










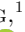
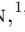




## A Snapshot Survey of Nearby Supernovae with the *Hubble Space Telescope*

RAPHAEL BAER-WAY <sup>1,2</sup> ASIA DEGRAW <sup>1</sup> WEIKANG ZHENG <sup>1,3</sup> SCHUYLER D. VAN DYK <sup>4</sup>  
ALEXEI V. FILIPPENKO <sup>1</sup> ORI D. FOX <sup>5</sup> THOMAS G. BRINK <sup>1,6</sup> PATRICK L. KELLY <sup>7</sup> NATHAN SMITH <sup>8</sup>  
SERGIY S. VASYLYEV <sup>1,9</sup> THOMAS DE JAEGER <sup>10,11</sup> KETO ZHANG <sup>1,4</sup> SAMANTHA STEGMAN <sup>1,12</sup> TIMOTHY ROSS <sup>1,13</sup>  
AND SAMEEN YUNUS <sup>1,14</sup>

<sup>1</sup>*Department of Astronomy, University of California, Berkeley, CA 94720-3411, USA*

<sup>2</sup>*Department of Astronomy, University of Virginia, 530 McCormick Road, Charlottesville, VA, 22904*

<sup>3</sup>*Eustace Specialist in Astronomy*

<sup>4</sup>*Caltech/IPAC, Mailcode 100-22, Pasadena, CA 91125, USA*

<sup>5</sup>*Space Telescope Science Institute, 3700 San Martin Drive, Baltimore, MD 21218, USA*

<sup>6</sup>*Wood Specialist in Astronomy*

<sup>7</sup>*University of Minnesota, School of Physics and Astronomy, 116 Church St. SE, Minneapolis, MN 55455, USA*

<sup>8</sup>*Steward Observatory, University of Arizona, 933 North Cherry Avenue, Tucson, AZ 85721, USA*

<sup>9</sup>*Steven Nelson Graduate Fellow*

<sup>10</sup>*Institute for Astronomy, University of Hawai'i, 2680 Woodlawn Dr., Honolulu, HI 96822, USA*

<sup>11</sup>*CNRS/IN2P3 (Sorbonne Université, Université Paris Cité), Laboratoire de Physique Nucléaire et de Hautes Énergies, 75005, Paris, France*

<sup>12</sup>*Department of Chemistry, University of Wisconsin, Madison, WI 53706, USA*

<sup>13</sup>*Lumentum, 1001 Ridder Park Dr., San Jose, CA 95131, USA*

<sup>14</sup>*Department of Physics, University of California, Merced, 5200 Lake Rd., Merced, CA 95343, USA*

### ABSTRACT

Over recent decades, robotic (or highly automated) searches for supernovae (SNe) have discovered several thousand events, many of them in quite nearby galaxies (distances  $< 30$  Mpc). Most of these SNe, including some of the best-studied events to date, were found before maximum brightness and have associated with them extensive follow-up photometry and spectroscopy. Some of these discoveries are so-called “SN impostors,” thought to be superoutbursts of luminous blue variable stars, although possibly a new, weak class of massive-star explosions. We conducted a Snapshot program with the *Hubble Space Telescope* (*HST*) and obtained images of the sites of 31 SNe and four impostors, to acquire late-time photometry through two filters. The primary aim of this project was to reveal the origin of any lingering energy for each event, whether it is the result of radioactive decay or, in some cases, ongoing late-time interaction of the SN shock with pre-existing circumstellar matter, or the presence of a light echo. Alternatively, lingering faint light at the SN position may arise from an underlying stellar population (e.g., a host star cluster, companion star, or a chance alignment). The results from this study complement and extend those from Snapshot programs by various investigators in previous *HST* cycles.

*Keywords:* Supernovae

### 1. INTRODUCTION

Supernovae (SNe) represent the final, explosive stage in the evolution of certain varieties of stars (e.g., Woosley & Weaver 1986; Wheeler & Harkness 1990; Filippenko 1997; Gal-Yam 2017). Studies of SNe, both observational and theoretical, are closely tied with the physics of stellar evolution, explosion mechanisms and nucleosynthesis, the chemical evolution of galaxies and the Universe, the formation of neutron stars and black

holes, and gamma-ray bursts. SNe Ia are also exceedingly useful cosmological tools, revealing the accelerating expansion of the Universe.

Despite the well-sampled early-time light curves of relatively nearby SNe, observations are quite sparse at late times ( $t \gtrsim 6$  months), primarily because the SNe are extremely faint or their ground-based photometry is contaminated by neighboring stars within the seeing disk. Thus, high-spatial-resolution observations, such as

with the *Hubble Space Telescope* (*HST*), are required to obtain accurate photometry. Following the multifilter light-curve shapes of these SNe over their long evolution provides important information on their progenitor systems and on the underlying physics leading to the lingering light, and can reveal “SN impostors” — events which are not genuine SNe involving a terminal explosion, but instead are powerful stellar outbursts which occasionally approach the peak luminosity of some kinds of true SNe.

There have been a number of *HST* Snapshot surveys of the sites of SNe. Various studies have conducted detailed analyses of the late-time emission of these SNe and of their immediate environments (e.g., Li et al. 2002; Fransson et al. 2002; Van Dyk et al. 2003; Sun et al. 2023). In each case it has been shown that *HST* can effectively resolve the faint SNe at late times from their immediate environments. In some cases, more than one epoch of *HST* observations was obtained, enabling the measurements of late-time decline rates and providing important information on the nebular evolution of SNe. Observed differences in late-time decline rates, particularly for those significantly diverging from power due to  $^{56}\text{Co}$  radioactive decay, motivate the need for larger samples of light curves to be collected.

Additional sources of late-time luminosity can originate via contribution from light echoes or from interaction of the SN shock with circumstellar matter (CSM). For instance, light echoes observed with *HST* have been spatially resolved around four nearby SNe Ia: SN 1991T (Sparks et al. 1999), SN 1998bu (Cappellaro et al. 2001), SN 2006X (Wang et al. 2008), and SN 2014J (Crotts 2015; Yang et al. 2017). The presence of light echoes is not limited to SNe Ia — resolved echoes have been detected around a number of core-collapse SNe as well, such as SN 1987A (e.g., Bond et al. 1990), SN 1993J (Sugerman & Crotts 2002; Liu et al. 2003), SN 2003gd (Sugerman 2005; Van Dyk et al. 2006), SN 2008bk (Van Dyk 2013), SN 2012aw (Van Dyk et al. 2015), and SN 2016adj (Stritzinger et al. 2022). Recently, a light echo has also been detected around SN 1987A as detailed by Ding et al. (2021) and Cikota et al. (2023). Snapshot programs, in particular, can provide statistics on the frequency of light echoes around various types of SNe.

The sustained late-time luminosity of some SNe II can be explained by interaction of the SN shock with large amounts of CSM set up by the pre-SN wind (e.g., Fox et al. 2013; Smith 2014, 2017; Smith et al. 2017). The sustained optical emission in this case likely arises from a radiatively-cooled shell. *HST* Snapshot programs can also help reveal the nature of the SN impostors, events similar to Type IIn SNe (with relatively narrow H emis-

sion lines in their spectra), but which are subluminal compared with core-collapse SNe ( $M_V \approx -14$  mag) near maximum brightness (Smith et al. 2011a; Van Dyk & Matheson 2012).

In this paper, we present the results of *HST* Snapshot program GO-16179 (PI A. Filippenko), along with some data from previous Snapshot programs such as GO-14668 and GO-15166 (PI A. Filippenko). The primary goal of this study is fairly simple: to determine whether the SNe at late times are essentially following the exponential light-curve decline, as a result of reprocessing of  $\gamma$ -rays and positrons from radioactive  $^{56}\text{Co}$  decay, or whether an additional power source is at work. In Section 2 we provide the details of the *HST* observations, and Section 3 describes our analysis, including the data reduction and results. The results as they pertain to all of the individual objects are discussed in Section 4. Section 5 provides our summary and conclusions.

## 2. OBSERVATIONS

The program was executed during *HST* Cycle 28 from 2020 November 11 through September 24 2021 (UTC dates are used throughout), with the Wide Field Camera 3 (WFC3) UVIS. The original observing request was for 55 visits, consisting of 9 SNe Ia, 27 SNe Ib/c, 12 SNe II, and 7 SN impostors (for reviews of SN spectral classification, see Filippenko (1997), Gal-Yam (2017)), of which 38 visits ( $\sim 70\%$ ) were actually executed. However, one visit, of the target SN IIn 2005ip, failed outright (all data lost), and two other visits, of the SN Ia 2018hfp and SN Ia 2019cth, experienced loss of guiding and were rendered useless. The final observed sample of 35 targets (3 SNe Ia, 9 SNe Ib/c, 19 SNe II, and 4 SN impostors) is summarized in Table 1. All of the data presented in this article were obtained from the Mikulski Archive for Space Telescopes (MAST) at the Space Telescope Science Institute. The specific observations analyzed can be accessed via the associated DOI.

The observing scheme for the program was to obtain all of the executed visits within an optimum “Snapshot” orbit of  $\sim 38$ – $40$  min, which was intended to increase the likelihood that a visit would be scheduled. To accomplish this, each visit orbit consisted of observations in two bands, with a total exposure time of 710 s in one band and 780 s in the other. Typically, we observed in the F555W band with the shorter exposures and in F814W with the longer ones, but varied the actual filter combination used depending on the specific science goal for each visit. The observations in each band per visit were split into two exposures of equal duration, employing a line dither between exposures to mitigate as best

as possible against cosmic-ray hits and detector cosmetic defects.

All of the data from the program had no exclusive access period and were publicly available from the Mikulski Archive for Space Telescopes (MAST)<sup>1</sup> as soon as they were processed through the Space Telescope Science Institute (STScI) *HST* standard pipeline. We note that at least one study not focused on SNe or related transients, but on the optical counterparts of extragalactic ultraluminous X-ray sources (Allak et al. 2022), has already made use of our data.

### 3. ANALYSIS

#### 3.1. Data Reduction

We ran the suite of STScI *Drizzlepac* routines (STScI Development Team 2012) on the data from each visit, to construct a drizzled image mosaic in each band. To locate the general sites of SNe in each of the image mosaics, coordinates from the Transient Name Server (TNS)<sup>2</sup> were first used. To more precisely isolate the SN site, either we directly compared the new data with previous *HST* images containing the SN from previous epochs (in many of the cases, from previous Snapshot programs) when the SN was brighter, or, if no prior *HST* data were available, astrometrically aligned the *HST* Snapshot mosaics with ground-based images of the SN (in many cases, obtained by us with the 0.76 m Katzman Automatic Imaging Telescope (KAIT; Filippenko 2003) or at the Nickel 1 m telescope, both at Lick Observatory). In the former cases, we could simply blink the Snapshot images with the previous *HST* images and visually identify the SN in the new data. In the latter cases, stars were found in common between the *HST* and ground-based images, and astrometric registration between the two datasets was performed. The SN position in the ground-based data was then transformed to the *HST* reference frame. The typical astrometric uncertainty was in the range of  $\sim 0.1''$ , and in no case where we performed this alignment were there any other sources in the error circle. In most cases, it was then readily apparent which object in the Snapshot data was the SN in question.

To obtain photometry from the data in both bands for each visit, we ran the individual frames for the entire

visit through the *Dolphot* package (Dolphin 2016), using one of the mosaics as the reference image for source detection. Generally, the recommended WFC3/UVIS parameters from Dolphin (2016) were used.

#### 3.2. Results

Once an SN location was isolated, its image coordinates were matched to the output from *Dolphot* to retrieve photometric information for the SN, along with any potential error/quality flags. The photometric results for all of the SNe are given in Table 2. The brightness measurements for the SNe are in Vega magnitudes for the *HST* flight system bands, as indicated in the table. In a number of cases, nothing was detected by *Dolphot* at the SN position, and subsequently we estimated upper limits to detection and provide these in the table. The upper limits were based on the formal estimations of signal-to-noise ratio ( $S/N$ ) from *Dolphot*, and we have set the significance at  $S/N = 5$ . The major caveat is that the uncertainties, particularly at low flux levels and in crowded environments, are underestimated by *Dolphot* (Williams et al. 2014), so the significance levels of the nondetections are likely overestimates; see Van Dyk et al. (2023) for a discussion of this issue.

For each event we also indicate in Table 2 our assessment of whether the late-time light curves appear to be powered by radioactive decay (the  $^{56}\text{Co}$  decay rate is shown for comparison in the light-curve figures; see Section 4), with either a “yes” or “no.” In some cases we were unable to make this assessment, since the event is either an SN impostor (and therefore still likely undergoing a superoutburst) or early-time photometry did not exist; these are listed as “N/A,” for “not applicable.” In a number of cases we were unable to confidently ascribe the decline to radioactive decay, primarily because we could only place an upper-limit constraint on the late-time emission, and these are indicated by a question mark.

In the next section we discuss each of the individual objects separately.

## 4. INDIVIDUAL OBJECTS

### 4.1. SN 1988Z

SN 1988Z was recognized early as an unusual SN II (Stathakis & Sadler 1991). From the luminous radio (Van Dyk et al. 1993; Williams et al. 2002) and X-ray (Fabian & Terlevich 1996; Schlegel & Petre 2006) emission detected from the SN, along with the characteristics of its optical photometric and spectroscopic emission (Turatto et al. 1993; Aretxaga et al. 1999), it was posited that long-lived interaction of the SN shock with a pre-existing dense CSM was the likely source of this

<sup>1</sup> <https://mast.stsci.edu/search/ui/#/hst>

<sup>2</sup> <https://www.wis-tns.org/>

**Table 1.** Properties of the Targeted Events and Their Hosts

SN	Type	$\alpha$ (h,m,s) (J2000)	$\delta$ ( $^{\circ}$ ,',") (J2000)	Discovery Date (UTC)	Host galaxy	$A_V$ (MW) (mag)	Distance (Mpc)	$v_{\text{hel}}$ (host) (km s $^{-1}$ )
SN 1988Z	IIn	10:51:50.10	+16:00:01.01	1988-12-12	MCG +03-28-022	0.07	70.7(11)	6748(3)
SN 1993J	IIb	09:55:25.00	+69:01:13.01	1993-03-28	NGC 3031	0.22	3.6(0.3)	−39(3)
SN 2000ch	Imp.	10:52:41.40	+36:40:08.51	2000-05-03	NGC 3432	0.04	11.7(4.2)	613(4)
SN 2010jl	IIn	09:42:53.33	+09:29:41.78	2010-11-03	UGC 5189A	0.08	...	3207(37)
SN 2010mc	IIn	17:21:30.67	+48:07:47.39	2010-08-20	GALEXASCJ172130.92+480747.6	0.05	...	10493
SN 2011dh	IIb	13:30:05.12	+47:10:10.81	2011-06-01	NGC 5194	0.10	7.2(2.1)	463(3)
SN 2012A	II-P	10:25:07.39	+17:09:14.62	2012-01-07	NGC 3239	0.09	9.7(1.6)	710(1)
SN 2012aw	II-P	10:43:53.76	+11:40:17.90	2012-03-16	NGC 3351	0.08	9.9(1.1)	1128(24)
SN 2013df	IIb	12:26:29.33	+31:13:38.32	2013-06-07	NGC 4414	0.05	18.1(3.1)	708(2)
SN 2013ej	II-P/II-L	01:36:48.16	+15:45:31.00	2013-07-25	NGC 628	0.19	7.5(3.1)	657(1)
SN 2014C	Ib	22:37:05.60	+34:24:31.90	2014-01-05	NGC 7331	0.25	13.4(2.7)	816(1)
SN 2015cp	Ia	03:09:12.76	+27:31:16.95	2015-12-28	WISEAJ030912.10+273106.9	0.74	...	...
SN 2016G	Ic-BL	03:03:57.70	+43:24:03.60	2016-01-09	NGC 1171	0.43	26.6(6.2)	2742(5)
SN 2016adj	Ic?	13:25:24.11	−43:00:57.50	2016-02-08	NGC 5128	0.32	3.8(0.8)	547(5)
SN 2016bkv	II-P	10:18:19.31	+41:25:39.30	2016-03-21	NGC 3184	0.05	12.3(2.2)	582(1)
AT 2016blu	Imp.	12:35:52.30	+27:55:55.9	2021-01-11	NGC 4559	0.05	8.9(0.2)	814(1)
SN 2016coi	Ic-BL	21:59:04.14	+18:11:10.46	2016-05-27	UGC 11868	0.23	17.2(7)	1093(5)
SN 2016coj	Ia	12:08:06.80	+65:10:37.80	2016-05-28	NGC 4125	0.05	22.8(7.6)	1281(14)
SN 2016gkg	IIb	01:34:14.46	−29:26:25.00	2016-09-20	NGC 613	0.05	20.9(5.7)	1481(5)
AT 2016jbu	Imp.?	07:36:25.96	−69:32:55.25	2016-12-01	NGC 2442	0.56	20.1(0.5)	1466(5)
SN 2017cfd	Ia	08:40:49.09	+73:29:15.11	2017-03-16	IC 511	0.06	...	3623(49)
SN 2017eaw	II-P	20:34:44.24	+60:11:35.84	2017-05-14	NGC 6946	0.94	7.3(1.5)	40(2)
SN 2017gax	Ib/c	04:45:49.50	−59:14:42.50	2017-08-14	NGC 1672	0.06	11.8(1.4)	1331(3)
SN 2017gkk	IIb	09:13:44.57	+76:28:44.54	2017-08-31	NGC 2748	0.07	19.2(2.8)	1476(2)
SN 2017ixv	Ic-BL	19:21:31.24	+61:08:51.76	2017-12-17	NGC 6796	0.19	36.2(2.8)	2189(6)
SN 2018aoq	II-P	12:10:38.22	+39:23:47.87	2018-04-01	NGC 4151	0.08	15.8(0.4)	997(2)
SN 2018gj	II-P	16:32:02.30	+78:12:40.93	2018-01-14	NGC 6217	0.12	20.6(7.3)	1361(3)
AT 2018cow	Ic-BL	16:16:00.22	+22:16:04.83	2018-06-16	CGCG 137−068	0.24	...	4241(39)
SN 2018ivc	II-pec	02:42:41.28	−00:00:31.92	2018-11-24	NGC 1068	0.09	10.6(3.0)	1137(3)
SN 2018zd	II-P	06:18:03.19	+78:22:01.16	2018-03-02	NGC 2146	0.26	19.6(8.2)	892(4)
SN 2019ehk	Ib/gap tr.	12:22:56.15	+15:49:34.03	2019-04-29	NGC 4321	0.09	16.2(3.1)	1571(1)
AT 2019krl	Imp.	01:36:49.65	+15:46:46.21	2019-07-06	NGC 628	0.19	7.5(3.1)	657(1)
SN 2020dpw	II-P	20:37:10.55	+66:06:10.66	2020-02-26	NGC 6951	1.02	23.1(3.5)	1424(1)
SN 2020hvp	Ib	16:21:45.39	−02:17:21.37	2020-04-21	NGC 6118	0.43	20.8(3.9)	1573(1)
SN 2020jfo	II-P	12:21:50.48	+04:28:54.05	2020-05-06	NGC 4303	0.06	14.6(7.3)	1566(2)

NOTE—SN positions and discovery dates are adopted from the TNS. Foreground Milky Way visual extinction,  $A_V$ (MW), is adopted in each case from the NASA/IPAC Extragalactic Database (NED; Schlafly & Finkbeiner 2011). Distances and heliocentric velocities ( $v_{\text{hel}}$ ) are also obtained from NED.

**Table 2.** *HST* Photometry of the Observed Supernovae

Object	Obs. Date (UTC)	MJD	Age (days)	Bands	Exp. Time (s)	Brightness (Vegamag)	Exponential Decline?
SN 1988Z	2021-02-19	59264.8	11757.8	F625W, F814W	710, 780	24.83(03), 24.98(10)	No
SN 1993J	2020-12-14	59197.2	10123.2	F336W, F814W	710, 780	23.38(03), 23.25(03)	No
SN 2000ch	2020-12-13	59196.8	7529.1	F555W, F814W	710, 780	20.90(03), 19.01(01)	N/A
SN 2010jl	2020-12-29	59213.0	3699.9	F336W, F814W	710, 780	>24.8, >25.6	No?
SN 2010mc	2021-09-24	59481.3	4053.3	F555W, F814W	710, 780	24.56(04), 25.44(12)	No
SN 2011dh	2020-12-10	59193.1	3480.1	F555W, F814W	710, 780	23.15(02), 23.22(03)	No
SN 2012A	2021-02-16	59261.8	3328.8	F606W, F814W	710, 780	>26.9, >25.8	Yes?
SN 2012aw	2021-02-17	59262.9	3260.9	F555W, F814W	710, 780	25.87(10), 25.17(13)	No
SN 2013df	2021-02-15	59260.9	2810.9	F336W, F555W	780, 710	23.62(03), 23.21(03)	No
SN 2013ej	2021-08-19	59446.0	2948.0	F555W, F814W	710, 780	24.37(03), 23.41(03)	No
SN 2014C	2021-08-20	59446.7	2785.7	F555W, F814W	710, 780	22.18(04), 20.88(01)	No
SN 2015cp	2020-11-30	59183.0	1799.0	F275W, F625W	710, 780	>25.1, >27.2	Yes?
SN 2016G	2020-12-20	59203.4	1807.4	F606W, F814W	710, 780	>25.8, >25.1	Yes?
SN 2016adj	2021-07-28	59423.6	1997.6	F438W, F555W	710, 780	>27.4, >26.5	Yes?
SN 2016bkv	2020-12-13	59196.0	1721.0	F555W, F814W	710, 780	23.39(02), 23.33(04)	No
AT 2016blu	2021-02-17	59262.9	1779.0	F606W, F814W	710, 780	19.51(00), 19.32(00)	N/A
SN 2016coi	2020-12-06	59189.7	1654.7	F336W, F814W	710, 780	>26.1, >26.0	Yes?
SN 2016coj	2020-12-09	59192.2	1656.2	F555W, F814W	710, 780	>26.8, >25.5	Yes?
SN 2016gkg	2021-08-19	59445.8	1794.8	F438W, F606W	710, 780	>26.1, 24.88(04)	No
AT 2016jbu	2021-08-21	59447.9	1724.9	F555W, F814W	710, 780	26.63(04), 25.69(05)	N/A
SN 2017cfd	2021-09-16	59473.5	1645.4	F555W, F814W	710, 780	>26.9, >26.0	Yes?
SN 2017eaw	2020-11-11	59164.8	1277.8	F555W, F814W	710, 780	23.66(02), 23.00(05)	No
SN 2017gax	2020-11-27	59180.2	1201.2	F336W, F814W	710, 780	>26.3, >26.0	Yes?
SN 2017gkk	2021-09-24	59481.0	1485.1	F555W, F814W	710, 780	24.69(05), 23.91(07)	No
SN 2017ixv	2021-01-11	59225.8	1121.8	F555W, F814W	710, 780	>26.4, >24.9	Yes?
SN 2018gj	2021-01-27	59241.4	1109.3	F555W, F814W	710, 780	24.77(04), 23.32(06)	No
SN 2018zd	2021-02-07	59252.6	1073.7	F555W, F814W	710, 780	>27.0, >26.1	Yes?
SN 2018aoq	2020-12-05	59188.8	983.8	F555W, F814W	710, 780	>26.9, >25.9	Yes?
AT 2018cow	2021-07-25	59420.8	1135.8	F555W, F814W	710, 780	25.69(09), 26.21(03)	No
SN 2018ivc	2020-12-02	59185.0	739.0	F555W, F814W	710, 780	22.71(02), 21.97(03)	No
SN 2019ehk	2021-02-21	59266.9	664.9	F438W, F625W	710, 780	>27.2, >26.6	Yes?
AT 2019krl	2021-02-15	59260.6	590.8	F438W, F625W	710, 780	23.85(04), 23.77(03)	N/A
SN 2020dpw	2020-12-13	59196.9	291.9	F555W, F814W	710, 780	20.33(00), 18.54(00)	Yes?
SN 2020hvp	2021-05-22	59356.8	396.8	F555W, F814W	710, 780	22.81(01), 22.20(02)	Yes
SN 2020jfo	2021-07-28	59423.5	448.5	F555W, F814W	710, 780	22.23(01), 21.34(01)	Yes

NOTE—Obs. Date is the Snapshot observation date. Modified Julian Date (MJD) is Julian date (JD) – 2,400,000.5. Age is days since discovery date. Exposure times (“Exp.”) are the total time in each *HST* band.

radiation. In fact, recent spectra show that SN 1988Z is still strongly interacting with dense CSM even three decades after explosion (Smith et al. 2017). SN 1988Z is generally considered to be a Type IIn SN, even a prototype of this subclass.

The Snapshot observations were obtained on 2021 February 19 in F625W ( $\sim R$ ) and F814W ( $\sim I$ ). As can be seen in Figure 1, amazingly the SN was still detectable in the *HST* images 11,758 d (32.2 yr) after discovery, at  $m_{F625W} = 24.83 \pm 0.03$  and  $m_{F814W} = 24.98 \pm 0.10$  mag. (We had intentionally used the F625W band, sensitive to any remaining  $H\alpha$  line emission, and the F814W band, potentially sensitive to hot dust, to increase the probability of detection at such late times.) We pinpointed the location of the faint SN in these images by employing previously unpublished imaging in 2013 February from our Snapshot program in Cycle 20 (GO-13029, PI A. Filippenko), when the SN was brighter ( $m_{F625W} = 24.08 \pm 0.04$  and  $m_{F814W} = 24.49 \pm 0.07$  mag).

We have included the two sets of Snapshot data together with the ground-based, earlier-time  $R$  light curves from Aretxaga et al. (1999) and Turatto et al. (1993). The light curve clearly does not follow the trend for radioactive-decay power, and the very late-time points from *HST* appear to follow the break in the light curve that began at  $\sim 2000$  d.

#### 4.2. SN 1993J

SN 1993J is one of the best-studied and historically prominent SNe ever discovered. It remains a benchmark SN IIB to which more recent discoveries are often compared, with a rich array of multiwavelength observations collected over the last 30 yr. The proximity of its host galaxy facilitated detection and characterization of its progenitor as a K-type supergiant, even from the ground (Filippenko et al. 1993; Aldering et al. 1994; Cohen et al. 1995; Van Dyk et al. 2002), and excess flux in the blue and near-ultraviolet (UV) bands suggested the presence of a binary companion, consistent with models of supergiant mass loss onto the secondary (e.g., Podsiadlowski et al. 1993; Maund et al. 2004; Fox et al. 2014). The optical light curve of the SN has been powered by ongoing interaction with the CSM in a relatively slow decline. The SN had faded enough by 2004 that it was evident that the supergiant progenitor had vanished (Maund & Smartt 2009). The SN had remained too luminous, however, for a binary companion to be isolated via imaging, until Fox et al. (2014) were able to claim detection of UV excess emission indicative of such a star in *HST* data from 2011 and 2012. Up to the present epoch, the visual-wavelength spectrum of

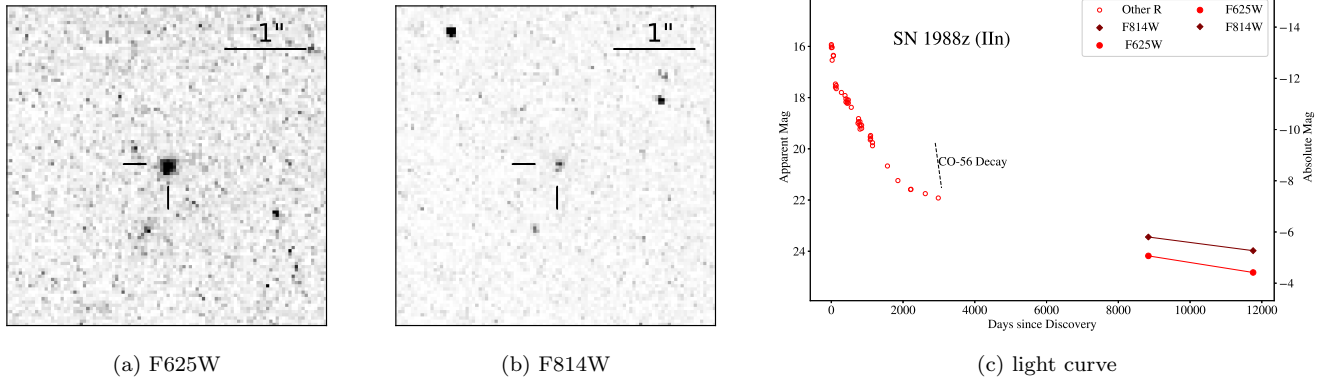
SN 1993J is still dominated by strong ongoing CSM interaction, with prominent broad emission lines of  $H\alpha$ , [O I], [O II], and [O III] (Smith et al. 2017).

We located the SN site in our Snapshot data in F336W ( $\sim U$ ) and F814W from 2020 December 14, when the SN was at 10,123 d (27.7 yr), by consulting Fox et al. (2014, their Figure 1) and also comparing with the data from 2012 February from program GO-12531 (PI A. Filippenko), when the SN was brighter in F336W and F814W ( $22.33 \pm 0.02$  and  $20.87 \pm 0.01$  mag, respectively). We also compared to previously-unpublished data from 2015 March at F336W from GO-13648 (PI O. Fox; the SN was at  $22.62 \pm 0.05$  mag); see Figure 2. SN 1993J clearly is not following the radioactive-decay trend, which has been the case for most of its late-time ( $\gtrsim 500$  d) history. However, the SN appears to have faded more rapidly, compared to the more gradual decline up to (and possibly beyond) 2015. This could be indicating that the SN shock was encountering a less dense circumstellar environment than previously, consistent with the results of modeling of the declines in both the radio and X-ray emission (Kundu et al. 2019).

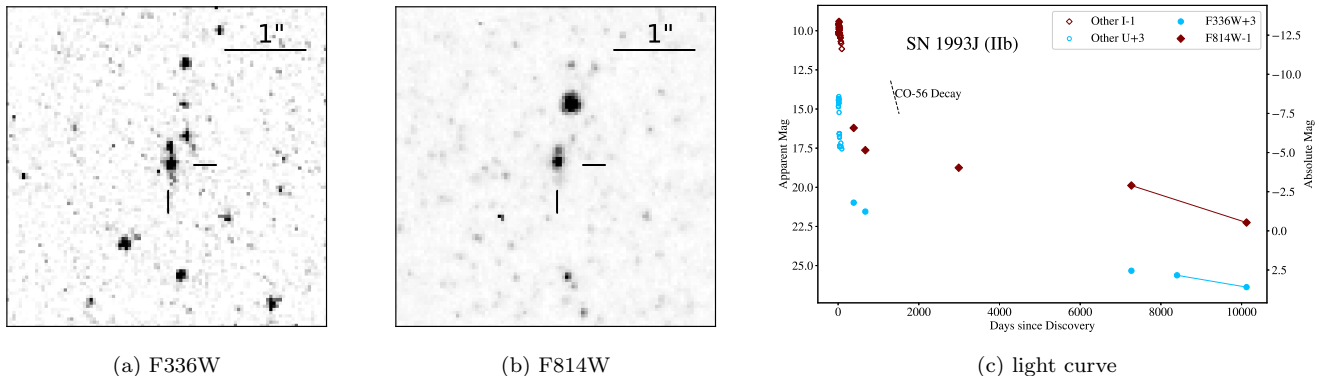
We can now clearly detect in F814W (see Figure 2) a star immediately to the northwest of the SN, the presence of which was just hinted at by Fox et al. (2014). Following the labeling scheme from Fox et al. (2014), this star “O” has  $m_{F814W} = 22.88$  mag. We have reprocessed the 2011 data from Fox et al. (2014), adopting the same *Dolphot* parameters that we used here (which differ somewhat from those used in that previous study); our results are presented in Table 3. We also include our measurements for F336W data (640 s) from GO-13648 (PI O. Fox). Furthermore, we present our results for these same stars from our Snapshot data. On average, the stars have essentially the same measured brightnesses in F814W, with the Snapshot values being slightly fainter (by  $\sim 0.06$  mag), whereas the F336W Snapshot measurements appear to differ by substantially more,  $\sim 0.46$  mag fainter, than our remeasurements of the Fox et al. (2014) data. We can potentially account for this large difference in that the 2011 total exposures (3000 s) in F336W were a factor of  $\sim 4.2$  deeper than the 710 s total Snapshot exposure, so the  $S/N$  was substantially higher for the former than the latter.

#### 4.3. SN 2000ch

SN 2000ch, discovered with KAIT at magnitude 17.4, was suspected early on to be an unusual and very luminous variable in NGC 3432. Wagner et al. (2004) initially described its erratic behavior, and Pastorello



**Figure 1.** A portion of the WFC3 image mosaic containing SN 1988Z, from observations on 2021 February 19, in (a) F625W and (b) F814W. Here, and in all other figures showing *HST* images in this paper, north is up and east is to the left; also, whenever the SN is visible, it is indicated by tick marks. Also shown are the (“Other”) *R* (c) light curves from [Aretxaga et al. \(1999\)](#) and [Turatto et al. \(1993\)](#), together with the Snapshot detections from programs GO-13029 and GO-16179.



**Figure 2.** A portion of the WFC3 image mosaic containing SN 1993J, from observations on 2020 December 14, in (a) F336W and (b) F814W. Also shown are the (“Other”) *U* and *I* (c) light curves from [Richmond et al. \(1996\)](#), together with prior *HST* data from [Van Dyk et al. \(2002\)](#), [Fox et al. \(2014\)](#), and previously-unpublished data from GO-13648 (PI O. Fox), as well as our Snapshots.

[et al. \(2010\)](#) later detailed the occurrence of multiple outbursts from the star. [Smith et al. \(2011a\)](#) compared SN 2000ch to a host of other objects considered to be luminous blue variables or SN impostors, which may survive their eruptive outbursts. SN 2000ch has continued to experience brief, regularly recurring outbursts ([Aghakhanloo et al. 2022a](#)), and can fool transient hunters as being a new event (e.g., [Van Dyk et al. 2013a](#)).

Our Snapshot observations were obtained in F555W ( $\sim V$ ) and F814W on 2020 December 13. As one can see in Figure 3, the object is easily detectable in the *HST* images, and its light curve appears very much unlike that of a typical SN. [Aghakhanloo et al. \(2022a\)](#) have recently analyzed the continued photometric evolution of SN 2000ch, finding periodicity to the cycle of repeating outbursts, which suggests a binary nature for the

transient. The object, since it is a likely SN impostor, is not powered at late times by radioactive decay.

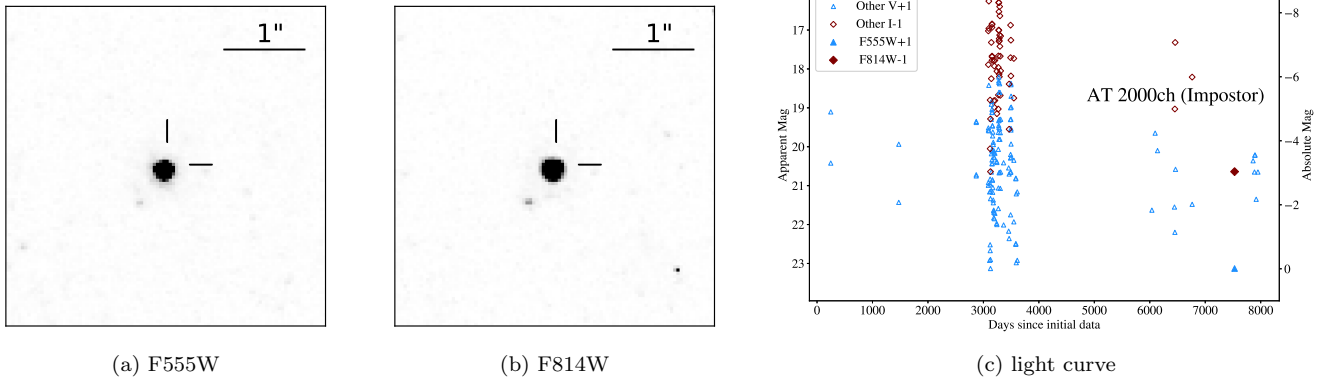
#### 4.4. SN 2010jl

SN 2010jl was classified as a luminous Type IIn SN, and [Stoll et al. \(2011\)](#) presented early-time light curves and spectra. [Smith et al. \(2011b\)](#) identified a luminous blue ( $M_{F300W} \approx -12.0$  mag) point source at the SN location that they identified as a candidate progenitor, although [Fox et al. \(2017\)](#) have since demonstrated that this is less likely. [Smith et al. \(2011b\)](#) noted that even if the blue source was a nearby star cluster, its young age suggested a high initial mass of  $> 30 M_{\odot}$  for the progenitor of SN 2010jl. Further optical and near-infrared (IR) monitoring of SN 2010jl has been presented by [Zhang et al. \(2012\)](#), [Ofek et al. \(2014\)](#), [Borish et al. \(2015\)](#), [Jencson et al. \(2016\)](#), and others. As an SN IIn, similar to the case of SN 1988Z (Section 4.1), there has

**Table 3.** SN 1993J Field Photometry Comparisons

Star	Fox et al. (2014)		GO-13648	This paper	
	F336W	F814W	F336W	F336W	F814W
	(mag)	(mag)	(mag)	(mag)	(mag)
SN	22.33 (0.02)	20.87 (0.01)	22.62 (0.05)	23.85 (0.10)	22.01 (0.02)
A	23.39 (0.03)	20.60 (0.01)	23.65 (0.09)	24.79 (0.21)	20.47 (0.01)
B	22.66 (0.02)	22.89 (0.03)	22.93 (0.05)	23.06 (0.05)	>25.6
C	22.55 (0.03)	23.71 (0.05)	22.82 (0.05)	22.93 (0.05)	23.56 (0.04)
D	22.44 (0.02)	24.19 (0.06)	22.63 (0.05)	22.73 (0.06)	24.04 (0.06)
E	23.29 (0.03)	24.21 (0.07)	23.54 (0.09)	23.65 (0.07)	24.22 (0.07)
F	23.90 (0.04)	24.98 (0.12)	24.07 (0.12)	24.04 (0.16)	>25.6
G	23.21 (0.03)	>25.7	23.53 (0.09)	23.65 (0.07)	>25.6
H	24.14 (0.04)	24.65 (0.10)	24.10 (0.13)	24.49 (0.12)	24.38 (0.08)
I	24.51 (0.06)	>25.7	24.44 (0.17)	>25.5	>25.6
J	>26.4	23.84 (0.05)	>26.1	>25.5	23.93 (0.06)
K	23.58 (0.03)	24.43 (0.07)	23.86 (0.10)	24.04 (0.09)	24.77 (0.11)
L	25.84 (0.13)	>25.7	>26.1	>25.5	>25.6
M	23.54 (0.03)	24.73 (0.10)	23.42 (0.08)	23.96 (0.09)	25.56 (0.21)
N	24.35 (0.06)	24.72 (0.10)	25.08 (0.27)	24.72 (0.14)	24.66 (0.10)
O	...	...	>26.1	>25.5	22.88 (0.03)

Uncertainties ( $1\sigma$ ) are in parentheses.



**Figure 3.** A portion of the WFC3 image mosaic containing SN 2000ch, from observations on 2020 December 13, in (a) F555W and (b) F814W. Also shown are the (“Other”)  $V$  and  $I$  (c) light curves from Pastorello et al. (2010) and Aghakhanloo et al. (2022a), together with the Snapshot detections.

long been multiwavelength evidence for strong circumstellar interaction (e.g., Smith et al. 2011b, 2012; Fransson et al. 2014; Chandra et al. 2015). Most notable is the observational and analytical indications for the presence of dust associated with the SN (e.g., Andrews et al. 2011; Smith et al. 2012; Gall et al. 2014; Sarangi et al. 2018; Bevan et al. 2020).

Fox et al. (2017) detected SN 2010jl in *HST* images up to 1618 d (4.4 yr) after discovery. Our Snapshots in F336W and F814W from 2020 December 29 are when the SN is significantly older, at 4118 d (11.3 yr); see Figure 4. We located the SN 2010jl site via comparison with prior *HST* images obtained in 2015 October by GO-14149 (PI A. Filippenko), when the SN was at  $m_{F336W} = 21.77 \pm 0.04$  and  $m_{F814W} = 22.23 \pm 0.02$  mag,



and October 2016 by GO-14668 (PI A. Filippenko), at  $m_{F336W} = 22.08 \pm 0.03$  and  $m_{F814W} = 22.67 \pm 0.03$  mag (see Fox et al. 2017). Analysis of a set of *HST* images from February 7 2018 (nearly 3 yr prior to our data), previously-unpublished data from GO-15166 (PI A. Filippenko), shows that SN 2010jl was still detectable at F814W, with  $m_{F814W} = 23.11 \pm 0.04$  mag, but had already become undetectable in F336W (with an upper limit of 23.5 mag). Given the late-time brightness of the SN, radioactive decay could not have been the object’s primary source of power. We conclude from analysis of our Snapshot images that the SN has now vanished, with upper limits of 24.8 mag in F336W and 25.6 mag in F814W.

#### 4.5. SN 2010mc

Ofek (2012) discovered SN 2010mc during the course of the PTF survey. Howell & Murray (2012) classified it subsequently as an SN IIn at redshift  $z = 0.035$ . Looking back in the PTF data, Ofek et al. (2013) discovered an astounding outburst event  $\sim 40$  d prior to the apparent SN. Smith et al. (2013) pointed out that SN 2010mc was a near twin of the remarkable event SN 2009ip, and Smith et al. (2014) proposed that both events were the terminal SN IIn explosions arising from eruptive blue supergiant progenitors. A terminal SN explosion has since been confirmed for SN 2009ip (Smith et al. 2022). The last published spectrum of SN 2010mc was from day 1024 (Smith et al. 2014), which at that time showed strong shock-broadened  $H\alpha$  emission indicative of ongoing CSM interaction.

We detected SN 2010mc in both our F555W and F814W Snapshots from 2021 September 24, 4053 d (11.1 yr) after discovery; see Figure 5. We had isolated the site of the SN using *HST* data from 2017 March 26 obtained by program GO-14668 (PI A. Filippenko), when the SN was at  $m_{F555W} = 24.26 \pm 0.04$  and  $m_{F814W} = 25.35 \pm 0.10$  mag. One will note that, both in 2017 and 2021, the SN is significantly brighter in F555W than in F814W, which we speculate must be the result of sustained luminous  $H\alpha$  emission from the SN within the F555W bandpass, with much less luminous continuum emission in F814W. SN 2010mc has diverged from radioactive-decay power since day  $\sim 400$  and continues to do so, most likely as a result of sustained CSM interaction. However, it is possible that some of the light is contributed by a star cluster coincident with the SN, as was the case for SN 2009ip; deeper and higher-resolution observations are needed to identify such a cluster.

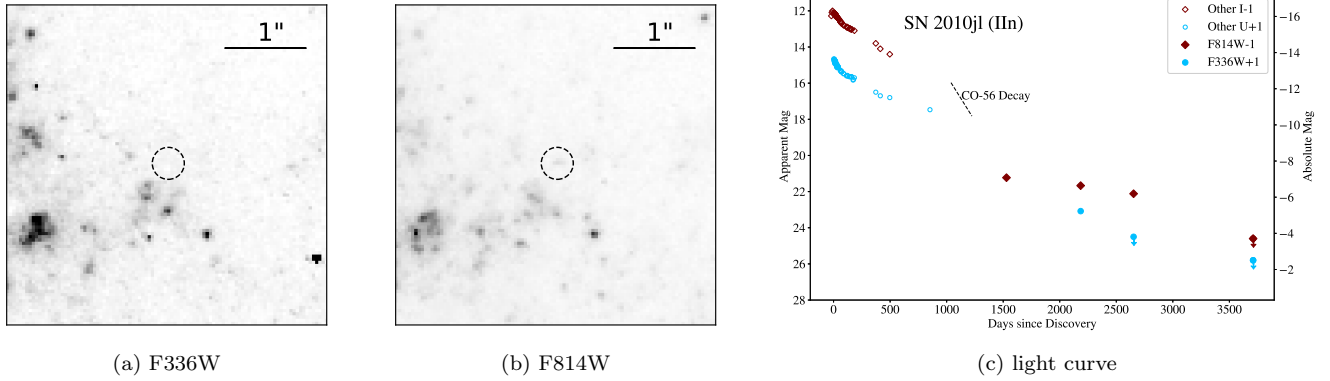
#### 4.6. SN 2011dh

The nearby SN 2011dh in M51 has become, along with SN 1993J, one of the best-studied SNe IIB, if not one of

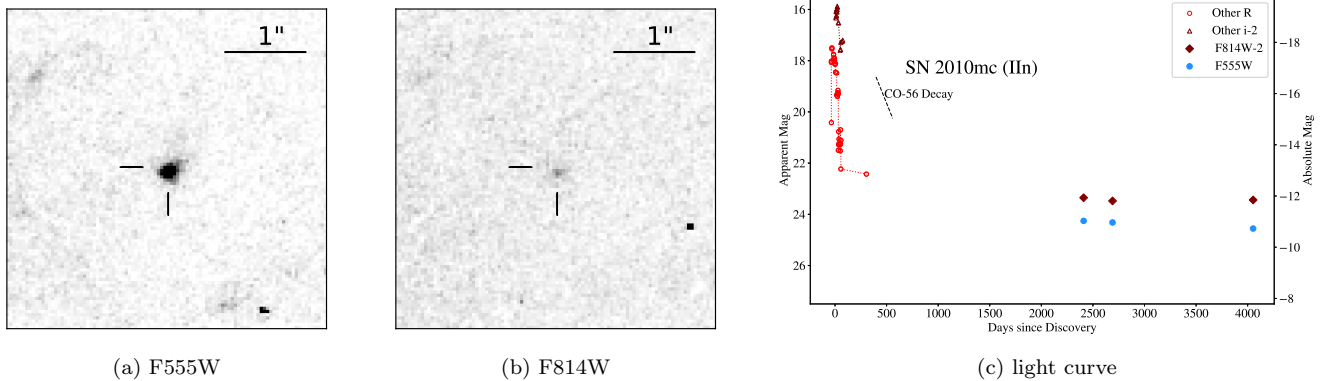
the best-studied SNe of any type thus far. Extensive UV, optical, and near-IR follow-up observations were carried out not long after discovery by Arcavi et al. (2011), Sahu et al. (2013), Shivvers et al. (2013), Ergon et al. (2014, 2015), Mauerhan et al. (2015), Marion et al. (2014), and others. Multiwavelength observations, including X-ray and radio, were indicative of circumstellar interaction; see, for example, Martí-Vidal et al. (2011), Krauss et al. (2012), Horesh et al. (2013), Maeda et al. (2014), de Witt et al. (2016), and Kundu et al. (2019). Both Maund et al. (2011) and Van Dyk et al. (2011) independently identified the SN’s progenitor. Soderberg et al. (2012), followed by Van Dyk et al. (2011), argued that the progenitor was compact, while Maund et al. (2011) pointed to the detected yellow supergiant as the star that exploded, and this was supported by the modeling by Bersten et al. (2012) and subsequently confirmed by the supergiant progenitor’s disappearance (Van Dyk et al. 2013b). Furthermore, detailed theoretical modeling of the progenitor by Benvenuto et al. (2013) supported the binary origin for the SN. Folatelli et al. (2014) claimed detection of a possible blue companion to the progenitor, although Maund et al. (2015) and Maund (2019) cast some doubt on that possibility.

Maund (2019), analyzing a veritable treasure trove of *HST* imaging serendipitously covering the SN site, argued that a light echo originating from dust with a preferred disk geometry could be responsible for the observed extended late-time emission. We pinpointed the location of the SN in our Snapshot images in F555W and F814W from 2020 December 10 (3480 d  $\approx 9.5$  yr after discovery), using a number of these prior *HST* images for comparison, and as can be seen, the emission is significantly fainter than from the analysis by Maund (2019); see Figure 6. Since that study, previously-unpublished *HST* observations also have been obtained of the SN site in 2019 on November 24 with the Advanced Camera for Surveys (ACS) Wide-Field Channel (WFC) in F814W by GO-15645 (PI D. Sand;  $m_{F814W} = 23.89 \pm 0.02$  mag) and in 2020 January 29 with WFC3/UVIS in F555W by GO-16024 (PI A. Filippenko;  $m_{F555W} = 25.02 \pm 0.05$  mag). (We note that data were also obtained by GO-16024 in F225W, not shown; however, the SN was not detected, to a limit of 24.0 mag; cf. Maund et al. 2015.) Taken together, these late-time *HST* data indicate a slow, steady fading of the SN emission — but clearly the SN at very late times has not followed a radioactive decay-powered decline.

#### 4.7. SN 2012A



**Figure 4.** A portion of the WFC3 image mosaic containing SN 2010jl, from observations on 2020 December 29, in (a) F336W and (b) F814W. As the SN is not detected in either band, its location is indicated by the dashed circle. Also shown are the (“Other”)  $U$  and  $I$  (c) light curves from Ofek et al. (2014) and Jencson et al. (2016), and F336W and F814W measurements from Fox et al. (2017), together with  $HST$  points from GO-15166 (PI A. Filippenko) and the Snapshot detections.

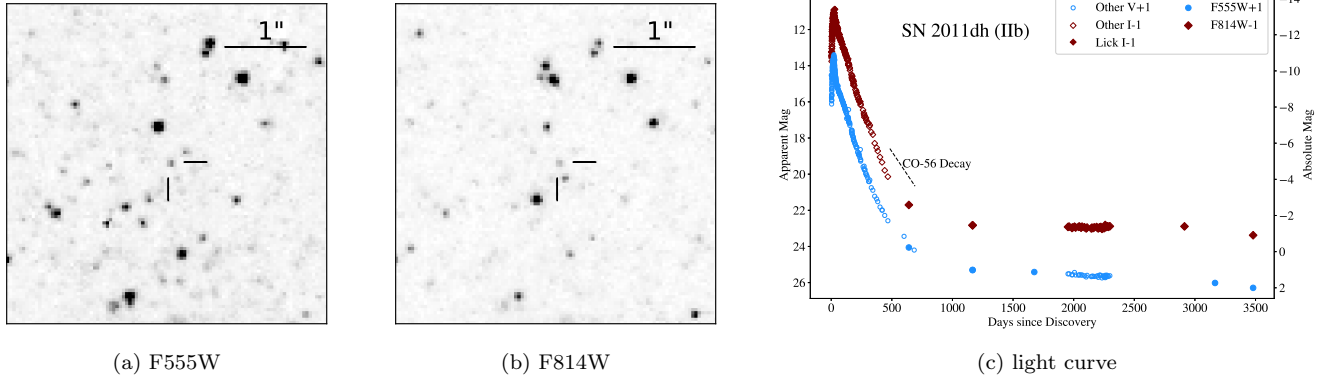


**Figure 5.** A portion of the WFC3 image mosaic containing SN 2010mc, from observations on 2021 September 24, in (a) F555W and (b) F814W. Also shown are the (“Other”)  $R$  and  $i$  (c) light curves from Ofek et al. (2013) and Smith et al. (2014), with the Snapshot data at the two  $HST$  bands for comparison.

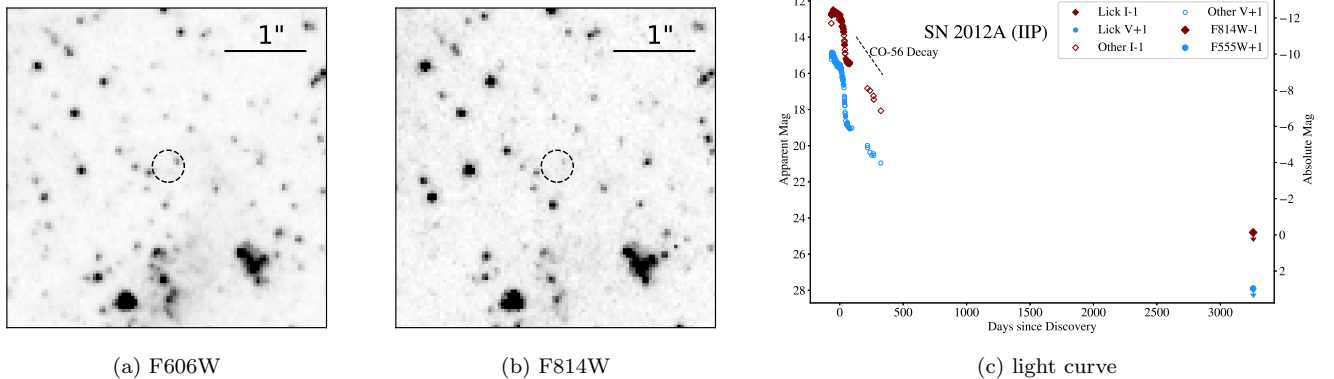
Tomasella et al. (2013) extensively monitored the normal SN II-P 2012A, beginning within a few days after discovery. The SN was also monitored in multiple bands and spectroscopically from Lick Observatory (de Jaeger et al. 2019). Silverman et al. (2017) analyzed a late-time Keck Observatory spectrum. Prieto et al. (2012) detected a progenitor candidate for the SN in pre-explosion Gemini ground-based adaptive optics (AO) imaging in the  $K$  band and characterized the star as a red supergiant (RSG). Tomasella et al. (2013) reanalyzed these data and estimated that the progenitor’s initial mass was  $\sim 10 M_{\odot}$ . Utrobin & Chugai (2015) also estimated the progenitor initial mass at  $13.1 \pm 0.7 M_{\odot}$  from hydrodynamical modeling of the clumpiness of the ejecta.

We obtained our Snapshot observations in F606W (“Wide”  $\sim V$ ) and F814W on 2021 February 16, 3329 d (9.1 yr) after discovery. We had purposely selected F606W in this case, rather than F555W, since the for-

mer is the preferred bandpass in which to acquire data, together with F814W, for use in tip-of-the-red-giant-branch (TRGB) distance estimates (Anand et al. 2021). Our intention was to obtain data that can better constrain the distance to SN 2012A, although that TRGB estimation is beyond the scope of this paper. (Our focus for the Snapshots was on the SN itself, which is within the main body of the host galaxy, and not the galaxy halo in which the TRGB would likely be more apparent.) We astrometrically aligned KAIT images from de Jaeger et al. (2019) with our Snapshot images, in order to isolate the SN site, and concluded from that analysis that the SN was no longer detectable, to 26.9 and 25.8 mag in F606W and F814W, respectively; see Figure 7. Van Dyk et al. (2023) performed a more precise alignment of the Snapshot F814W image with the AO data and concluded that the RSG progenitor star had vanished.



**Figure 6.** A portion of the WFC3 image mosaic containing SN 2011dh, from observations on 2020 December 10, in (a) F555W and (b) F814W. Also shown are the Lick (Zheng et al. 2022)  $V$  and  $I$  (c) light curves, along with (“Other”) data in these bands from Arcavi et al. (2011), Tsvetkov et al. (2012), Sahu et al. (2013), Marion et al. (2014), and Ergon et al. (2015), together with F555W and F814W data from Maund (2019) and Maund et al. (2015), *HST* programs GO-15645 (PI D. Sand) and GO-16024 (PI A. Filippenko), and our Snapshot observations.



**Figure 7.** A portion of the WFC3 image mosaic containing SN 2012A, from observations on 2021 February 16, in (a) F606W and (b) F814W. The SN was not detected in either band; the site is indicated by the dashed circle. Also shown are the Lick (de Jaeger et al. 2019)  $V$  and  $I$  (c) light curves, along with (“Other”) data in these bands from Tomasella et al. (2013), together with the detection upper limits from our Snapshot data.

#### 4.8. SN 2012aw

SN 2012aw in M95 is a nearby, well-studied normal SN II-P. Multiwavelength follow-up observations have been conducted by a number of investigators, including Bose et al. (2013), Dall’Ora et al. (2014), Jerkstrand et al. (2014), and de Jaeger et al. (2019)). Not long after discovery both Van Dyk et al. (2012b) and Fraser et al. (2012) identified a candidate progenitor RSG in pre-explosion *HST* WFPC2 images. The progenitor was confirmed, as it had disappeared in late-time *HST* imaging (Fraser 2016). In the same late-time imaging, Van Dyk et al. (2015) discovered a resolved light echo around the SN.

We pinpointed the location of the SN in our Snapshot data in F555W and F814W from 2021 February 17, using *HST* data obtained on 2016 October 24 by GO-14668

(PI A. Filippenko), as well as the pre-explosion WFPC2 images in which the progenitor had been identified; see Figure 8. What is most strikingly apparent is the continued presence of the light echo in both bands around the SN site. Whereas the SN was obscured by the echo at earlier times (Van Dyk et al. 2015), the SN had become recoverable in both the *HST* F814W and F555W images 3261 d (8.9 yr) after discovery.

The echo itself is seen almost as a perfect ring, although asymmetric relative to the SN position, with the SN offset by  $\sim 2.6$  pixels ( $\sim 0''.103$  at the UVIS pixel scale) southeast from the ring center. The surface brightness of the echo is still highest to the east and southeast, as reported by Van Dyk et al. (2015). We estimate that the radius of the echo is  $\sim 7.4$  pixels ( $\sim 0''.293$ ). This is nearly double the radius, at  $\sim 2492$  d

later than when first discovered by Van Dyk et al. (2015) in 2014. A detailed analysis of the echo and its evolution is beyond the scope of this paper.

#### 4.9. SN 2013df

SN 2013df is an SN IIB in NGC 4414 and was first studied in detail by Van Dyk et al. (2014), who also identified its yellow supergiant progenitor. Morales-Garoffolo et al. (2014), Maeda et al. (2015), and Szalai et al. (2016) performed additional optical and near-IR follow-up observations. It was established early that SN 2013df strongly resembled SN 1993J (Section 4.2), both in SN and progenitor properties. The radio and X-ray emission from the SN (Kamble et al. 2016), together with the late-time ( $\sim 670$  d) optical spectral characteristics (Maeda et al. 2015), were indicative of circumstellar interaction.

We pinpointed the exact location of SN 2013df by comparing directly with *HST* observations from 2013 July 15 (GO-12888; PI S. Van Dyk), when the SN had  $m_{F555W} = 16.15 \pm 0.01$  mag. As one can see from Figure 9, the SN was clearly detected in our Snapshot images from 2021 February 15, both in F336W and F555W, 2811 d (7.7 yr) after discovery. That the SN is still relatively bright in F336W indicates that the interaction was still ongoing at the time of our observations. The brightness in F555W is likely dominated within the bandpass by continued luminous  $H\alpha$  emission, as well as less prominent He I/Na I emission, as seen in the late-time spectra (Maeda et al. 2015). In the figure we have overlaid the F336W light curve of SN 1993J (see Section 4.2) on the light curve of SN 2013df in this same band. As one can see, the two agree amazingly well, which would imply that, based on the photometric evolution over more than 2800 d (7.7 yr), SN 2013df is essentially a twin of SN 1993J, as the early-time data, including the progenitor identification, tended to indicate as well.

#### 4.10. SN 2013ej

SN 2013ej in M74 has been considered an atypical SN II, possibly an SN II-P/II-L hybrid (Mauerhan et al. 2017). A number of investigators have observed and analyzed the SN; see Van Dyk et al. (2023) and references therein. Early-time monitoring was also undertaken by KAIT; see de Jaeger et al. (2019). Our *HST* Snapshots were obtained in F555W and F814W on 2021 August 19, 2948 d (8.1 yr) after discovery. The location of the SN in our data was established based on Mauerhan et al. (2017, their Figure 11); see Figure 10. The SN 2013ej light curves in both bands have flattened out significantly at late times, showing essentially no decline in

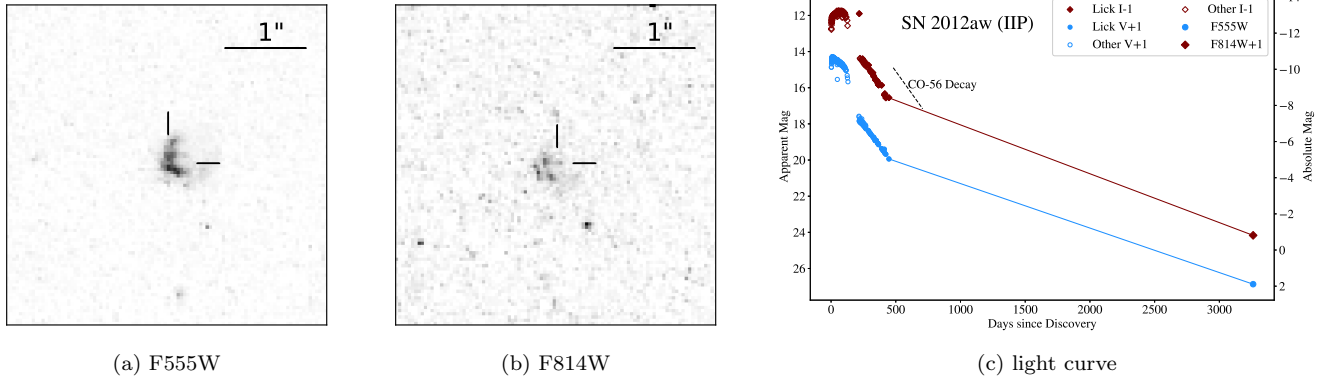
brightness ( $< 1$  mag decline in both F555W and F814W) over more than 2000 d (5.5 yr). Van Dyk et al. (2023), based on the brightness of the SN in these Snapshot data, concluded that the progenitor identified by Fraser et al. (2014) had vanished (confirming an earlier inference made by Mauerhan et al. 2017).

Technically, we covered the field again in bands F438W ( $\sim B$ ) and F625W when we observed AT 2019krl (see Section 4.32); however, unfortunately the SN 2013ej site fell within the chip gap for both of those bands.

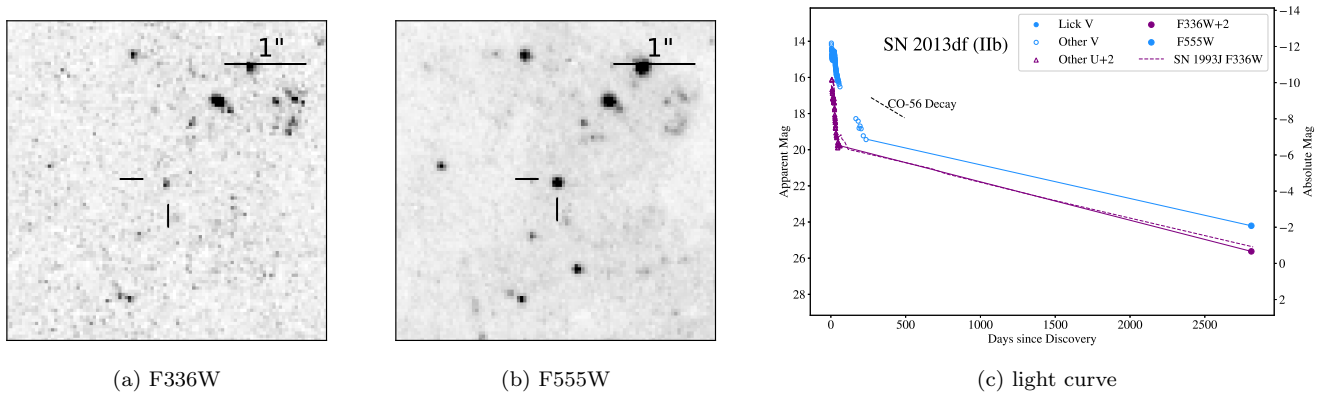
#### 4.11. SN 2014C

SN 2014C in NGC 7331 is a fascinating event, having been classified soon after explosion as an SN Ib (without H) and, after  $\sim 1$  yr, exhibited distinct and strong signs of circumstellar interaction, similar to an SN IIn, with strong  $H\alpha$  emission (e.g., Milisavljevic et al. 2015). From radio and X-ray monitoring Margutti et al. (2017) inferred that the progenitor star had ejected a massive ( $\sim 1 M_{\odot}$ ) H shell decades to centuries before explosion, and that possibly as many as  $\sim 10\%$  of all SN Ib progenitors might experience a similar history. Brethauer et al. (2022) have since interpreted that the shell, with as much as  $\sim 2 M_{\odot}$ , has a radius of  $\sim 2 \times 10^{16}$  to  $\sim 10^{17}$  cm. Milisavljevic et al. (2015) identified in pre-explosion F658N *HST* imaging a luminous  $H\alpha$  source at the SN’s position, which they inferred was a stellar cluster that was home to the progenitor. Sun et al. (2020) performed a detailed analysis of this cluster and estimated an age for it of  $\sim 20$  Myr, which they found consistent with a  $\sim 11 M_{\odot}$  star stripped partially of its envelope via mass transfer with a companion in a relatively wide binary system, followed by an eruptive ejection of the remaining H prior to explosion.

We located the SN in our Snapshot images obtained in F336W and F625W on 2021 August 20 (2786 d  $\approx 7.6$  yr after discovery), using *HST* data obtained in 2016 October for program GO-14668 (PI A. Filippenko); see Figure 11. We intentionally selected the F336W band, to sample any late-time UV emission from the SN, and F625W, to sample  $H\alpha$  emission, both being indicators of ongoing interaction. Zheng et al. (2022) undertook early-time optical monitoring with KAIT, during the “Ib” phase of the SN, prior to the onset of strong interaction, and we combine that photometry here with our Snapshots and other available late-time *HST* data. What can be seen in the figure is the contribution to the light curves from the circumstellar interaction and that the UV emission, in particular, has declined somewhat in strength since day  $\sim 1500$ . This behavior would be consistent with the decline in the observed X-ray luminosity after day  $\sim 1000$  (Brethauer et al. 2022).



**Figure 8.** A portion of the WFC3 image mosaic containing SN 2012aw, from observations on 2021 February 17, in (a) F555W and (b) F814W. One can also clearly see the light echo surrounding the SN. Also shown are the Lick (de Jaeger et al. 2019) *V* and *I* (c) light curves, along with (“Other”) data in these bands from Spogli et al. (2020), Bose et al. (2013), and Dall’Ora et al. (2014), together with the Snapshot detections.



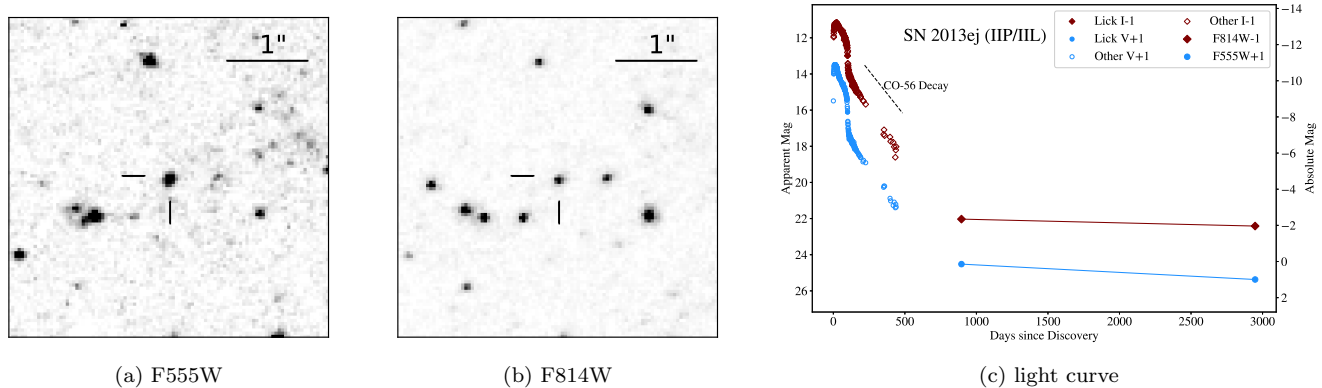
**Figure 9.** A portion of the WFC3 image mosaic containing SN 2013df, from observations on 2021 February 15, in (a) F336W and (b) F555W. Also shown is the Lick + RATIR (Van Dyk et al. 2014) *V* (c) light curve, along with (“Other”) data in *U* and *V* from Morales-Garoffolo et al. (2014) and Szalai et al. (2016), together with the Snapshot detections. Furthermore, we have overlaid, by adjusting in time and in magnitude, the F336W light curve (dashed line) of SN 1993J (Section 4.2) on the F336W curve of SN 2013df.

#### 4.12. SN 2015cp

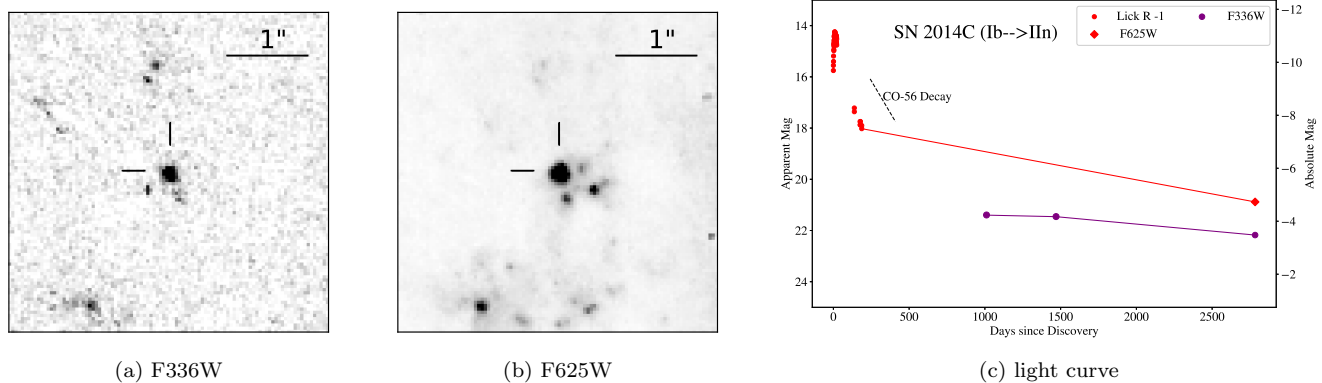
SN 2015cp (also known as PS15dpq), in a host at  $z \approx 0.04$ , was originally classified as a “91T-like” over-luminous SN Ia at  $\sim 40$  d post-peak, but was shown to be experiencing circumstellar interaction at 681 d after explosion, based on a near-UV (NUV) *HST* detection (Graham et al. 2019 and references therein). Harris et al. (2018), based on radio and X-ray follow-up observations of this “SN Ia-CSM,” constrained the total circumstellar mass at  $< 0.5 M_{\odot}$ . Graham et al. (2019) estimated constraints on the inner radius of the CSM of  $R_{\text{CSM}} > 10^{16}$  and  $< 10^{17}$  cm. There was little early-time optical follow-up photometry of the SN, beyond a minimal iPTF light curve in the *g* and *R* bands.

Our Snapshot observations were obtained on 2020 November 30 (1798 d  $\approx 4.9$  yr after discovery) in

F275W (NUV) and F625W. We first rereduced with *Astrodrizzle* (STSCI Development Team 2012) and *Dolphot* the *HST* F275W image (858 s) from Graham et al. (2019; GO-14779, PI M. Graham) and confirmed the detection of the SN, at  $m_{\text{F275W}} = 23.25 \pm 0.08$  mag (in this case, Vega mag, whereas Graham et al. 2019 present the brightness in AB mag). We used the resulting mosaic to isolate the location of SN 2015cp in our Snapshot mosaics. As can be seen in Figure 12 the SN was not detected to a limit of 25.1 and 27.2 mag in F275W and F625W, respectively. The upper limit to detection in F275W implies that the SN shock may have ceased interacting with the CSM some time between 681 d and 1798 d, when our Snapshots were executed (at least to the detection depth of our F275W data). If we assume that the SN shock expanded through the CSM at  $\sim 2000$  km s $^{-1}$  (Graham et al. 2019), then we



**Figure 10.** A portion of the WFC3 image mosaic containing SN 2013ej, from observations on 2021 August 19, in (a) F555W and (b) F814W. Also shown are the Lick (de Jaeger et al. 2019)  $V$  and  $I$  (c) light curves, along with (“Other”) data from Richmond (2014), Bose et al. (2015), Huang et al. (2015), Dhungana et al. (2016), Yuan et al. (2016), and Mauerhan et al. (2017), together with the Snapshot detections.



**Figure 11.** A portion of the WFC3 image mosaic containing SN 2014C, from observations on 2021 August 20, in (a) F336W and (b) F625W. Also shown is the Lick (Zheng et al. 2022)  $R$  (c) light curve, together with measurements from late-time F336W observations by Sun et al. (2020, which were originally from our previous Snapshot programs GO-14668 and GO-15166, PI A. Filippenko), as well as our Snapshot detections.

can place a limit on the outer radius of the CSM at  $\lesssim 3.1 \times 10^{16}$  cm based on our nondetection.

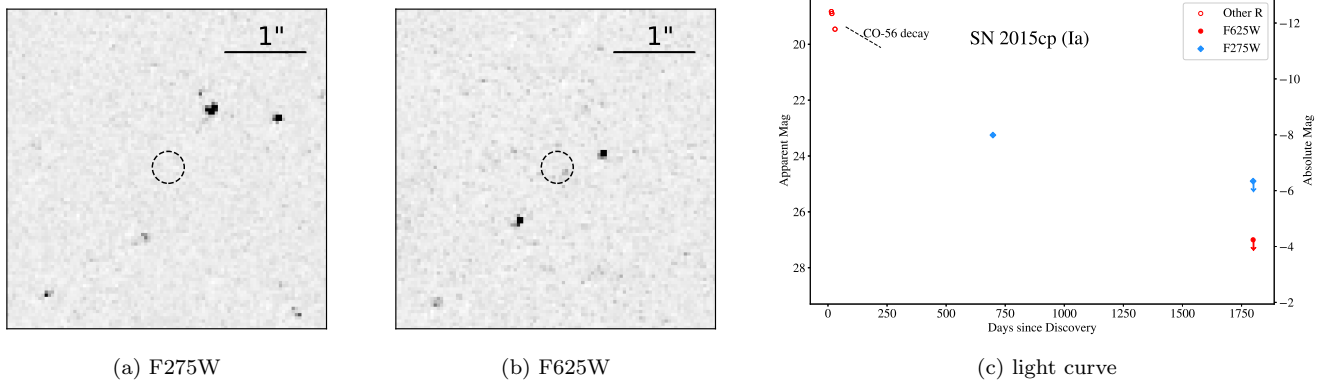
#### 4.13. SN 2016G

SN 2016G in NGC 1171 was classified as a broad-lined SN Ic (Ic-BL) by Zhang & Wang (2016). Zheng et al. (2022) conducted early-time, multiband optical monitoring of the SN with KAIT. Our Snapshot observations were obtained on 2020 December 20, 1807 d (5.1 yr) after discovery, in F555W and F814W. We attempted to locate the SN in the *HST* data astrometrically aligning to the ground-based KAIT images from 2016 February. The SN was not detected in either *HST* band; see Figure 13. It appears from our data that the SN may have been located in a dust lane within the host galaxy, possibly complicating our recovery of the SN at late times; the  $B - V$  color curve for SN 2016G in Zheng et al. (2022) implies that the SN may have experienced significant

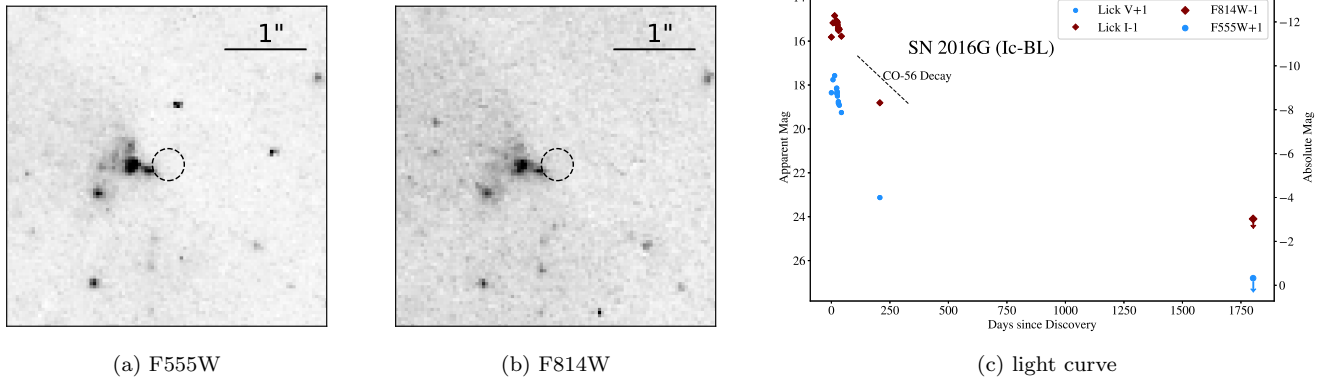
internal reddening (also consistent with the lack of detection of the SN in early times in the UV with *Swift*; Campana & Margutti 2016).

#### 4.14. SN 2016adj

SN 2016adj in NGC 5128 (Centaurus A) is certainly one of the nearest SNe (at 3.42 Mpc) of any type in recent years. The object was classified as a core-collapse SN, potentially with a stripped-envelope progenitor, with a C-rich SN Ic classification inevitably proposed (Stritzinger et al. 2023). It became readily apparent at early stages that SN 2016adj was heavily reddened ( $A_V \approx 2-4$  mag) by internal host dust (Stritzinger et al. 2016). In time it also became obvious that there was, at first, one (Sugerman & Lawrence 2016) and then several prominent light echoes apparent around the SN (Stritzinger et al. 2022).



**Figure 12.** A portion of the WFC3 image mosaic containing SN 2015cp, from observations on 2020 November 30, in (a) F275W and (b) F625W. The SN was not detected in either band; the site is indicated by the dashed circle. Also shown is the iPTF *R* (c) light curve (adjusted from AB mag to Vegamag) and our rereduction of the *HST* F275W detection on 2017 September 12 from [Graham et al. \(2019\)](#), together with our Snapshot upper limits.



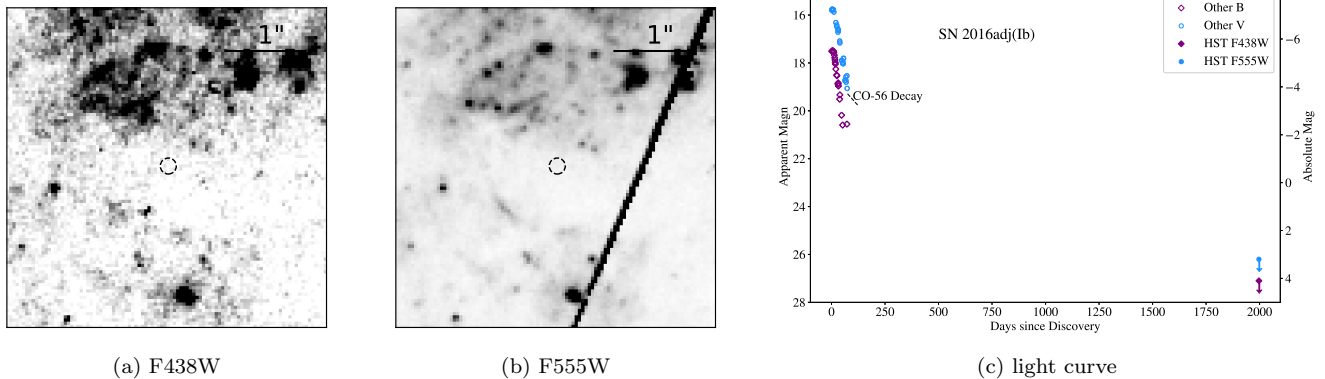
**Figure 13.** A portion of the WFC3 image mosaic containing SN 2016G, from observations on 2020 December 20, in (a) F555W and (b) F814W. As the SN was not detected in either band, its location is denoted by the dashed circle. Also shown are the Lick ([Zheng et al. 2022](#)) *V* and *I* (c) light curves, together with the Snapshot upper limits.

We observed the SN as part of our Snapshot program on 2021 July 28, 1998 d (5.5 yr) after discovery, in F438W and F555W. The former band was chosen intentionally to capture the blue light from the echoes, whereas the latter was used to establish the echo colors. We found the precise position of the SN in our *HST* data comparing with images obtained on 2016 February 22 for GO-14115 (PI S. Van Dyk) in F438W and F814W; see Figure 14. The SN was not detected in the current Snapshots, at 27.4 and 26.5 mag in F438W and F555W, respectively. The echoes, however, are quite prominent (see also [Stritzinger et al. 2022](#), who used our Snapshot data as well in their work). A detailed analysis of the light echoes is beyond the scope of this paper.

#### 4.15. SN 2016bkv

SN 2016bkv is an exceptional example of a low-luminosity SN II-P, with an extraordinarily long plateau

phase ( $\gtrsim 140$  d) and very low expansion velocities, in addition to a strong initial bump in the light curve, as well as “flash-ionization” features, all signs of short-lived, early-time circumstellar interaction ([Nakaoka et al. 2018](#); [Hosseinzadeh et al. 2018](#)). [Nakaoka et al. \(2018\)](#) concluded that the progenitor mass-loss rate within a few years of explosion was quite high,  $\sim 1.7 \times 10^{-2} M_{\odot} \text{ yr}^{-1}$  (although see [Deckers et al. 2021](#)), possibly indicating that the star had experienced a violent outburst. [Hosseinzadeh et al. \(2018\)](#) further suggested that SN 2016bkv is an example of an electron-capture (EC) SN. Through radiative-transfer modeling of the spectra, [Deckers et al. \(2021\)](#) inferred an odd surface composition for the progenitor, implying that it was more likely a binary rather than a single star, with the primary either accreting unprocessed material from its companion or undergoing a merger before explosion.



**Figure 14.** A portion of the WFC3 image mosaic containing SN 2016adj, from observations on 2021 July 28, in (a) F438W and (b) F555W. The SN was not detected in either band; the site is indicated by the dashed circle. What is most obvious in both bands are the light echoes around the SN site; see also [Stritzinger et al. \(2022\)](#). Also shown are (“Other”) *B* and *V* (c) light-curve data ([Stritzinger et al. 2023](#)), together with our upper limits. We see a diffraction spike going straight through the F555W image, but it does not affect the SN site.

Our Snapshot data were obtained on 2020 December 13, 1721 d (4.7 yr) after discovery, in F555W and F814W. The location of the SN was pinpointed by referring to early-time *HST* F555W data from 2016 April 14 (GO-14115, PI S. Van Dyk), when the SN was at  $m_{F555W} = 16.06 \pm 0.01$  mag. The SN was still clearly detected in our Snapshots in both bands; see Figure 15.

#### 4.16. AT 2016blu

AT 2016blu, also known as NGC 4559-OT1, PSN J12355230+2755559, and Gaia16ada, was actually discovered by the Lick Observatory Supernova Search earlier, in 2012 ([Kandrashoff et al. 2012](#)), and classified as a luminous blue variable (LBV) or SN impostor (see also [Sheehan et al. 2014](#)). The object is highly variable and has been “rediscovered” a number of times over the years thereafter (e.g., [Vinokurov et al. 2021](#)) — hence, the multiple identifiers for the same object. Not long after discovery, [Van Dyk et al. \(2012a\)](#) identified a possible precursor in *HST* images from 2005 and, based on preliminary photometry, estimated that the star had  $M_V = -9.4$  mag with intrinsic colors  $B - V = 0.10$  and  $V - I = 0.36$  mag, consistent with an early-F spectral type. [Aghakhanloo et al. \(2022b\)](#) recently conducted an analysis of the recurring outbursts from the transient. They found a periodicity to the outbursts, and proposed that AT 2016blu is probably an LBV in an eccentric interacting binary very much like SN 2000ch.

Our *HST* program obtained observations on 2021 February 17 (3320 d since discovery) in F606W and F814W. The F606W band was used rather than F555W, expressly in order to probe the TRGB for estimation of the distance to the host galaxy (NGC 4559; however, [McQuinn et al. 2017](#) had already performed a TRGB

analysis, with different *HST* data, and found a distance of 8.91 Mpc).

We pinpointed the AT’s location by astrometrically aligning with KAIT ground-based data from 2016 April, as well as precursor *HST* images from 2005 March (GO-10214, PI R. Soria). AT 2016blu is still strongly detected in our Snapshot images in both bands (see Figure 16).

#### 4.17. SN 2016coi

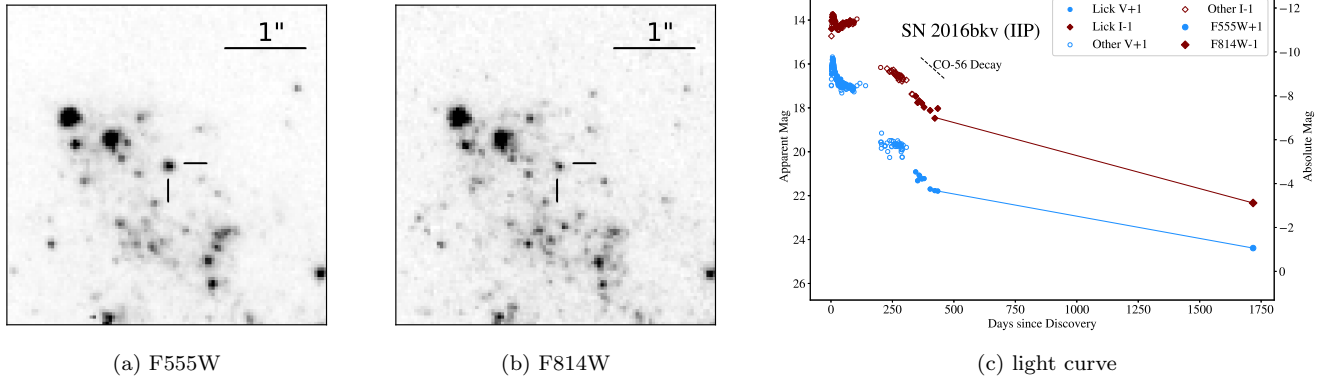
SN 2016coi (ASASSN-16fp) in UGC 11868 is an SN Ic-BL, or possibly a transitional event between a normal and broad-lined SN Ic, with evidence for some residual He — extensive multiwavelength follow-up observations were performed by [Yamanaka et al. \(2017\)](#), [Kumar et al. \(2018\)](#), [Prentice et al. \(2018\)](#), [Terreran et al. \(2019\)](#), and [Tsvetkov et al. \(2020\)](#). Early-time photometry was obtained with KAIT as well ([Zheng et al. 2022](#)).

Our Snapshot observations of the SN were executed on 2020 December 6, 1655 d (4.5 yr) after discovery, in F336W and F814W. In order to pinpoint the SN location in the Snapshots, we compared with *HST* data from 2016 October 4 for our previous Snapshot program GO-14668 (PI A. Filippenko), when the younger SN was at  $m_{F555W} = 16.79 \pm 0.01$  and  $m_{F814W} = 16.18 \pm 0.01$  mag. The SN was not detected in our late-time Snapshots, to limits of 26.1 and 26.0 mag in F336W and F814W, respectively; see Figure 17.

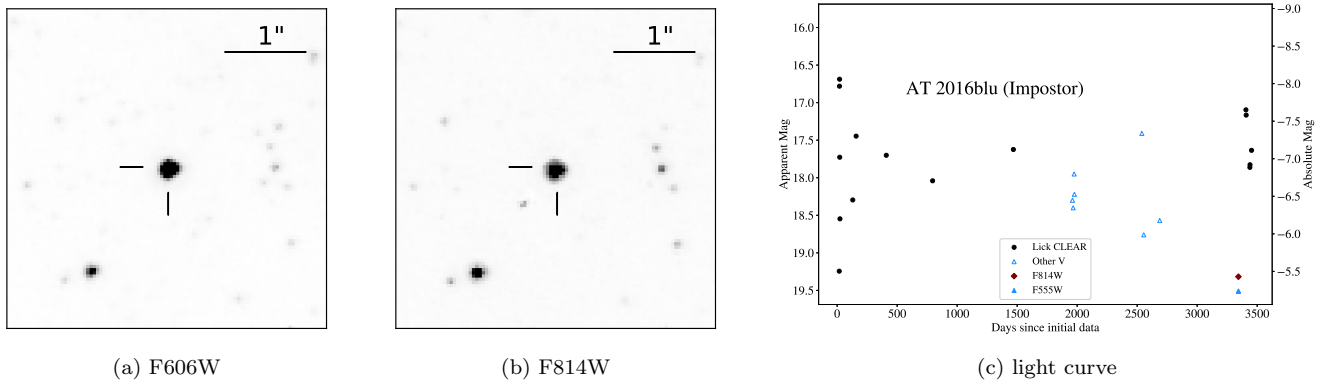
#### 4.18. SN 2016coj

SN 2016coj in NGC 4125 was discovered on 2016 May 28 with KAIT and was subsequently classified as a normal SN Ia ([Zheng et al. 2017](#)). [Richmond & Vietje \(2017\)](#) and [Stahl et al. \(2019\)](#) have presented further optical multiband follow-up photometry.





**Figure 15.** A portion of the WFC3 image mosaic containing SN 2016bkv, from observations on 2020 December 13, in (a) F555W and (b) F814W. Also shown are previously unpublished Lick  $V$  and  $I$  (c) light curves, along with (“Other”) data including upper limits from Nakaoka et al. (2018) and Hosseinzadeh et al. (2018), together with the Snapshot detections.



**Figure 16.** A portion of the WFC3 image mosaic containing AT 2016blu, from observations on 2021 February 17, in (a) F606W and (b) F814W. Also shown is the Lick “clear” (unfiltered) and  $V$  (Aghakhanloo et al. 2022b) (c) light curves, together with the Snapshot detections in the two *HST* bands.

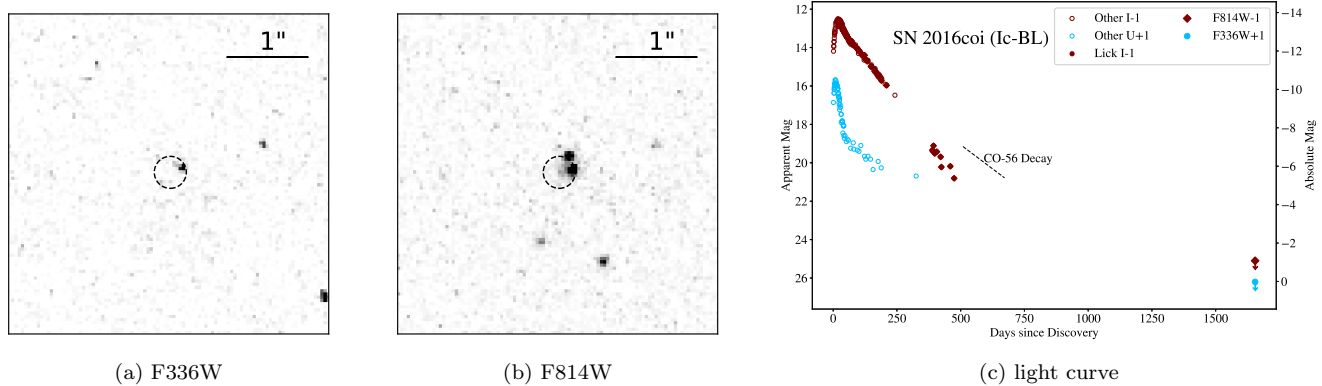
The Snapshot observations occurred on 2020 December 9, 1656 d (4.5 yr) after discovery, in F555W and F814W. The location of the SN was pinpointed using *HST* data from 2017 December 25 as part of our previous Snapshot program GO-15166 (PI A. Filippenko), when SN 2016coj was at  $m_{F555W} = 24.20 \pm 0.04$  and  $m_{F814W} = 23.46 \pm 0.07$  mag. The SN was not detected in the current Snapshots to limits of 26.8 and 25.5 mag in F555W and F814W, respectively.

#### 4.19. SN 2016gkg

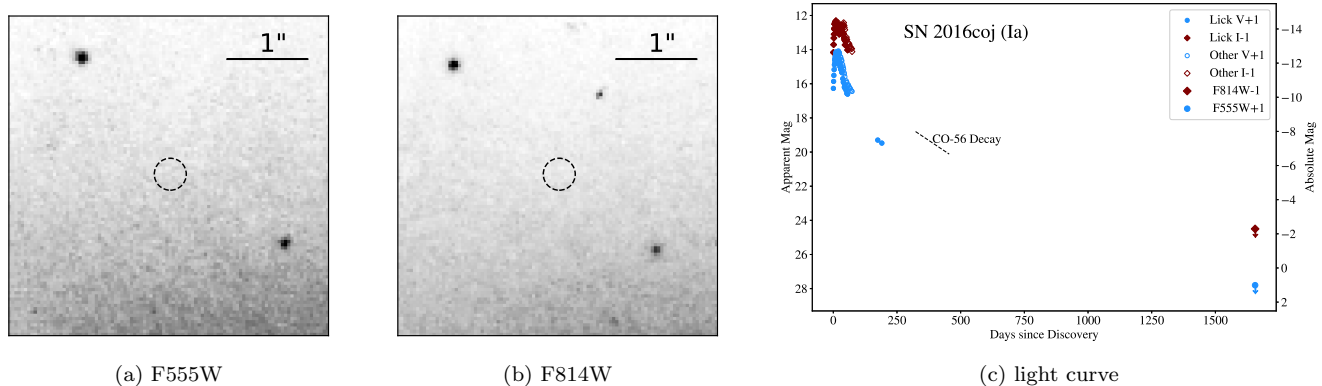
SN 2016gkg in NGC 613 is an SN IIb with properties that are intermediate between those of SN 1993J (Section 4.2 and SN 2011dh (Section 4.6; Tartaglia et al. 2017b). Both Arcavi et al. (2017) and Piro et al. (2017) modeled the first cooling peak of the SN to infer properties of the progenitor. Tartaglia et al. (2017b) and Kilpatrick et al. (2017) independently identified a progenitor candidate in pre-explosion *HST* images. Bersten et al. (2018) also identified and characterized the pro-

genitor, as well as the SN itself (which included KAIT photometry, enhanced with further data by Zheng et al. 2022).

The *HST* Snapshots were obtained on 2021 August 19, 1795 d (4.9 yr) after discovery, in F438W and F606W. The SN location was found using *HST* data taken 2016 October 10 for GO-14116 (PI S. Van Dyk), when the SN was young and bright, at  $m_{F555W} = 15.11 \pm 0.01$  mag. Kilpatrick et al. (2022) revisited the SN and, using our Snapshots found that  $m_{F606W} = 25.10 \pm 0.07$  and  $m_{F438W} = 26.61 \pm 0.27$  mag. Our results differ from these, with  $m_{F606W} = 24.95 \pm 0.04$  and  $m_{F438W} > 26.1$  mag. We can potentially ascribe the discrepancy in F606W as due to differences in assumed DoPhot input parameters; however, as can be seen in Figure 19, the SN is clearly not visually detected at F438W. Based on our results, Van Dyk et al. (2023) concluded that the progenitor candidate had vanished. The behavior



**Figure 17.** A portion of the WFC3 image mosaic containing SN 2016coi, from observations on 2020 December 6, in (a) F336W and (b) F814W. The SN was not detected in either band; the site is indicated by the dashed circle. Also shown is the Lick (Zheng et al. 2022)  $I$  (c) light curve, along with (“Other”) data in  $I$ , as well as  $U$ , from Kumar et al. (2018), Terreran et al. (2019), Prentice et al. (2018), and Tsvetkov et al. (2020), together with the Snapshot upper limits.



**Figure 18.** A portion of the WFC3 image mosaic containing SN 2016coj, from observations on 2020 December 9, in (a) F555W and (b) F814W. The SN was not detected in either band; the site is indicated by the dashed circle. Also shown are the Lick (Stahl et al. 2019)  $V$  and  $I$  (c) light curves, along with (“Other”) data from Richmond & Vietje (2017), together with the Snapshot upper limits.

of the late-time light curve in F606W implies that CSM interaction may be a source of additional power.

#### 4.20. AT 2016jbu

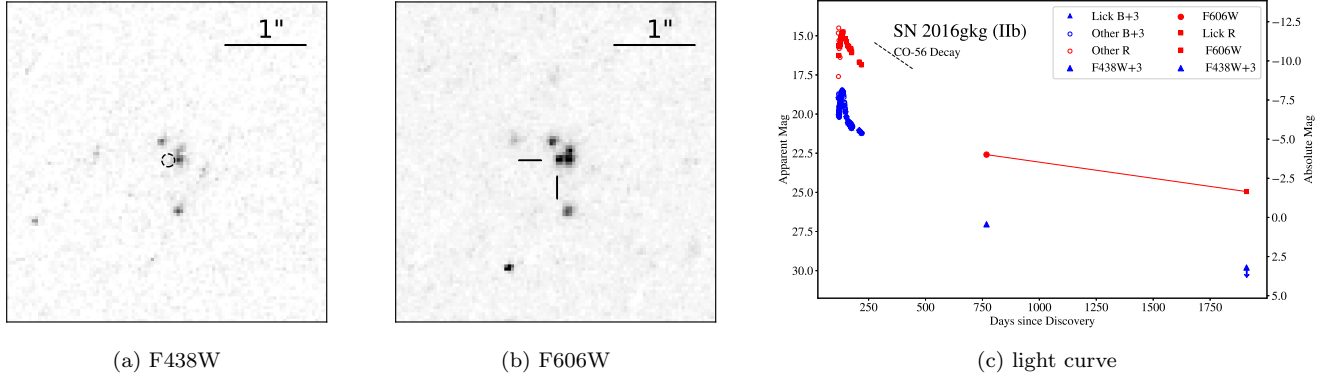
AT 2016jbu (Gaia16cfr) in NGC 2442 has been considered since early after discovery to be an SN impostor, although it has been argued that it should actually be considered a pre-explosion LBV (Kilpatrick et al. 2018b) or simply an interacting, SN 2009ip-like transient (Brennan et al. 2022b). Both Kilpatrick et al. (2018b) and Brennan et al. (2022c) independently identified in pre-outburst *HST* images and subsequently characterized the precursor: a massive ( $\sim 22\text{--}30 M_{\odot}$ ) yellow supergiant enshrouded by a dusty circumstellar shell.

The object was detected in our Snapshots in F555W and F814W on 2021 August 21, 1725 d (4.7 yr) after discovery. We isolated the location of the object using *HST* data obtained on 2019 March 21 for our previ-

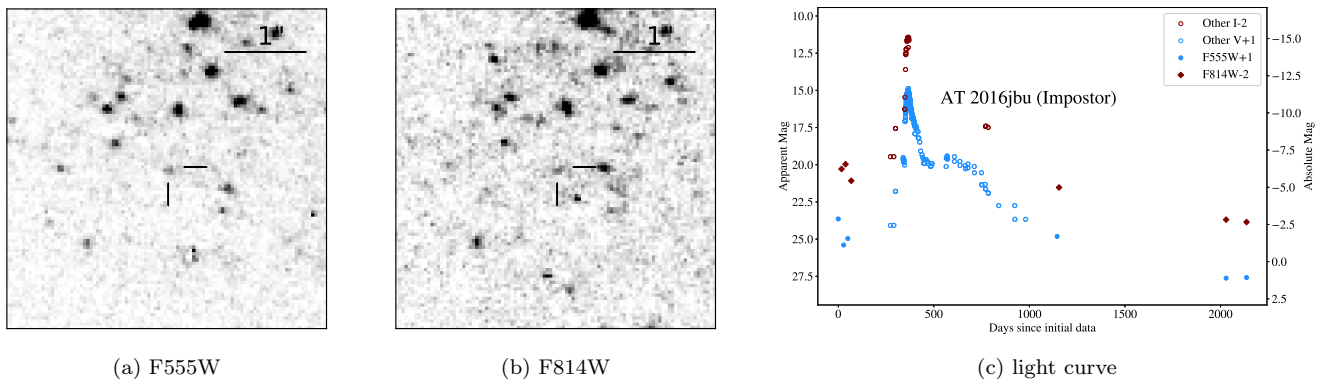
ous Snapshot program GO-15166 (PI A. Filippenko), together with finder charts from the ensemble of *HST* observations presented by Brennan et al. (2022c); see Figure 20. Brennan et al. (2022a) also obtained multi-band *HST* observations of AT 2016jbu on 2021 December 6, only 107 d later, and discovered that the observed brightness of the transient was less than the precursor levels. Those authors further found that it was difficult to explain this dimming in terms of increasing dust obscuration and therefore concluded that the precursor had likely vanished — thus, AT 2016jbu may have actually been a terminal explosion. Our Snapshot data also confirm the dimming and precursor disappearance.

#### 4.21. SN 2017cfd

SN 2017cfd in IC 511 was discovered on 2017 March 16 with KAIT and classified as a normal SN Ia (Han et al.



**Figure 19.** A portion of the WFC3 image mosaic containing SN 2016gkg, from observations on 2021 August 19, in (a) F438W and (b) F606W. The SN is detected in F606W, as indicated by tick marks, but not detected in F438W; the site in that band is indicated by the dashed circle. Also shown are the Lick (Bersten et al. 2018; Zheng et al. 2022)  $V$  and  $I$  (c) light curves, along with (“Other”) data from Tartaglia et al. (2017b) and additional previous *HST* and  $B$  data from Kilpatrick et al. (2022), together with the Snapshot detections.



**Figure 20.** A portion of the WFC3 image mosaic containing AT 2016jbu, from observations on 2021 August 21, in (a) F555W and (b) F814W. Also shown are the combined  $V$  (c) and  $I$  (c) light curves from Kilpatrick et al. (2018b) and Brennan et al. (2022a), together with *HST* data from Brennan et al. (2022c), Brennan et al. (2022b), and this paper (the second-to-latest data points).

2020). Stahl et al. (2019) presented further early-time multiband optical monitoring with KAIT.

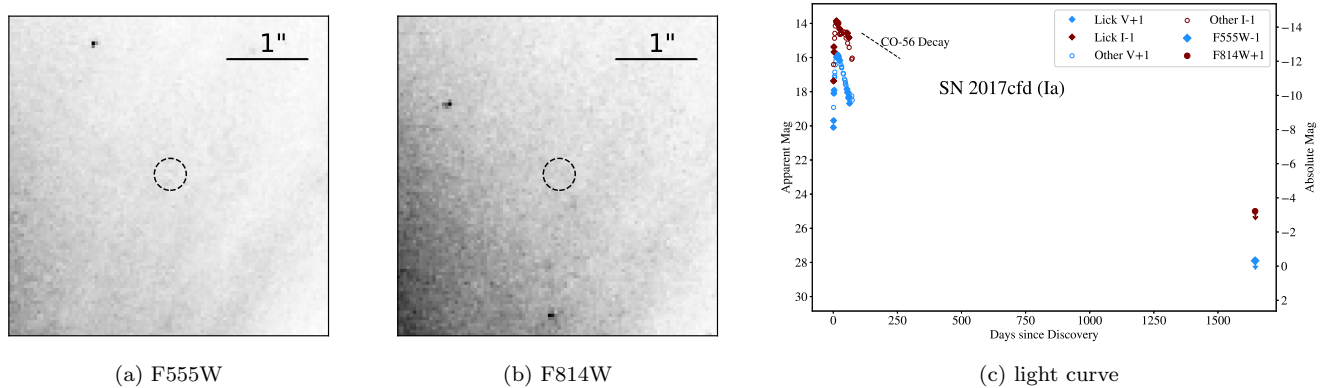
Our Snapshots were obtained on 2021 February 17, 1654 d (4.5 yr) after discovery, in F555W and F814W. We astrometrically aligned ground-based KAIT images from 2017 April with the Snapshot image mosaics, in order to locate the SN position; see Figure 21. The SN was not detected in either of the *HST* bands, to limits of 26.9 and 26.0 mag in F555W and F814W, respectively.

#### 4.22. SN 2017eaw

SN 2017eaw is the tenth SN discovered in the nearby galaxy NGC 6946 and was likely a normal SN II-P of intermediate luminosity (Van Dyk et al. 2019). Buta & Keel (2019), Van Dyk et al. (2019), Szalai et al. (2019b), and Buta & Keel (2019) all undertook extensive optical and near-IR follow-up campaigns. Van Dyk et al. (2019)

pointed out the early “bump” in the light curves, which Morozova et al. (2020) interpreted as CSM set up by a pre-SN outburst  $\sim 50$ – $350$  d induced by a nuclear-burning episode  $\sim 150$ – $450$  d prior to the SN. Furthermore, Weil et al. (2020) found evidence spectroscopically of continued circumstellar interaction at late times. Kilpatrick & Foley (2018), Van Dyk et al. (2019), and Rui et al. (2019) all independently identified in pre-explosion *HST* images and characterized the progenitor candidate for the SN; Van Dyk et al. (2019) modeled the star as a dusty, luminous  $M_{\text{ZAMS}} \approx 15 M_{\odot}$  RSG. Bostroem et al. (2023) suggested that SN 2017eaw may arise from a binary progenitor, based on analysis of the surrounding stellar population.

Snapshots for our program were obtained on 2020 November 11, 1273 d (3.5 yr) after discovery, in F555W and F814W. The location of the SN was confirmed us-



**Figure 21.** A portion of the WFC3 image mosaic containing SN 2017cfd, from observations on 2021 February 17, in (a) F555W and (b) F814W. The SN was not detected in either band; the site is indicated by the dashed circle. Also shown are the Lick (Stahl et al. 2019)  $V$  and  $I$  (c) light curves, along with additional (“Other”; in this case, non-Lick) data from Han et al. (2020), together with the Snapshot upper limits.

ing *HST* images taken 2018 January 5 for GO-15166 (PI A. Filippenko), when the SN was at  $m_{F814W} = 18.62 \pm 0.01$  mag and  $m_{F555W} = 19.83 \pm 0.01$  mag. The SN was still quite bright in the current images; see Figure 22. Based on the change in brightness of the SN in both bands in our Snapshots, relative to pre-SN observations, Van Dyk et al. (2023) concluded that the RSG candidate was indeed the progenitor, and also confirmed the late-time CSM interaction, manifested as a UV excess.

#### 4.23. SN 2017gax

SN 2017gax (DLT17ch) was discovered in NGC 1672 by Tartaglia et al. (2017a) on 2017 August 14. The SN was spectroscopically classified, within a day of discovery, as an SN Ic by Jha et al. (2017). The SN location was established in our F336W and F814W Snapshots from 2020 November 27, 1202 d (3.5 yr) after discovery, using *HST* data from 2017 October 19 (GO-14645, PI S. Van Dyk), when the SN was at  $m_{F555W} = 15.94 \pm 0.01$  mag. The SN was not detected in the Snapshot data in either band; see Figure 23. Unfortunately, no published photometry exists, beyond the report by Maguire et al. (2017) of the SN at  $V = 16.1 \pm 0.1$  mag on 2017 November 9; thus, we are unable to show a light curve for this SN.

#### 4.24. SN2017gkk

SN 2017gkk was discovered in NGC 2748 on 2017 August 19 at 15.6 mag by Balanutsa et al. (2017), and then later rediscovered at 14.7 mag (both unfiltered) by Itagaki (2017). The classification spectrum obtained just days after discovery by Onori (2017) showed it was an SN IIb. The SN was detected in our Snapshot images on 2021 September 24, 1485 d (4.1 yr) after discovery,

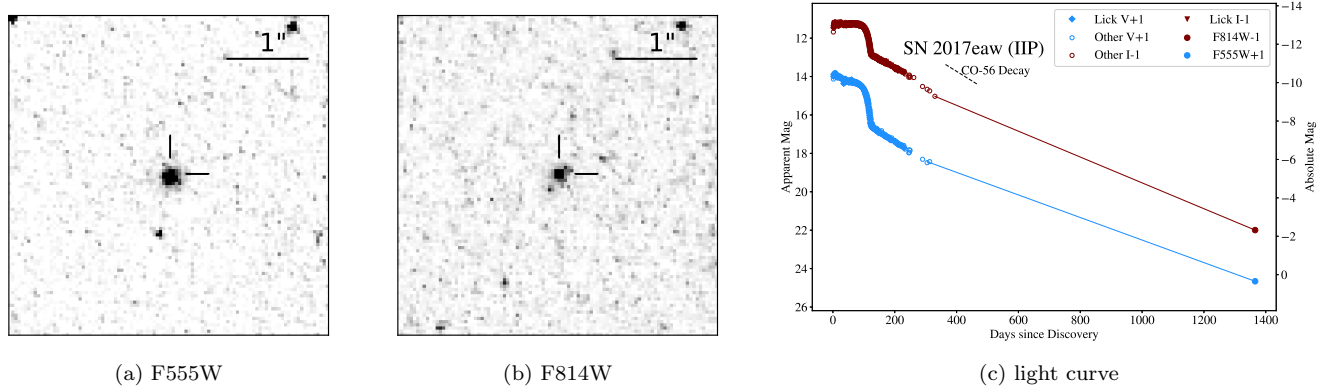
in both F555W and F814W; see Figure 24. The location of the SN was established using data obtained on 2019 February 22 for our previous Snapshot program GO-15166 (PI A. Filippenko), when the SN was at  $m_{F555W} = 23.55 \pm 0.02$  and  $m_{F814W} = 23.10 \pm 0.04$  mag. Limited early-time unfiltered (“clear”;  $\sim R$ ) photometry was obtained with KAIT. The light-curve behavior at late times in both Snapshot bands may imply that CSM interaction is contributing to the SN luminosity.

#### 4.25. SN 2017ixv

SN 2017ixv was discovered in NGC 6796 on 2017 December 17 by Cortini (2017). It was classified shortly thereafter as an SN Ic-BL by Leadbeater (2017). Unfortunately, we are not aware of any published follow-up photometry. SN 2017ixv was not detectable in our F555W and F814W Snapshots from 2021 January 11, 1122 d (3.1 yr) after discovery. We note that the SN site is in an edge-on spiral galaxy, and therefore the exact location is difficult to confirm without any earlier imaging data, owing to the crowded environment. In order to locate the SN, we used the absolute position (Cortini 2017), assuming a  $0''.2$  uncertainty. We further added this in quadrature with a quoted uncertainty of  $0''.03$  in the *Gaia*-based *HST* astrometric grid, and the total uncertainty is reflected in the radius of the dashed circle in Figure 25. Based on this position, it appears that the SN may have been in or near a patch of nebulosity in the host galaxy.

#### 4.26. SN 2018gj

SN 2018gj was discovered in NGC 6217 by Wiggins (2018) on 2018 January 1. It was classified as an SN IIb (and possible II-P) by Bertrand (2018) and as an SN II by Kilpatrick et al. (2018a). Teja et al. (2023) conducted extensive photometric and spectroscopic monitoring of



**Figure 22.** A portion of the WFC3 image mosaic containing SN 2017eaw, from observations on 2020 November 11, in (a) F555W and (b) F814W. Also shown are the Lick (Van Dyk et al. 2019)  $V$  and  $I$  (c) light curves, along with (“Other”) data from Tsvetkov et al. (2018), Szalai et al. (2019b), and Buta & Keel (2019), together with the Snapshot detections.



**Figure 23.** A portion of the WFC3 image mosaic containing SN 2017gax, from observations on 2020 November 27, in (a) F336W and (b) F814W. Nothing is detected in either band at the SN location, which is denoted by the dashed circle. No photometry has been published for this SN, aside from a single  $V$  measurement.

the SN. Previously-unpublished early-time photometric monitoring also exists from KAIT. Our Snapshots were obtained on 2021 January 27, 1109 d (3.0 yr) after discovery. The exact location of the SN was isolated in our *HST* images using data obtained on 2019 May 16 for GO-15151 (PI S. Van Dyk), when the SN was at  $m_{F625W} = 22.43 \pm 0.01$  and  $m_{F814W} = 21.90 \pm 0.01$  mag.

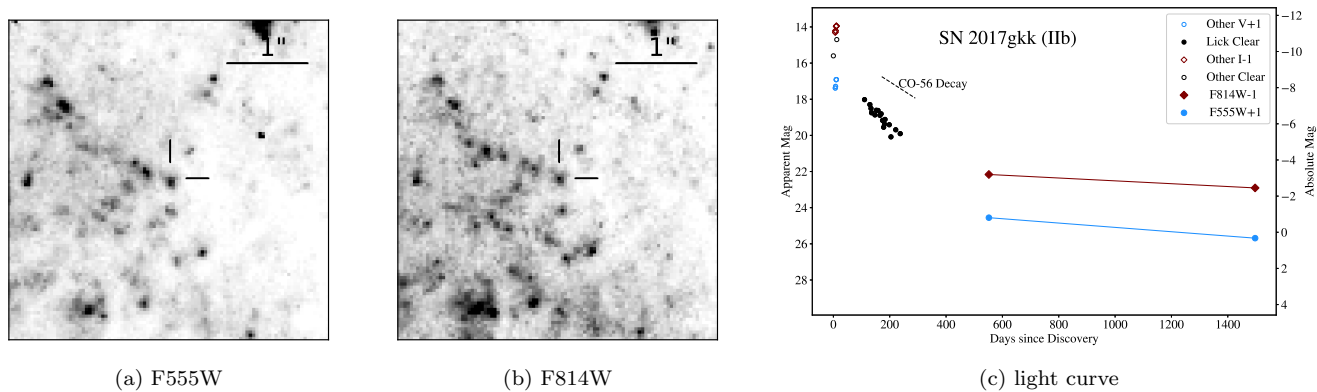
#### 4.27. SN 2018zd

SN 2018zd in NGC 2146 was monitored and analyzed independently by Zhang et al. (2020) and Hiramatsu et al. (2021). Both studies considered the event to be a low-luminosity SN II; however, the latter considered this to be the best example so far for an electron-capture SN, whereas the former found it to have properties more consistent with a normal SN II-P. Both studies found it likely that the progenitor candidate, identified in pre-explosion *HST* images, could have been a super-asymptotic-giant-branch star.

Our F606W and F814W Snapshots were obtained on 2021 February 7, 1074 d (2.9 yr) after discovery. (These two bands, and in particular F606W, were chosen for purposes of estimating a TRGB distance to the host galaxy, which is beyond the scope of this paper.) The location of the SN was isolated using *HST* data obtained on 2019 May 19 for GO-15151 (PI S. Van Dyk; Hiramatsu et al. 2021). The SN was not detected in either band. Van Dyk et al. (2023) took advantage of this fact to conclude that the candidate was indeed the SN 2018zd progenitor.

#### 4.28. SN 2018aoq

SN 2018aoq is a low-luminosity SN II-P. Both O’Neill et al. (2019) and Tsvetkov et al. (2019) undertook photometric monitoring campaigns of the SN, with the latter study including spectral coverage over the first  $\sim 70$  d. Furthermore, based on the available multi-band, pre-explosion *HST* images, O’Neill et al. (2019)



**Figure 24.** A portion of the WFC3 image mosaic containing SN 2017gkk, from observations on 2021 September 24, in (a) F555W and (b) F814W. Also shown is a light curve containing previously unpublished Lick “clear” (unfiltered) (c) points, together with data taken near discovery by Balanutsa et al. (2017), Itagaki (2017), and Vinko et al. (2017), along with our Snapshot detections.



**Figure 25.** A portion of the WFC3 image mosaic containing SN 2017ixv, from observations on 2021 January 11, in (a) F555W and (b) F814W. The SN was not detected in either band; the site is indicated by the dashed circle (the radius of which, in this case, represents the uncertainty in the SN position). No photometry has been published for this SN.

estimated the initial mass of a RSG progenitor candidate at  $\sim 10 M_{\odot}$ .

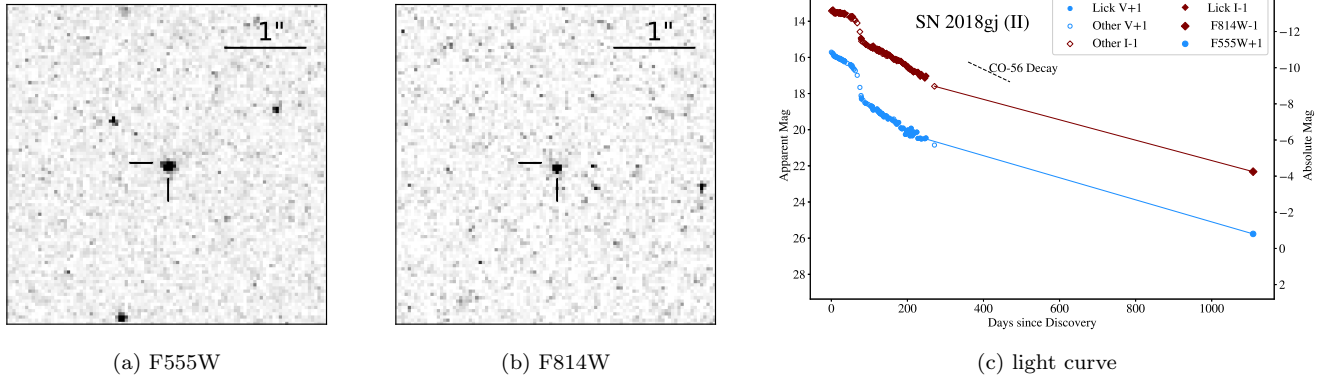
Our Snapshot observations were executed in F555W and F814W on 2020 December 5, 984 d (2.7 yr) after discovery. We located the SN position in the Snapshots using *HST* data from 2018 April 23 (GO-15151; PI S. Van Dyk), when the SN was at  $m_{F555W} = 15.93 \pm 0.01$  mag. SN 2018aoq was not detected in either of our Snapshots. Van Dyk et al. (2023) exploited that fact to conclude that the O’Neill et al. (2019) candidate was indeed the progenitor.

#### 4.29. AT 2018cow

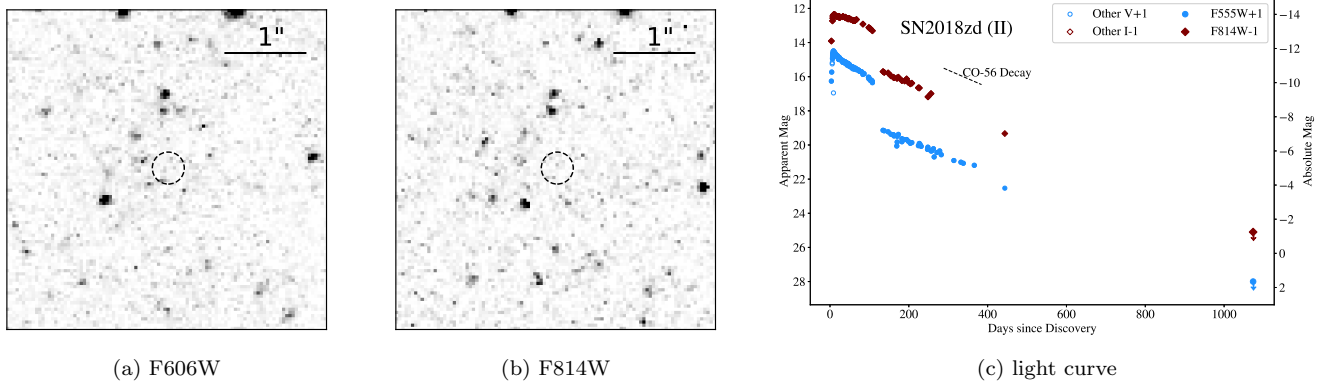
AT 2018cow, in CGCG 137–068 at  $z = 0.0141$ , is a particularly intriguing object. It very rapidly became exceedingly luminous ( $\sim -22$  mag absolute) and blue, and is considered a prototypical “fast blue optical transient,” or FBOT. “The Cow,” as it has been dubbed, stimulated intense interest in the community, leading to

several multiwavelength monitoring campaigns and theoretical analyses, including those of Perley et al. (2019), Margutti et al. (2019), and Xiang et al. (2021). Despite all of the focused effort, the nature of AT 2018cow and its precursor is still not settled. For instance, Fox & Smith (2019) surmised, based on similarities with various interacting SNe, that CSM interaction in a relatively H-depleted system could explain some its observed properties. Chen et al. (2023) concluded that a fading transient UV source persists, which may be from ejecta-CSM interaction or from a central engine, more specifically a precessing accretion disk. Additionally, Inkenhaag et al. (2023) studied the late-time brightness of AT 2018cow and estimated the potential black hole’s mass using our Snapshot data.

Our F555W and F814W Snapshots F555W and F814W were obtained on 2021 July 25, 1134 d (3.1 yr) after discovery. The location of the object was con-



**Figure 26.** A portion of the WFC3 image mosaic containing SN 2018gj, from observations on 2021 January 27, in (a) F555W and (b) F814W. Also shown are unpublished Lick  $V$  and  $I$  (c) light curves, along with (“Other”) data from Teja et al. (2023), together with the Snapshot detections.



**Figure 27.** A portion of the WFC3 image mosaic containing SN 2018zd, from observations on 2021 February 7, in (a) F606W and (b) F814W. The SN was not detected in either band; the site is indicated by the dashed circle. Also shown are  $V$  and  $I$  (c) light curves based on (“Other”) data from Zhang et al. (2020), Hiramatsu et al. (2021), and Callis et al. (2021), together with F555W and F814W data from Hiramatsu et al. (2021) and the Snapshot upper limits.

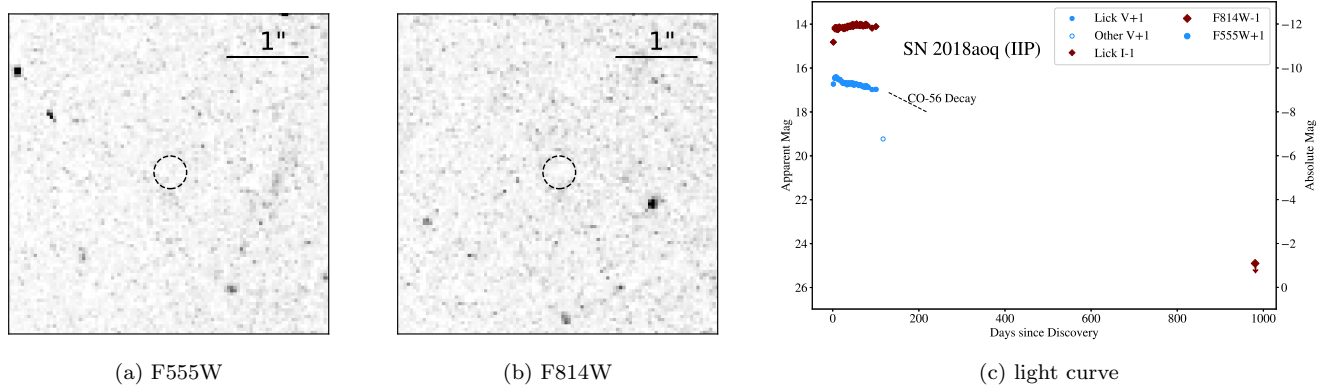
firmed using prior *HST* data taken on 2018 August 6 for GO-15600 (PI R. Foley), as well as from finding charts in prior literature on the object, such as Perley et al. (2019) and Margutti et al. (2019); see Figure 29. Chen et al. (2023) used our Snapshots as part of a larger work, looking at a variety of late-time observations (from 50 to 1423 d post-discovery) to better understand the object. They concluded that the nature of a putative black hole at the center of the accretion disk is still up for debate, given the various intriguing properties of the late-time emission. (Both Sun et al. 2022 and Sun et al. 2023 also made use of our Snapshot data.) The final identity of the precursor object therefore remains unknown.

#### 4.30. SN 2018ivc

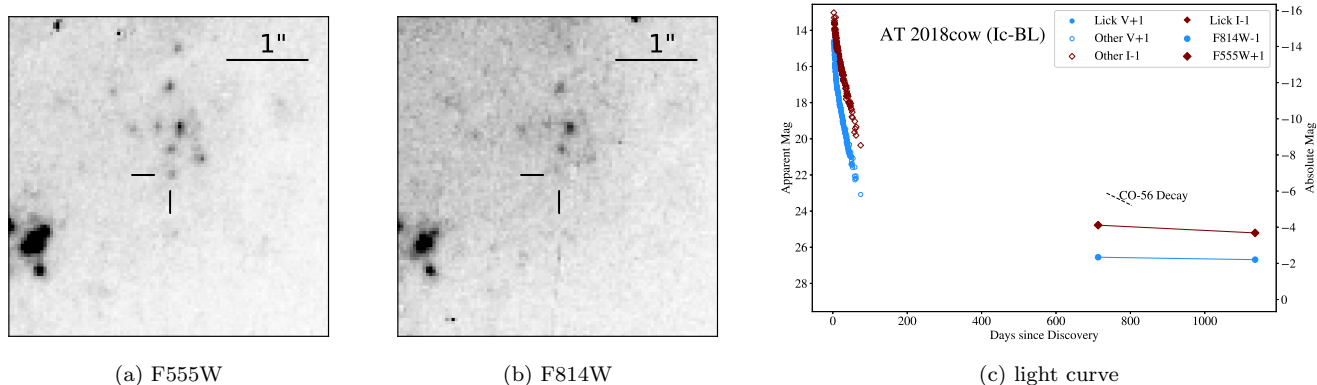
From high-cadence follow-up spectroscopic and photometric observations since discovery, Bostroem et al. (2020) concluded that SN 2018ivc in NGC 1068 is an un-

usual SN II. That study placed limits on the properties of the progenitor, based on available pre-explosion *HST* of this famous Seyfert galaxy. Maeda et al. (2023b) considered SN 2018ivc as a possible variant of SN II-L, with transitional characteristics between II-P and IIb. Interaction of the SN shock with pre-existing wind matter appears to be playing a strong role in the SN’s emission (Maeda et al. 2023b), with origins in a progenitor experiencing an extreme form of binary evolution (Maeda et al. 2023a). The SN was detected in our *HST* F555W and F814W Snapshots obtained on 2020 November 27, 739 d (2.0 yr) after discovery. The SN location was confirmed using *HST* data obtained for GO-15151 (PI S. Van Dyk), in which the SN was at  $m_{F555W} = 20.33 \pm 0.01$  and  $m_{F814W} = 19.03 \pm 0.01$  mag.

#### 4.31. SN 2019ehk



**Figure 28.** A portion of the WFC3 image mosaic containing SN 2018aoq, from observations on 2020 December 5, in (a) F555W and (b) F814W. The SN was not detected in either band; the site is indicated by the dashed circle. Also shown are previously unpublished Lick  $V$  and  $I$  (c) light curves, along with (“Other”) data from O’Neill et al. (2019) and Tsvetkov et al. (2019), together with the Snapshot upper limits.



**Figure 29.** A portion of the WFC3 image mosaic containing AT 2018cow, from observations on 2021 July 25, in (a) F555W and (b) F814W. Also shown are Lick (Zheng et al. 2022)  $V$  and  $I$  (c) light curves, along with (“Other”) data from Perley et al. (2019), Margutti et al. (2019), Xiang et al. (2021), and Tsvetkov et al. (2022), together with the Snapshot detections.

SN 2019ehk in NGC 4321 (M100) has been characterized as a “Ca-rich transient,” possibly evolving from a Type Ib SN, based on photometric and spectroscopic monitoring of the event by Jacobson-Galán et al. (2020; 2021) and Nakaoka et al. (2021). We located the SN 2019ehk site in our Snapshot data using *HST* data from 2020 May for program GO-16075 (PI W. Jacobson-Galán), in which the transient was at  $m_{F555W} = 25.91 \pm 0.09$  mag. However, interestingly, it was not detected in our *HST* F438W and F625W images obtained on 2021 February 21, 665 d (1.8 yr) after discovery; see Figure 31. The detection upper limits are 27.0 and 26.6 mag in F438W and F606W, respectively.

#### 4.32. AT 2019krl

Andrews et al. (2021) characterized the intermediate-luminosity transient AT 2019krl in NGC 628 (M74) as either a relatively unobscured blue supergiant or a more extinguished LBV in eruption. We located the position

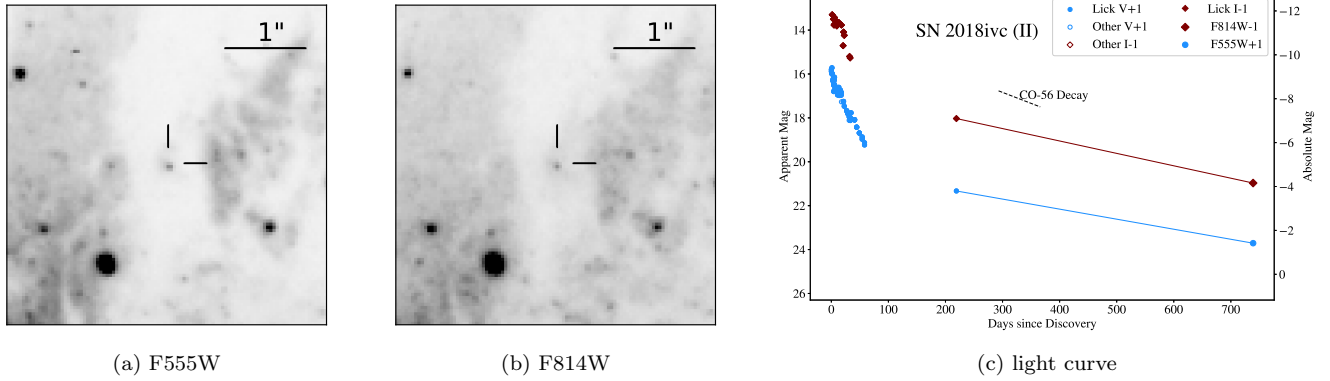
of the transient in our Snapshot images using 2019 *HST* data from GO-15151 (PI S. Van Dyk), in which the AT was at  $m_{F555W} = 21.91 \pm 0.02$  mag. The AT was clearly visible in the more recent F438W and F625W Snapshots from 2021 February 15; see Figure 32.

#### 4.33. SN 2020dpw

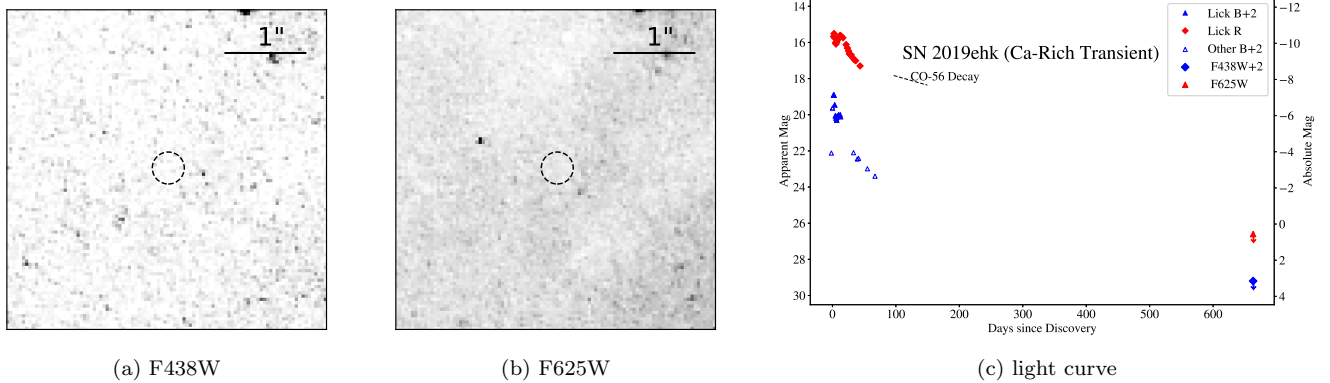
Wiggins (2020) discovered SN 2020dpw in NGC 6951 (based on the discovery position, the host must have been incorrectly reported as NGC 6952) and Kawabata (2020) classified it as an SN II-P. Unfortunately, we have no knowledge of existing early-time photometry, although the SN was easily detected in our *HST* F555W and F814W Snapshots from 2020 December 13, near the reported discovery location 292 d (0.8 yr) after discovery; see Figure 33.

#### 4.34. SN 2020hvp





**Figure 30.** A portion of the WFC3 image mosaic containing SN2018ivc, from observations on 2020 November 27, in (a) F555W and (b) F814W. Also shown are previously unpublished Lick *V* and *I* (c) light curves, along with (“Other”) data from [Bostroem et al. \(2020\)](#); which include F555W and F814W data from GO-15151, PI S. Van Dyk), together with the Snapshot detections.



**Figure 31.** A portion of the WFC3 image mosaic containing SN 2019ehk, from observations on 2021 February 21, in (a) F438W and (b) F625W. The transient was not detected in either band; the site is indicated by the dashed circle. Also shown are previously unpublished Lick *V* and *I* (c) light curves, along with (“Other”) data from [Nakaoka et al. \(2021\)](#) and [Jacobson-Galán et al. \(2021\)](#), together with the Snapshot upper limits.

[Tonry et al. \(2020\)](#) discovered SN 2020hvp in NGC 6118 and [Burke et al. \(2020\)](#) subsequently classified it as an SN Ib. The SN was easily detected near the reported discovery position in the Snapshot images obtained on 2021 May 22, 397 d (1.1 yr) after discovery; see Figure 34. In the figure we complement previously-unpublished early-time photometry obtained with KAIT with the *HST* data.

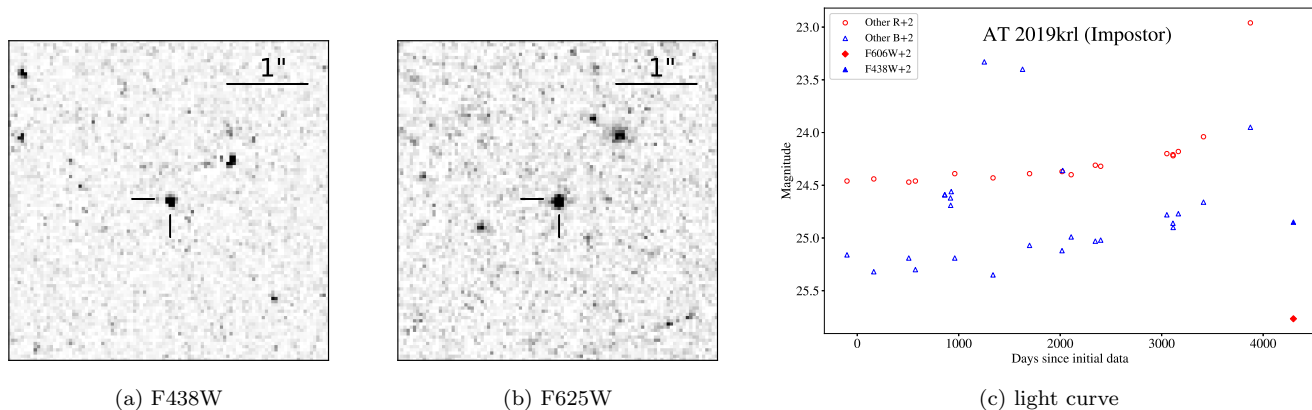
#### 4.35. SN 2020jfo

The SN II-P 2020jfo in NGC 4303 (M61) was monitored by [Sollerman et al. \(2021\)](#), [Teja et al. \(2022\)](#), and [Ailawadhi et al. \(2022\)](#), in which early-time photometry obtained by KAIT was presented. The SN was clearly detected in both Snapshot bands F555W and F814W obtained on 2021 July 28, 449 d (1.2 yr) after discovery; see Figure 35. These *HST* observations were first discussed by [Sollerman et al. \(2021\)](#), as confirmation of

the SN progenitor candidate identification. [Kilpatrick et al. \(2023\)](#) also identified the progenitor through pre-explosion images.

## 5. DISCUSSION AND CONCLUSIONS

We have conducted an analysis of images that we obtained from an *HST* Snapshot survey during Cycle 28 of nearby SNe at late times. We were ultimately able to observe successfully the targeted sites of 31 SNe of various types and 4 SN impostors. The goal of the program was to reveal the possible origins of their late-time emission or lack thereof. Only 2 of the 31 SNe (SN 2020hvp and SN 2020jfo) listed in Table 2 convincingly exhibited lingering emission most likely ascribed to radioactive decay of  $^{56}\text{Co}$ . For 12 of the remaining SNe (indicated by “Yes?” in Table 2) we could not determine the source of the late-time emission, since these events were no longer detectable, and upper limits to their lu-



**Figure 32.** A portion of the WFC3 image mosaic containing AT 2019krl, from observations on 2021 February 15, in (a) F438W and (b) F625W. Also shown are *B* and *R* (“Other”) (c) light curves from Andrews et al. (2021), together with the Snapshot detections.



**Figure 33.** A portion of the WFC3 image mosaic containing SN 2020dpw, from observations on 2020 December 13, in (a) F555W and (b) F814W. No photometry has been published for this SN.

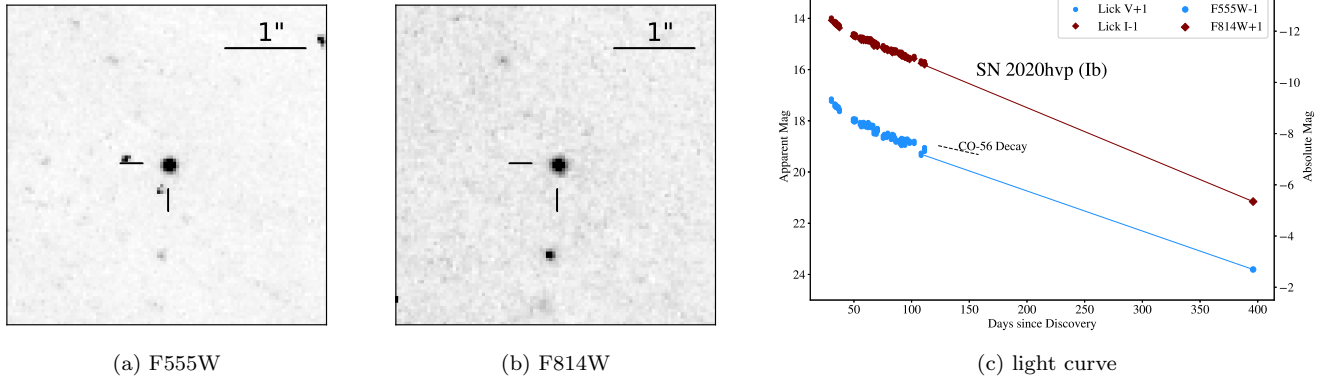
minosities were not sufficiently constraining. All three of the observed SNe Ia fall in this category. For three of the SNe in the observed sample (SN 2017gax, SN 2017ixv, and SN 2020dpw), no early-time photometry was available, and the former two SNe were no longer detectable, so it was not possible to determine whether radioactive decay was powering the light at late times. A remaining 15 SNe were detected; however, it was clear from their extended light curves that the emission was in excess of what we would expect for radioactive decay. We can infer in these cases that the emission may arise, at least in part, from sustained CSM interaction or a light echo, or both. SN 2010jl had exhibited previous indications of CSM interaction, but was no longer detectable in our Snapshot data. It is also worth mentioning the possibility that the sustained late-time luminosity could at least partially be due to radioactive decay of elements with longer lifetimes.

We have also detected the known resolved light echoes around SN 2012aw and SN 2016adj, and we note that

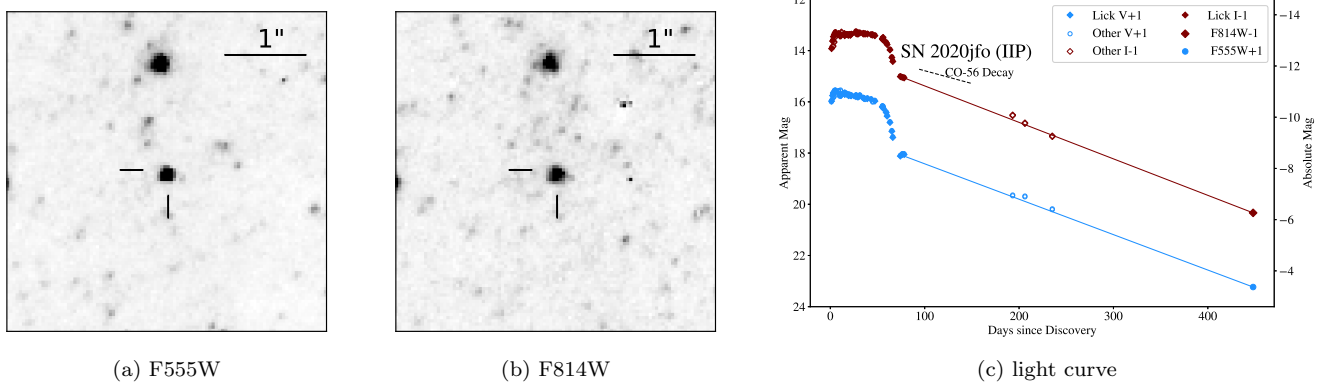
their geometries have evolved since they were first discovered (Van Dyk et al. 2015; Stritzinger et al. 2022).

Of the four events that we consider to be SN impostors, all are still detectable in our Snapshots, implying that their eruptive behavior is persisting even at late times. Note that we have considered SN 2016jbu as an SN impostor, although Brennan et al. (2022a) concluded that the event may have actually been a terminal explosion and that the precursor has vanished.

Whereas we can likely infer from the few observed SNe Ia that their late-time emission was consistent with radioactive decay, for a significant number of core-collapse SNe II, CSM interaction may contribute to the luminosity even as late as  $\sim 10,000$  d. This is not entirely surprising for the SNe II<sub>n</sub> in our sample, and also to some extent for the SNe II<sub>b</sub>, which have largely shown signs of CSM interaction at early times. However, for otherwise-normal SNe II-P, such as SN 2016bvk and SN 2017eaw, the SN shock unexpectedly continues to interact at  $\gtrsim 1000$  d with the pre-existing CSM lost by the



**Figure 34.** A portion of the WFC3 image mosaic containing SN 2020hvp, from observations on 2021 May 22, in (a) F555W and (b) F814W. Also shown are previously unpublished Lick  $V$  and  $I$  (c) light curves, together with the Snapshot detections.



**Figure 35.** A portion of the WFC3 image mosaic containing SN 2020jfo, from observations on 2021 July 28, in (a) F555W and (b) F814W. Also shown are the Lick (Ailawadhi et al. 2022)  $V$  and  $I$  (c) light curves, along with (“Other”) data from Sollerman et al. (2021) and Teja et al. (2022), together with the Snapshot detections.

progenitor prior to explosion. The presence of such interaction provides important information about the extent of the CSM and the duration and nature of the mass loss (which can be further constrained through information gathered from the SN spectrum), with further implications for the evolution of the massive progenitor.

Snapshot surveys, such as ours, can efficiently provide a broad overview of the late-time properties of SNe and SN impostors and represent a reasonable use of valuable *HST* observing time. Approximately 70% of our originally proposed program was actually completed. The only wrinkle is that one has no control over which targets actually get executed, yet developing a relatively comprehensive sample is important in order to obtain a set of statistically significant results. Here we chose to target a large range of object types, to obtain knowledge of the late-time luminosity across a range of events from different astrophysical conditions. However, one could limit the sample to a large number of one particular SN type, nominally arising from a distinct progenitor population.

Such is the case for *HST* programs pointedly targeting samples of SNe Ia (Graham et al. 2019; in Cycle 24) and SNe II (PI C. Kilpatrick in Cycle 30; PI W. Jacobson-Galán in Cycle 31). *HST* Snapshot programs have been executed specifically to detect light echoes at late times around SNe (PI P. Garnavich in Cycle 10, in this case those around SNe Ia).

A number of investigators have already exploited our publicly-available Snapshot data, and we have cited those studies in this paper, including our own spin-off study on disappearing progenitors (Van Dyk et al. 2023). We anticipate that other scientists will find this dataset valuable for their own use in the future, further proving that such surveys possess an archival legacy. To that end, we have examined our data for the possible detection of SNe other than the ones we had originally targeted, the sites of which are also serendipitously covered by our Snapshots. We provide a summary of those results in Section A in the Appendix.

## 6. ACKNOWLEDGMENTS

This research is based on observations, associated with programs GO-14668, GO-15166, GO-16179, and others, made with the NASA/ESA *Hubble Space Telescope* and obtained from STScI, which is operated by the Association of Universities for Research in Astronomy, Inc., under NASA contract NAS 5–26555. *HST* archival data were analyzed through program AR-14259. Support for these programs was provided by NASA through grants from STScI. This research has made use of NED, which is funded by NASA and operated by the California Institute of Technology. A.V.F.’s SN team at U.C. Berkeley also received generous support from the Miller Institute for Basic Research in Science (where A.V.F. was a Miller Senior Fellow), Gary and Cynthia Bengier (T. deJ. was a Bengier Postdoctoral Fellow), the Christopher R. Redlich Fund, Alan Eustace, Briggs and Kathleen Wood, and many other donors.

KAIT and its ongoing operation were made possible by donations from Sun Microsystems, Inc., the Hewlett-Packard Company, AutoScope Corporation, Lick Ob-

servatory, the U.S. National Science Foundation (NSF), the University of California, the Sylvia & Jim Katzman Foundation, and the TABASGO Foundation. Research at Lick Observatory is partially supported by a generous gift from Google, Inc.

We thank (mostly U.C. Berkeley undergraduate students) Yukei Murakami, Kevin Tang, Benjamin Jeffers, Andrew Hoffman, Sanyum Channa, Sahana Kumar, Jeremy Wayland, Jeffrey Molloy, Julia Hestenes, James Sunseri, Goni Halevi, Costas Solar, Connor Jennings, Andrew Halle, Teagan Chapman, Shaunak Modak, Nick Choksi, Jackson Sipple, Heechan Yuk, Emily Ma, Edward Falcon, Nachiket Girish, Maxime de Kouchkovsky, Evelyn Liu, Derek Perera, Andrew Rikhter, Matt Chu, Kevin Hayakawa, Ivan Altunin, Haynes Stephens for their effort in taking Lick/Nickel data.

*Facilities:* HST(WFC3)

*Software:* Drizzlepac, Astrodrizzle (STSCI Development Team 2012), Dolphot (Dolphin 2016)

## APPENDIX

### A. SERENDIPITOUS EVENTS

A number of SNe or SN impostors could also have been caught serendipitously in our Snapshot data. Of those events that were in our Snapshot footprints, we provide a summary in the subsections below. We show only the images and dispense with measuring photometry and including it with earlier-time light curves, since these events were not originally targets of our Snapshot survey. We leave this for the interested reader.

Several SN sites were not in our Snapshot images despite being in targeted the host galaxies, as follows. For the SN 2011dh observation, the sites of neither the SN Ic 1994I nor the SN II-P 2005cs were covered; for both of the SN 2013ej and AT 2019krl observations, the sites of the SN Ic 2002ap and SN II-P 2003gd were not covered; for the SN 2016adj observation, the site of the SN Ia 1986G was not covered; for the AT 2016jbu observation, the site of the SN Ia 2015F was not covered; for the SN 2017eaw observation, of the other nine SNe in the host galaxy, none of the SNe within the last few decades are in the Snapshot pointing; the site of the intriguing interacting SN Ib 2004dk (e.g., Mauerhan et al. 2018), which occurred in the same host as SN 2020hvp, was not in the Snapshot footprint; and, for the SN 2020jfo observation, the sites of the SN II-P 2008in and SN II-P 1999gn are not in the pointing, and the SN Iax 2014dt site is too near the edge.

#### A.1. SN 1999el

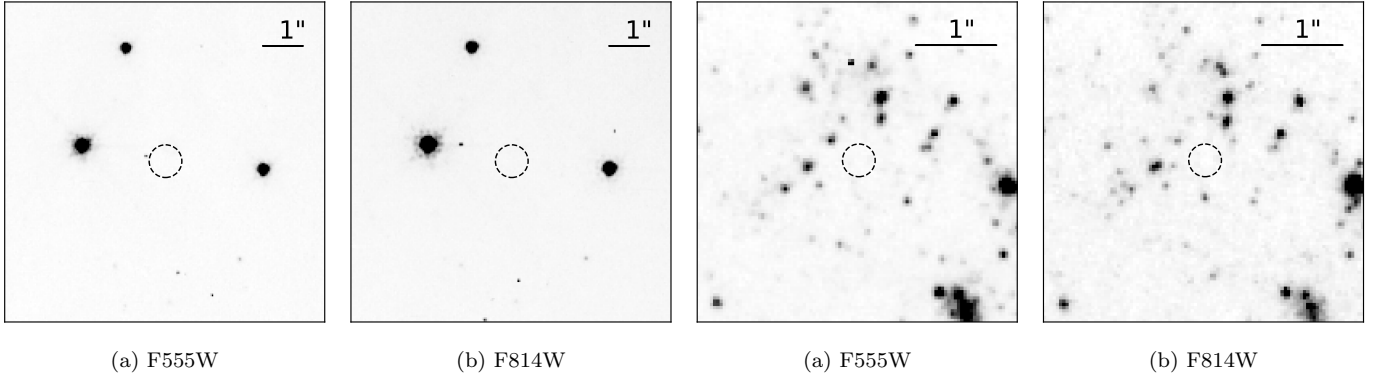
The site of the SN IIn 1999el (Di Carlo et al. 2002) was captured in our SN 2020dpw Snapshots (Section 4.33). However, it was not detected; see Figure 36.

#### A.2. SN 1999gi

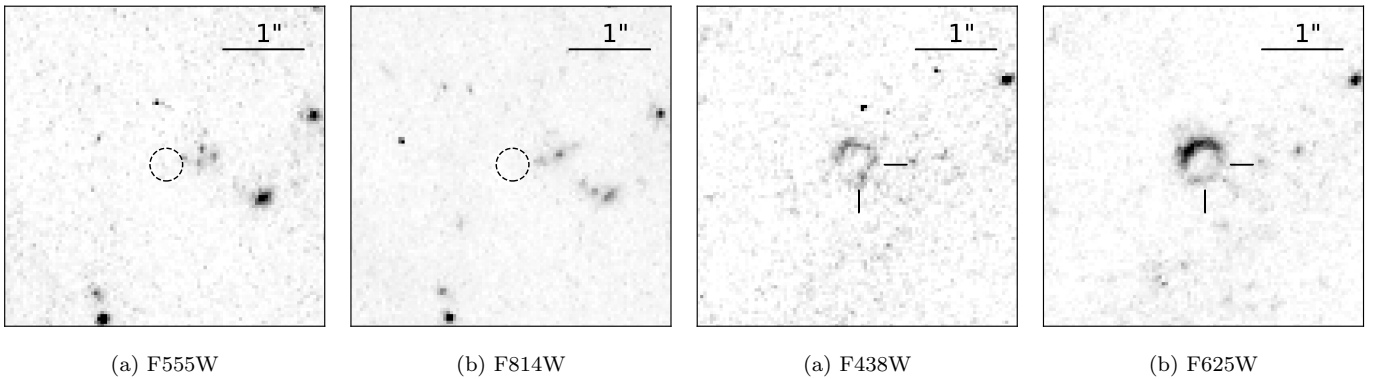
The site of the SN II-P 1999gi (e.g., Leonard et al. 2002) was in our Snapshots of SN 2016bkv (Section 4.15). However, the SN was no longer detectable at this late time. We pinpointed the location via comparison with WFPC2 images from one of our previous Snapshot programs (GO-8602; PI A. Filippenko); see Figure 36.

#### A.3. SN 2000E

The site of the SN Ia 2000E (Valentini et al. 2003) was captured in our SN 2020dpw Snapshots (Section 4.33). However, it was no longer detectable in either band; see Figure 37.



**Figure 36.** *Left two panels:* A portion of the WFC3 image mosaic containing SN 1999el, caught serendipitously in observations of SN 2020dpw (Section 4.33), in (a) F555W and (b) F814W. The SN is no longer detectable in either band; the site is indicated by the dashed circle. *Right two panels:* A portion of the WFC3 image mosaic containing SN 1999gi (e.g., Leonard et al. 2002), caught serendipitously in observations of SN 2016bkv (Section 4.15), in (a) F555W and (b) F814W. The SN is no longer detectable; the site is indicated by the dashed circle.



**Figure 37.** *Left two panels:* A portion of the WFC3 image mosaic containing SN 2000E (Valentini et al. 2003), caught serendipitously in observations of SN 2020dpw (Section 4.33), in (a) F555W and (b) F814W. The SN is no longer detectable; the site is indicated by the dashed circle. *Right two panels:* A portion of the WFC3 image mosaic containing SN 2006X, caught serendipitously in observations on 2021 February 21 of SN 2019ehk (Section 4.31), in (a) F438W and (b) F625W. Whereas the SN is no longer detectable (the site is indicated by tick marks), the light echo around it is still quite apparent.

#### A.4. SN 2006X

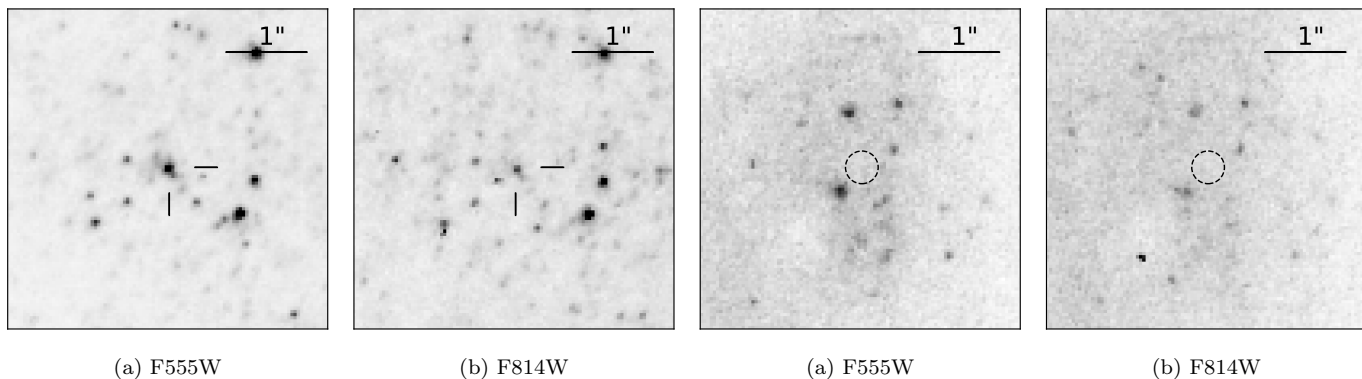
We managed to catch the light echo around the SN Ia 2006X (Wang et al. 2008; Crotts & Yourdon 2008) in our SN 2019ehk Snapshots (Section 4.31). The SN itself has disappeared, with upper limits of 26.2 and 25.8 mag in F438W and F625W, respectively; see Figure 37. An analysis of the evolution of the echo is beyond the scope of this paper.

#### A.5. SN 2006ov

The SN II-P 2006ov (e.g., Spiro et al. 2014) was serendipitously captured in our SN 2020jfo Snapshots in F555W and F814W (Section 4.35); see Figure 38. We ascertained the continued presence of the SN using *HST* ACS images from program GO-10877 (PI W. Li) obtained around the time of discovery.

#### A.6. SN 2012bv

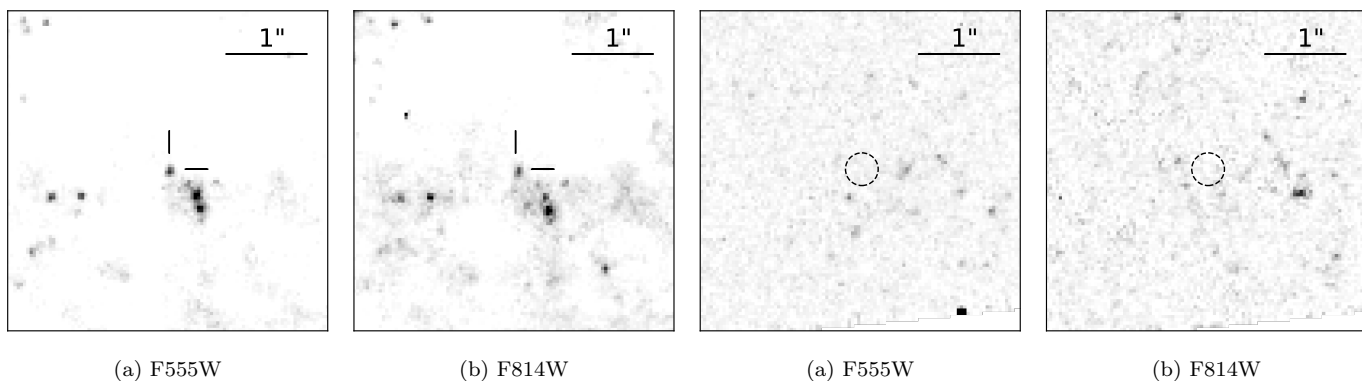
The SN II 2012bv was serendipitously observed in our observations of SN 2017ixv (Section 4.25). There was no prior *HST* or optical ground-based imaging of the SN, and thus the absolute position was used to locate the site of the SN. The SN was no longer detectable in either band; see Figure 38.



**Figure 38.** *Left two panels:* A portion of the WFC3 image mosaic containing SN 2006ov, caught serendipitously in observations of SN 2020jfo (Section 4.35), in (a) F555W and (b) F814W. The SN is still quite apparent, as indicated by the tick marks. *Right two panels:* A portion of the WFC3 image mosaic containing SN 2012bv, caught serendipitously in observations of SN 2017ixv (Section 4.25), in (a) F555W and (b) F814W. The SN is no longer detectable; the site is indicated by the dashed circle.

#### A.7. SN 2013ff

The SN Ic 2013ff site is in our Snapshots of SN 2017gkk (Section 4.24). Szalai et al. (2019a) claimed that SN 2013ff was detected by *Spitzer* in 2014 January (at  $\sim 180$  d). We isolated a probable detection of the SN in both bands by comparing the Snapshots from this program to those from our previous programs GO-14668 and GO-15166 (PI A. Filippenko), when it appeared much fainter; see Figure 39. This implies that, sometime between 2019 February and 2021 September, the SN shock may have encountered and was interacting with dense, or denser, CSM. This is quite unusual for an SN Ic and would further imply that SN 2013ff may be similar to SN 2014C (Section 4.11).



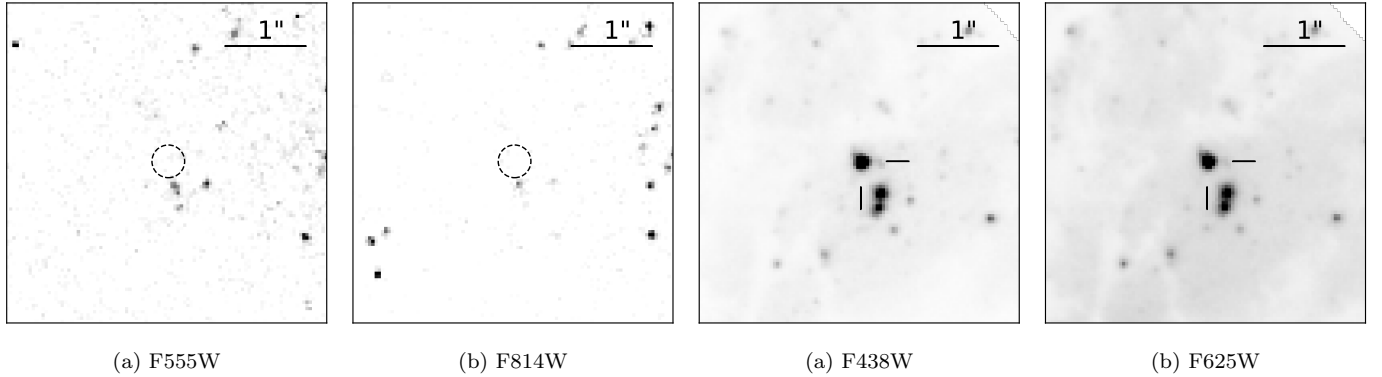
**Figure 39.** *Left two panels:* A portion of the WFC3 image mosaic containing SN 2013ff, caught serendipitously in observations of SN 2017gkk (Section 4.24), in (a) F555W and (b) F814W. The SN is detected in our Snapshots, as indicated by the tick marks. *Right two panels:* A portion of the WFC3 image mosaic containing PSN J09132750+7627410 caught serendipitously in observations of SN 2017gkk (Section 4.24), in (a) F555W and (b) F814W. The impostor is no longer detectable; the site is indicated by the dashed circle.

#### A.8. PSN J09132750+7627410

The SN impostor PSN J09132750+7627410 was captured in our SN 2017gkk Snapshots (Section 4.24). Based on a direct comparison with detections shown by Tartaglia et al. (2016), we determined that the object was no longer detectable; see Figure 39.

## A.9. SN 2015G

The site of the Type Ibn SN 2015G (Shivvers et al. 2017) was included in our SN 2020dpw Snapshots as well (Section 4.33). The SN is not detected in the Snapshots, however, and had likely vanished based on comparisons with the images shown by Shivvers et al. (2017); see Figure 40.



**Figure 40.** *Left two panels:* A portion of the WFC3 image mosaic containing SN 2015G, caught serendipitously in observations of SN 2020dpw (Section 4.33), in (a) F555W and (b) F814W. The SN is no longer detectable and the site is indicated by the dashed circle. *Right two panels:* A portion of the WFC3 image mosaic containing SN 2020oi, caught serendipitously in observations on 2021 February 21 of SN 2019ehk (Section 4.31), in (a) F438W and (b) F625W. The SN is detected in our Snapshots, as indicated by the tick marks.

## A.10. SN 2020oi

The SN Ic 2020oi was serendipitously detected in our SN 2019ehk Snapshots (Section 4.31) at  $m_{F438W} = 19.41 \pm 0.01$  and  $m_{F625W} = 19.47 \pm 0.01$  mag; see Figure 40. Gagliano et al. (2022) made use of these Snapshots in their analysis of this SN.

## A.11. SN 2021J

We managed to capture serendipitously the SN Ia 2021J, which occurred in the same host galaxy (NGC 4414) as SN 2013df (Section 4.9). Gallego-Cano et al. (2022) undertook early-time photometric and spectroscopic monitoring of SN 2021J. Unfortunately, the SN was saturated in both bands of our Snapshot observations and therefore cannot complement the ground-based light curves; see Figure 41.

## A.12. SN 2021sjt

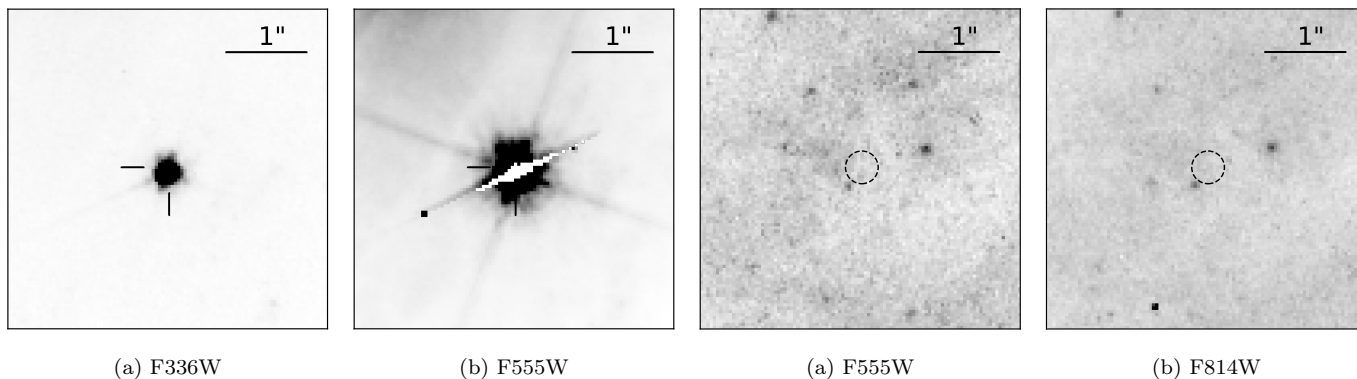
We further managed to capture the site of the SN Iib 2021sjt, pre-explosion, in the pointing for our observations of SN 2020dpw (Section 4.33) on 2020 December 13. However, based on a spectrum posted to TNS, it appears that the extinction at the site is very large and thus any progenitor identification would likely not be possible. This lack of detection is evident from our Snapshots; see Figure 41.

## A.13. SN 2022aau

For the SN 2017gax observation (Section 4.23), the site of SN II 2022aau is in the field of view and observed somewhat over a year prior to its discovery. However, based on the classification spectrum (Siebert et al. 2021), it appears that the extinction at the site is very large and therefore any progenitor identification would likely not be possible; see Figure 42.

## REFERENCES

- Aghakhanloo, M., Smith, N., Milne, P., et al. 2022a, arXiv e-prints, arXiv:2212.00113.  
<https://arxiv.org/abs/2212.00113>
- . 2022b, arXiv e-prints, arXiv:2212.09708,  
 doi: [10.48550/arXiv.2212.09708](https://doi.org/10.48550/arXiv.2212.09708)



**Figure 41.** *Left two panels:* A portion of the WFC3 image mosaic containing SN 2021J, caught serendipitously in observations on 2021 February 15 of SN 2013df, in (a) F336W and (b) F555W. The SN, which was at  $V = 13.63$  and  $I = 12.70$  mag (Gallego-Cano et al. 2022), is hopelessly saturated in both bands; hence, the Snapshots do not provide any additional photometric information. *Right two panels:* A portion of the WFC3 image mosaic containing the location of SN 2021sjt, caught serendipitously in observations of SN 2020dpw, in (a) F555W and (b) F814W. A progenitor candidate is not detectable, as indicated by the dashed circle.



**Figure 42.** A portion of the WFC3 image mosaic containing the location of SN 2022aau, caught serendipitously in observations of SN 2017gax, in (a) F336W and (b) F814W. The progenitor is not detectable, as indicated by the dashed circle.

- Ailawadhi, B., Dastidar, R., Misra, K., et al. 2022, MNRAS, doi: [10.1093/mnras/stac3234](https://doi.org/10.1093/mnras/stac3234)
- Aldering, G., Humphreys, R. M., & Richmond, M. 1994, AJ, 107, 662, doi: [10.1086/116886](https://doi.org/10.1086/116886)
- Allak, S., Akyuz, A., Sonbas, E., & Dhuga, K. S. 2022, MNRAS, 515, 3632, doi: [10.1093/mnras/stac1992](https://doi.org/10.1093/mnras/stac1992)
- Anand, G. S., Rizzi, L., Tully, R. B., et al. 2021, AJ, 162, 80, doi: [10.3847/1538-3881/ac0440](https://doi.org/10.3847/1538-3881/ac0440)
- Andrews, J. E., Clayton, G. C., Wesson, R., et al. 2011, AJ, 142, 45, doi: [10.1088/0004-6256/142/2/45](https://doi.org/10.1088/0004-6256/142/2/45)
- Andrews, J. E., Jencson, J. E., Van Dyk, S. D., et al. 2021, ApJ, 917, 63, doi: [10.3847/1538-4357/ac09e1](https://doi.org/10.3847/1538-4357/ac09e1)
- Arcavi, I., Gal-Yam, A., Yaron, O., et al. 2011, ApJL, 742, L18, doi: [10.1088/2041-8205/742/2/L18](https://doi.org/10.1088/2041-8205/742/2/L18)
- Arcavi, I., Hosseinzadeh, G., Brown, P. J., et al. 2017, ApJL, 837, L2, doi: [10.3847/2041-8213/aa5be1](https://doi.org/10.3847/2041-8213/aa5be1)
- Aretxaga, I., Benetti, S., Terlevich, R. J., et al. 1999, MNRAS, 309, 343, doi: [10.1046/j.1365-8711.1999.02830.x](https://doi.org/10.1046/j.1365-8711.1999.02830.x)
- Balanutsa, P., Lipunov, V., Gress, O., et al. 2017, The Astronomer's Telegram, 10667, 1
- Benvenuto, O. G., Bersten, M. C., & Nomoto, K. 2013, ApJ, 762, 74, doi: [10.1088/0004-637X/762/2/74](https://doi.org/10.1088/0004-637X/762/2/74)
- Bersten, M. C., Benvenuto, O. G., Nomoto, K., et al. 2012, ApJ, 757, 31, doi: [10.1088/0004-637X/757/1/31](https://doi.org/10.1088/0004-637X/757/1/31)
- Bersten, M. C., Folatelli, G., García, F., et al. 2018, Nature, 554, 497, doi: [10.1038/nature25151](https://doi.org/10.1038/nature25151)
- Bertrand, E. 2018, Transient Name Server Classification Report, 2018-56, 1
- Bevan, A. M., Krafton, K., Wesson, R., et al. 2020, ApJ, 894, 111, doi: [10.3847/1538-4357/ab86a2](https://doi.org/10.3847/1538-4357/ab86a2)
- Bond, H. E., Gilmozzi, R., Meakes, M. G., & Panagia, N. 1990, ApJL, 354, L49, doi: [10.1086/185720](https://doi.org/10.1086/185720)



**Table 2.** Photometry of Seven Supernovae with Unpublished Data (mag)<sup>1</sup>

MJD	<i>B</i>	1 $\sigma$	<i>V</i>	1 $\sigma$	<i>R</i>	1 $\sigma$	<i>Clear</i>	1 $\sigma$	<i>I</i>	1 $\sigma$	tel
2016bkv											
57470.3553	...	...	...	...	...	...	15.762	0.073	...	...	KAIT
57471.2635	15.412	0.052	15.463	0.031	15.399	0.029	15.243	0.031	15.402	0.041	KAIT
57472.3798	14.914	0.073	15.166	0.042	15.024	0.048	14.911	0.107	15.042	0.050	KAIT
57473.3044	14.606	0.066	14.984	0.032	14.971	0.032	14.806	0.036	15.007	0.038	KAIT
57474.3330	14.624	0.053	14.806	0.034	14.829	0.031	14.666	0.037	14.871	0.033	KAIT
57476.3319	14.685	0.048	14.754	0.027	14.751	0.035	14.635	0.033	14.756	0.040	KAIT
57477.3040	14.769	0.038	14.827	0.023	14.801	0.030	14.687	0.049	14.765	0.036	KAIT
57478.2828	14.873	0.042	14.924	0.025	14.885	0.030	14.770	0.035	14.818	0.036	KAIT

<sup>1</sup>Only a portion of the table is shown here; the full table is available in the electronic version.

- Borish, H. J., Huang, C., Chevalier, R. A., et al. 2015, ApJ, 801, 7, doi: [10.1088/0004-637X/801/1/7](https://doi.org/10.1088/0004-637X/801/1/7)
- Bose, S., Kumar, B., Sutaria, F., et al. 2013, MNRAS, 433, 1871, doi: [10.1093/mnras/stt864](https://doi.org/10.1093/mnras/stt864)
- Bose, S., Sutaria, F., Kumar, B., et al. 2015, ApJ, 806, 160, doi: [10.1088/0004-637X/806/2/160](https://doi.org/10.1088/0004-637X/806/2/160)
- Bostroem, K. A., Zapartas, E., Koplitz, B., et al. 2023, AJ, 166, 255, doi: [10.3847/1538-3881/acffc7](https://doi.org/10.3847/1538-3881/acffc7)
- Bostroem, K. A., Valenti, S., Sand, D. J., et al. 2020, ApJ, 895, 31, doi: [10.3847/1538-4357/ab8945](https://doi.org/10.3847/1538-4357/ab8945)
- Brennan, S. J., Elias-Rosa, N., Fraser, M., Van Dyk, S. D., & Lyman, J. D. 2022a, A&A, 664, L18, doi: [10.1051/0004-6361/202244262](https://doi.org/10.1051/0004-6361/202244262)
- Brennan, S. J., Fraser, M., Johansson, J., et al. 2022b, MNRAS, 513, 5642, doi: [10.1093/mnras/stac1243](https://doi.org/10.1093/mnras/stac1243)
- . 2022c, MNRAS, 513, 5666, doi: [10.1093/mnras/stac1228](https://doi.org/10.1093/mnras/stac1228)
- Brethauer, D., Margutti, R., Milisavljevic, D., et al. 2022, ApJ, 939, 105, doi: [10.3847/1538-4357/ac8b14](https://doi.org/10.3847/1538-4357/ac8b14)
- Burke, J., Hiramatsu, D., Howell, D. A., et al. 2020, Transient Name Server Classification Report, 2020-1129, 1
- Buta, R. J., & Keel, W. C. 2019, MNRAS, 487, 832, doi: [10.1093/mnras/stz1291](https://doi.org/10.1093/mnras/stz1291)
- Callis, E., Fraser, M., Pastorello, A., et al. 2021, arXiv e-prints, arXiv:2109.12943, <https://arxiv.org/abs/2109.12943>
- Campana, S., & Margutti, R. 2016, The Astronomer’s Telegram, 8535, 1
- Cappellaro, E., Patat, F., Mazzali, P. A., et al. 2001, ApJL, 549, L215, doi: [10.1086/319178](https://doi.org/10.1086/319178)
- Chandra, P., Chevalier, R. A., Chugai, N., Fransson, C., & Soderberg, A. M. 2015, ApJ, 810, 32, doi: [10.1088/0004-637X/810/1/32](https://doi.org/10.1088/0004-637X/810/1/32)
- Chen, Y., Drout, M. R., Piro, A. L., et al. 2023, arXiv e-prints, arXiv:2303.03501, doi: [10.48550/arXiv.2303.03501](https://doi.org/10.48550/arXiv.2303.03501)
- Cikota, A., Ding, J., Wang, L., et al. 2023, ApJL, 949, L9, doi: [10.3847/2041-8213/acd37c](https://doi.org/10.3847/2041-8213/acd37c)
- Cohen, J. G., Darling, J., & Porter, A. 1995, AJ, 110, 308, doi: [10.1086/117520](https://doi.org/10.1086/117520)
- Cortini, G. 2017, Transient Name Server Discovery Report, 2017-1423, 1
- Crotts, A. P. S. 2015, ApJL, 804, L37, doi: [10.1088/2041-8205/804/2/L37](https://doi.org/10.1088/2041-8205/804/2/L37)
- Crotts, A. P. S., & Yourdon, D. 2008, ApJ, 689, 1186, doi: [10.1086/592318](https://doi.org/10.1086/592318)
- Dall’Ora, M., Botticella, M. T., Pumo, M. L., et al. 2014, ApJ, 787, 139, doi: [10.1088/0004-637X/787/2/139](https://doi.org/10.1088/0004-637X/787/2/139)
- de Jaeger, T., Zheng, W., Stahl, B. E., et al. 2019, MNRAS, 490, 2799, doi: [10.1093/mnras/stz2714](https://doi.org/10.1093/mnras/stz2714)
- de Witt, A., Bietenholz, M. F., Kamble, A., et al. 2016, MNRAS, 455, 511, doi: [10.1093/mnras/stv2306](https://doi.org/10.1093/mnras/stv2306)
- Deckers, M., Groh, J. H., Boian, I., & Farrell, E. J. 2021, MNRAS, 507, 3726, doi: [10.1093/mnras/stab2423](https://doi.org/10.1093/mnras/stab2423)
- Dhungana, G., Kehoe, R., Vinko, J., et al. 2016, ApJ, 822, 6, doi: [10.3847/0004-637X/822/1/6](https://doi.org/10.3847/0004-637X/822/1/6)
- Di Carlo, E., Massi, F., Valentini, G., et al. 2002, ApJ, 573, 144, doi: [10.1086/340496](https://doi.org/10.1086/340496)
- Ding, J., Wang, L., Brown, P., & Yang, P. 2021, ApJ, 919, 104, doi: [10.3847/1538-4357/ac1069](https://doi.org/10.3847/1538-4357/ac1069)
- Dolphin, A. 2016, DOLPHOT: Stellar photometry, Astrophysics Source Code Library, record ascl:1608.013, <http://ascl.net/1608.013>
- Ergon, M., Sollerman, J., Fraser, M., et al. 2014, A&A, 562, A17, doi: [10.1051/0004-6361/201321850](https://doi.org/10.1051/0004-6361/201321850)

- Ergon, M., Jerkstrand, A., Sollerman, J., et al. 2015, *A&A*, 580, A142, doi: [10.1051/0004-6361/201424592](https://doi.org/10.1051/0004-6361/201424592)
- Fabian, A. C., & Terlevich, R. 1996, *MNRAS*, 280, L5, doi: [10.1093/mnras/280.1.L5](https://doi.org/10.1093/mnras/280.1.L5)
- Filippenko, A. V. 1997, *ARA&A*, 35, 309, doi: [10.1146/annurev.astro.35.1.309](https://doi.org/10.1146/annurev.astro.35.1.309)
- Filippenko, A. V. 2003, in *From Twilight to Highlight: The Physics of Supernovae*, ed. W. Hillebrandt & B. Leibundgut, 171, doi: [10.1007/10828549\\_23](https://doi.org/10.1007/10828549_23)
- Filippenko, A. V., Matheson, T., Kirshner, R. P., et al. 1993, *IAUC*, 5740, 1
- Folatelli, G., Bersten, M. C., Benvenuto, O. G., et al. 2014, *ApJL*, 793, L22, doi: [10.1088/2041-8205/793/2/L22](https://doi.org/10.1088/2041-8205/793/2/L22)
- Fox, O. D., Filippenko, A. V., Skrutskie, M. F., et al. 2013, *AJ*, 146, 2, doi: [10.1088/0004-6256/146/1/2](https://doi.org/10.1088/0004-6256/146/1/2)
- Fox, O. D., & Smith, N. 2019, *MNRAS*, 488, 3772, doi: [10.1093/mnras/stz1925](https://doi.org/10.1093/mnras/stz1925)
- Fox, O. D., Azalee Bostroem, K., Van Dyk, S. D., et al. 2014, *ApJ*, 790, 17, doi: [10.1088/0004-637X/790/1/17](https://doi.org/10.1088/0004-637X/790/1/17)
- Fox, O. D., Van Dyk, S. D., Dwek, E., et al. 2017, *ApJ*, 836, 222, doi: [10.3847/1538-4357/836/2/222](https://doi.org/10.3847/1538-4357/836/2/222)
- Fransson, C., Chevalier, R. A., Filippenko, A. V., et al. 2002, *ApJ*, 572, 350, doi: [10.1086/340295](https://doi.org/10.1086/340295)
- Fransson, C., Ergon, M., Challis, P. J., et al. 2014, *ApJ*, 797, 118, doi: [10.1088/0004-637X/797/2/118](https://doi.org/10.1088/0004-637X/797/2/118)
- Fraser, M. 2016, *MNRAS*, 456, L16, doi: [10.1093/mnras/slv168](https://doi.org/10.1093/mnras/slv168)
- Fraser, M., Maund, J. R., Smartt, S. J., et al. 2012, *ApJL*, 759, L13, doi: [10.1088/2041-8205/759/1/L13](https://doi.org/10.1088/2041-8205/759/1/L13)
- . 2014, *MNRAS*, 439, L56, doi: [10.1093/mnras/slt179](https://doi.org/10.1093/mnras/slt179)
- Gagliano, A., Izzo, L., Kilpatrick, C. D., et al. 2022, *ApJ*, 924, 55, doi: [10.3847/1538-4357/ac35ec](https://doi.org/10.3847/1538-4357/ac35ec)
- Gal-Yam, A. 2017, in *Handbook of Supernovae*, ed. A. W. Alsabti & P. Murdin, 195, doi: [10.1007/978-3-319-21846-5\\_35](https://doi.org/10.1007/978-3-319-21846-5_35)
- Gall, C., Hjorth, J., Watson, D., et al. 2014, *Nature*, 511, 326, doi: [10.1038/nature13558](https://doi.org/10.1038/nature13558)
- Gallego-Cano, E., Izzo, L., Dominguez-Tagle, C., et al. 2022, *arXiv e-prints*, arXiv:2204.10668. <https://arxiv.org/abs/2204.10668>
- Graham, M. L., Harris, C. E., Nugent, P. E., et al. 2019, *ApJ*, 871, 62, doi: [10.3847/1538-4357/aaf41e](https://doi.org/10.3847/1538-4357/aaf41e)
- Han, X., Zheng, W., Stahl, B. E., et al. 2020, *ApJ*, 892, 142, doi: [10.3847/1538-4357/ab7a27](https://doi.org/10.3847/1538-4357/ab7a27)
- Harris, C. E., Nugent, P. E., Horesh, A., et al. 2018, *ApJ*, 868, 21, doi: [10.3847/1538-4357/aae521](https://doi.org/10.3847/1538-4357/aae521)
- Hiramatsu, D., Howell, D. A., Van Dyk, S. D., et al. 2021, *Nature Astronomy*, 5, 903, doi: [10.1038/s41550-021-01384-2](https://doi.org/10.1038/s41550-021-01384-2)
- Horesh, A., Stockdale, C., Fox, D. B., et al. 2013, *MNRAS*, 436, 1258, doi: [10.1093/mnras/stt1645](https://doi.org/10.1093/mnras/stt1645)
- Hosseinzadeh, G., Valenti, S., McCully, C., et al. 2018, *ApJ*, 861, 63, doi: [10.3847/1538-4357/aac5f6](https://doi.org/10.3847/1538-4357/aac5f6)
- Howell, D. A., & Murray, D. 2012, *Central Bureau Electronic Telegrams*, 3313, 2
- Huang, F., Wang, X., Zhang, J., et al. 2015, *ApJ*, 807, 59, doi: [10.1088/0004-637X/807/1/59](https://doi.org/10.1088/0004-637X/807/1/59)
- Inkenhaag, A., Jonker, P. G., Levan, A. J., et al. 2023, *MNRAS*, 525, 4042, doi: [10.1093/mnras/stad2531](https://doi.org/10.1093/mnras/stad2531)
- Itagaki, K. 2017, *Transient Name Server Discovery Report*, 2017-940, 1
- Jacobson-Galán, W. V., Margutti, R., Kilpatrick, C. D., et al. 2020, *ApJ*, 898, 166, doi: [10.3847/1538-4357/ab9e66](https://doi.org/10.3847/1538-4357/ab9e66)
- . 2021, *ApJL*, 908, L32, doi: [10.3847/2041-8213/abdebc](https://doi.org/10.3847/2041-8213/abdebc)
- Jencson, J. E., Prieto, J. L., Kochanek, C. S., et al. 2016, *MNRAS*, 456, 2622, doi: [10.1093/mnras/stv2795](https://doi.org/10.1093/mnras/stv2795)
- Jerkstrand, A., Smartt, S. J., Fraser, M., et al. 2014, *MNRAS*, 439, 3694, doi: [10.1093/mnras/stu221](https://doi.org/10.1093/mnras/stu221)
- Jha, S. W., Camacho, Y., Dettman, K., et al. 2017, *The Astronomer's Telegram*, 10640, 1
- Kamble, A., Margutti, R., Soderberg, A. M., et al. 2016, *ApJ*, 818, 111, doi: [10.3847/0004-637X/818/2/111](https://doi.org/10.3847/0004-637X/818/2/111)
- Kandrashoff, M., Cenko, S. B., Li, W., et al. 2012, *Central Bureau Electronic Telegrams*, 2976, 1
- Kawabata, M. 2020, *Transient Name Server Classification Report*, 2020-657, 1
- Kilpatrick, C. D., Coulter, D. A., Foley, R. J., Pan, Y. C., & Siebert, M. R. 2018a, *The Astronomer's Telegram*, 11172, 1
- Kilpatrick, C. D., Coulter, D. A., Foley, R. J., et al. 2022, *ApJ*, 936, 111, doi: [10.3847/1538-4357/ac8a4c](https://doi.org/10.3847/1538-4357/ac8a4c)
- Kilpatrick, C. D., & Foley, R. J. 2018, *MNRAS*, 481, 2536, doi: [10.1093/mnras/sty2435](https://doi.org/10.1093/mnras/sty2435)
- Kilpatrick, C. D., Foley, R. J., Abramson, L. E., et al. 2017, *MNRAS*, 465, 4650, doi: [10.1093/mnras/stw3082](https://doi.org/10.1093/mnras/stw3082)
- Kilpatrick, C. D., Foley, R. J., Drout, M. R., et al. 2018b, *MNRAS*, 473, 4805, doi: [10.1093/mnras/stx2675](https://doi.org/10.1093/mnras/stx2675)
- Kilpatrick, C. D., Izzo, L., Bentley, R. O., et al. 2023, *MNRAS*, 524, 2161, doi: [10.1093/mnras/stad1954](https://doi.org/10.1093/mnras/stad1954)
- Krauss, M. I., Soderberg, A. M., Chomiuk, L., et al. 2012, *ApJL*, 750, L40, doi: [10.1088/2041-8205/750/2/L40](https://doi.org/10.1088/2041-8205/750/2/L40)
- Kumar, B., Singh, A., Srivastav, S., Sahu, D. K., & Anupama, G. C. 2018, *MNRAS*, 473, 3776, doi: [10.1093/mnras/stx2498](https://doi.org/10.1093/mnras/stx2498)
- Kundu, E., Lundqvist, P., Sorokina, E., et al. 2019, *ApJ*, 875, 17, doi: [10.3847/1538-4357/ab0d81](https://doi.org/10.3847/1538-4357/ab0d81)
- Leadbeater, R. 2017, *Transient Name Server Classification Report*, 2017-1435, 1

- Leonard, D. C., Filippenko, A. V., Li, W., et al. 2002, *AJ*, 124, 2490, doi: [10.1086/343771](https://doi.org/10.1086/343771)
- Li, W., Filippenko, A. V., Van Dyk, S. D., et al. 2002, *PASP*, 114, 403, doi: [10.1086/342493](https://doi.org/10.1086/342493)
- Liu, J.-F., Bregman, J. N., & Seitzer, P. 2003, *ApJ*, 582, 919, doi: [10.1086/344719](https://doi.org/10.1086/344719)
- Maeda, K., Katsuda, S., Bamba, A., Terada, Y., & Fukazawa, Y. 2014, *ApJ*, 785, 95, doi: [10.1088/0004-637X/785/2/95](https://doi.org/10.1088/0004-637X/785/2/95)
- Maeda, K., Michiyama, T., Chandra, P., et al. 2023a, *ApJL*, 945, L3, doi: [10.3847/2041-8213/acb25e](https://doi.org/10.3847/2041-8213/acb25e)
- Maeda, K., Hattori, T., Milisavljevic, D., et al. 2015, *ApJ*, 807, 35, doi: [10.1088/0004-637X/807/1/35](https://doi.org/10.1088/0004-637X/807/1/35)
- Maeda, K., Chandra, P., Moriya, T. J., et al. 2023b, *ApJ*, 942, 17, doi: [10.3847/1538-4357/aca1b7](https://doi.org/10.3847/1538-4357/aca1b7)
- Maguire, C., McDonnell, L., McGlinchey, M., et al. 2017, *The Astronomer's Telegram*, 10956, 1
- Margutti, R., Kamble, A., Milisavljevic, D., et al. 2017, *ApJ*, 835, 140, doi: [10.3847/1538-4357/835/2/140](https://doi.org/10.3847/1538-4357/835/2/140)
- Margutti, R., Metzger, B. D., Chornock, R., et al. 2019, *ApJ*, 872, 18, doi: [10.3847/1538-4357/aafa01](https://doi.org/10.3847/1538-4357/aafa01)
- Marion, G. H., Vinko, J., Kirshner, R. P., et al. 2014, *ApJ*, 781, 69, doi: [10.1088/0004-637X/781/2/69](https://doi.org/10.1088/0004-637X/781/2/69)
- Martí-Vidal, I., Tudose, V., Paragi, Z., et al. 2011, *A&A*, 535, L10, doi: [10.1051/0004-6361/201118195](https://doi.org/10.1051/0004-6361/201118195)
- Mauerhan, J. C., Filippenko, A. V., Zheng, W., et al. 2018, *MNRAS*, 478, 5050, doi: [10.1093/mnras/sty1307](https://doi.org/10.1093/mnras/sty1307)
- Mauerhan, J. C., Williams, G. G., Leonard, D. C., et al. 2015, *MNRAS*, 453, 4467, doi: [10.1093/mnras/stv1944](https://doi.org/10.1093/mnras/stv1944)
- Mauerhan, J. C., Van Dyk, S. D., Johansson, J., et al. 2017, *ApJ*, 834, 118, doi: [10.3847/1538-4357/834/2/118](https://doi.org/10.3847/1538-4357/834/2/118)
- Maund, J. R. 2019, *ApJ*, 883, 86, doi: [10.3847/1538-4357/ab2386](https://doi.org/10.3847/1538-4357/ab2386)
- Maund, J. R., & Smartt, S. J. 2009, *Science*, 324, 486, doi: [10.1126/science.1170198](https://doi.org/10.1126/science.1170198)
- Maund, J. R., Smartt, S. J., Kudritzki, R. P., Podsiadlowski, P., & Gilmore, G. F. 2004, *Nature*, 427, 129, doi: [10.1038/nature02161](https://doi.org/10.1038/nature02161)
- Maund, J. R., Fraser, M., Ergon, M., et al. 2011, *ApJL*, 739, L37, doi: [10.1088/2041-8205/739/2/L37](https://doi.org/10.1088/2041-8205/739/2/L37)
- Maund, J. R., Arcavi, I., Ergon, M., et al. 2015, *MNRAS*, 454, 2580, doi: [10.1093/mnras/stv2098](https://doi.org/10.1093/mnras/stv2098)
- McQuinn, K. B. W., Skillman, E. D., Dolphin, A. E., Berg, D., & Kennicutt, R. 2017, *AJ*, 154, 51, doi: [10.3847/1538-3881/aa7aad](https://doi.org/10.3847/1538-3881/aa7aad)
- Milisavljevic, D., Margutti, R., Kamble, A., et al. 2015, *ApJ*, 815, 120, doi: [10.1088/0004-637X/815/2/120](https://doi.org/10.1088/0004-637X/815/2/120)
- Morales-Garoffolo, A., Elias-Rosa, N., Benetti, S., et al. 2014, *MNRAS*, 445, 1647, doi: [10.1093/mnras/stu1837](https://doi.org/10.1093/mnras/stu1837)
- Morozova, V., Piro, A. L., Fuller, J., & Van Dyk, S. D. 2020, *ApJL*, 891, L32, doi: [10.3847/2041-8213/ab77c8](https://doi.org/10.3847/2041-8213/ab77c8)
- Nakaoka, T., Kawabata, K. S., Maeda, K., et al. 2018, *The Astrophysical Journal*, 859, 78, doi: [10.3847/1538-4357/aabee7](https://doi.org/10.3847/1538-4357/aabee7)
- Nakaoka, T., Maeda, K., Yamanaka, M., et al. 2021, *ApJ*, 912, 30, doi: [10.3847/1538-4357/abe765](https://doi.org/10.3847/1538-4357/abe765)
- Ofek, E. O., Sullivan, M., Cenko, S. B., et al. 2013, *Nature*, 494, 65, doi: [10.1038/nature11877](https://doi.org/10.1038/nature11877)
- Ofek, E. O., Zoglauer, A., Boggs, S. E., et al. 2014, *ApJ*, 781, 42, doi: [10.1088/0004-637X/781/1/42](https://doi.org/10.1088/0004-637X/781/1/42)
- Ofek, O. 2012, *Central Bureau Electronic Telegrams*, 3313, 1
- O'Neill, D., Kotak, R., Fraser, M., et al. 2019, *A&A*, 622, L1, doi: [10.1051/0004-6361/201834566](https://doi.org/10.1051/0004-6361/201834566)
- Onori, F. 2017, *Transient Name Server Classification Report*, 2017-964, 1
- Pastorello, A., Botticella, M. T., Trundle, C., et al. 2010, *MNRAS*, 408, 181, doi: [10.1111/j.1365-2966.2010.17142.x](https://doi.org/10.1111/j.1365-2966.2010.17142.x)
- Perley, D. A., Mazzali, P. A., Yan, L., et al. 2019, *MNRAS*, 484, 1031, doi: [10.1093/mnras/sty3420](https://doi.org/10.1093/mnras/sty3420)
- Piro, A. L., Muhleisen, M., Arcavi, I., et al. 2017, *ApJ*, 846, 94, doi: [10.3847/1538-4357/aa8595](https://doi.org/10.3847/1538-4357/aa8595)
- Podsiadlowski, P., Hsu, J. J. L., Joss, P. C., & Ross, R. R. 1993, *Nature*, 364, 509, doi: [10.1038/364509a0](https://doi.org/10.1038/364509a0)
- Prentice, S. J., Ashall, C., Mazzali, P. A., et al. 2018, *MNRAS*, 478, 4162, doi: [10.1093/mnras/sty1223](https://doi.org/10.1093/mnras/sty1223)
- Prieto, J. L., Osip, D., & Palunas, P. 2012, *The Astronomer's Telegram*, 3863, 1
- Richmond, M., & Vietje, B. 2017, *JAAVSO*, 45, 65. <https://arxiv.org/abs/1706.03289>
- Richmond, M. W. 2014, *JAAVSO*, 42, 333. <https://arxiv.org/abs/1405.7900>
- Richmond, M. W., Treffers, R. R., Filippenko, A. V., & Paik, Y. 1996, *AJ*, 112, 732, doi: [10.1086/118048](https://doi.org/10.1086/118048)
- Rui, L., Wang, X., Mo, J., et al. 2019, *MNRAS*, 485, 1990, doi: [10.1093/mnras/stz503](https://doi.org/10.1093/mnras/stz503)
- Sahu, D. K., Anupama, G. C., & Chakradhari, N. K. 2013, *MNRAS*, 433, 2, doi: [10.1093/mnras/stt647](https://doi.org/10.1093/mnras/stt647)
- Sarangi, A., Dwek, E., & Arendt, R. G. 2018, *ApJ*, 859, 66, doi: [10.3847/1538-4357/aabfc3](https://doi.org/10.3847/1538-4357/aabfc3)
- Schlafly, E. F., & Finkbeiner, D. P. 2011, *ApJ*, 737, 103, doi: [10.1088/0004-637X/737/2/103](https://doi.org/10.1088/0004-637X/737/2/103)
- Schlegel, E. M., & Petre, R. 2006, *ApJ*, 646, 378, doi: [10.1086/504890](https://doi.org/10.1086/504890)
- Sheehan, P., Follette, K., McCarthy, D., et al. 2014, *The Astronomer's Telegram*, 6303, 1
- Shivvers, I., Mazzali, P., Silverman, J. M., et al. 2013, *MNRAS*, 436, 3614, doi: [10.1093/mnras/stt1839](https://doi.org/10.1093/mnras/stt1839)

- Shivvers, I., Zheng, W., Van Dyk, S. D., et al. 2017, *MNRAS*, 471, 4381, doi: [10.1093/mnras/stx1885](https://doi.org/10.1093/mnras/stx1885)
- Siebert, M. R., Davis, K., Tinyanont, S., Foley, R. J., & Strasburger, E. 2021, *Transient Name Server Classification Report*, 2021-2383, 1
- Silverman, J. M., Pickett, S., Wheeler, J. C., et al. 2017, *MNRAS*, 467, 369, doi: [10.1093/mnras/stx058](https://doi.org/10.1093/mnras/stx058)
- Smith, N. 2014, *ARA&A*, 52, 487, doi: [10.1146/annurev-astro-081913-040025](https://doi.org/10.1146/annurev-astro-081913-040025)
- . 2017, in *Handbook of Supernovae*, ed. A. W. Alsabti & P. Murdin, 403, doi: [10.1007/978-3-319-21846-5\\_38](https://doi.org/10.1007/978-3-319-21846-5_38)
- Smith, N., Andrews, J. E., Filippenko, A. V., et al. 2022, *MNRAS*, 515, 71, doi: [10.1093/mnras/stac1669](https://doi.org/10.1093/mnras/stac1669)
- Smith, N., Li, W., Silverman, J. M., Ganeshalingam, M., & Filippenko, A. V. 2011a, *MNRAS*, 415, 773, doi: [10.1111/j.1365-2966.2011.18763.x](https://doi.org/10.1111/j.1365-2966.2011.18763.x)
- Smith, N., Mauerhan, J. C., Kasliwal, M. M., & Burgasser, A. J. 2013, *MNRAS*, 434, 2721, doi: [10.1093/mnras/stt944](https://doi.org/10.1093/mnras/stt944)
- Smith, N., Mauerhan, J. C., & Prieto, J. L. 2014, *MNRAS*, 438, 1191, doi: [10.1093/mnras/stt2269](https://doi.org/10.1093/mnras/stt2269)
- Smith, N., Silverman, J. M., Filippenko, A. V., et al. 2012, *AJ*, 143, 17, doi: [10.1088/0004-6256/143/1/17](https://doi.org/10.1088/0004-6256/143/1/17)
- Smith, N., Li, W., Miller, A. A., et al. 2011b, *ApJ*, 732, 63, doi: [10.1088/0004-637X/732/2/63](https://doi.org/10.1088/0004-637X/732/2/63)
- Smith, N., Kilpatrick, C. D., Mauerhan, J. C., et al. 2017, *MNRAS*, 466, 3021, doi: [10.1093/mnras/stw3204](https://doi.org/10.1093/mnras/stw3204)
- Soderberg, A. M., Margutti, R., Zauderer, B. A., et al. 2012, *ApJ*, 752, 78, doi: [10.1088/0004-637X/752/2/78](https://doi.org/10.1088/0004-637X/752/2/78)
- Sollerman, J., Yang, S., Schulze, S., et al. 2021, *A&A*, 655, A105, doi: [10.1051/0004-6361/202141374](https://doi.org/10.1051/0004-6361/202141374)
- Sparks, W. B., Macchetto, F., Panagia, N., et al. 1999, *ApJ*, 523, 585, doi: [10.1086/307766](https://doi.org/10.1086/307766)
- Spiro, S., Pastorello, A., Pumo, M. L., et al. 2014, *MNRAS*, 439, 2873, doi: [10.1093/mnras/stu156](https://doi.org/10.1093/mnras/stu156)
- Spogli, C., Fagotti, P., Vergari, D., Rocchi, G., & Ciprini, S. 2020, *JAAVSO*, 48, 131
- Stahl, B. E., Zheng, W., de Jaeger, T., et al. 2019, *MNRAS*, 490, 3882, doi: [10.1093/mnras/stz2742](https://doi.org/10.1093/mnras/stz2742)
- Stathakis, R. A., & Sadler, E. M. 1991, *MNRAS*, 250, 786, doi: [10.1093/mnras/250.4.786](https://doi.org/10.1093/mnras/250.4.786)
- Stoll, R., Prieto, J. L., Stanek, K. Z., et al. 2011, *ApJ*, 730, 34, doi: [10.1088/0004-637X/730/1/34](https://doi.org/10.1088/0004-637X/730/1/34)
- Stritzinger, M., Hsiao, E. Y., Morrell, N., et al. 2016, *The Astronomer's Telegram*, 8657, 1
- Stritzinger, M. D., Taddia, F., Lawrence, S. S., et al. 2022, *ApJL*, 939, L8, doi: [10.3847/2041-8213/ac93f8](https://doi.org/10.3847/2041-8213/ac93f8)
- Stritzinger, M. D., Baron, E., Taddia, F., et al. 2023, *arXiv e-prints*, arXiv:2309.05031. <https://arxiv.org/abs/2309.05031>
- STSCI Development Team. 2012, *DrizzlePac: HST image software*, Astrophysics Source Code Library, record ascl:1212.011. <http://ascl.net/1212.011>
- Sugerman, B., & Lawrence, S. 2016, *The Astronomer's Telegram*, 8890, 1
- Sugerman, B. E. K. 2005, *ApJL*, 632, L17, doi: [10.1086/497578](https://doi.org/10.1086/497578)
- Sugerman, B. E. K., & Crofts, A. P. S. 2002, *ApJL*, 581, L97, doi: [10.1086/346016](https://doi.org/10.1086/346016)
- Sun, N.-C., Maund, J. R., & Crowther, P. A. 2020, *MNRAS*, 497, 5118, doi: [10.1093/mnras/staa2277](https://doi.org/10.1093/mnras/staa2277)
- . 2023, *MNRAS*, 521, 2860, doi: [10.1093/mnras/stad690](https://doi.org/10.1093/mnras/stad690)
- Sun, N.-C., Maund, J. R., Crowther, P. A., & Liu, L.-D. 2022, *MNRAS*, 512, L66, doi: [10.1093/mnras/lsac023](https://doi.org/10.1093/mnras/lsac023)
- Szalai, T., Zsíros, S., Fox, O. D., Pejcha, O., & Müller, T. 2019a, *ApJS*, 241, 38, doi: [10.3847/1538-4365/ab10df](https://doi.org/10.3847/1538-4365/ab10df)
- Szalai, T., Vinkó, J., Nagy, A. P., et al. 2016, *MNRAS*, 460, 1500, doi: [10.1093/mnras/stw1031](https://doi.org/10.1093/mnras/stw1031)
- Szalai, T., Vinkó, J., Könyves-Tóth, R., et al. 2019b, *ApJ*, 876, 19, doi: [10.3847/1538-4357/ab12d0](https://doi.org/10.3847/1538-4357/ab12d0)
- Tartaglia, L., Sand, D., Wyatt, S., et al. 2017a, *The Astronomer's Telegram*, 10638, 1
- Tartaglia, L., Elias-Rosa, N., Pastorello, A., et al. 2016, *ApJL*, 823, L23, doi: [10.3847/2041-8205/823/2/L23](https://doi.org/10.3847/2041-8205/823/2/L23)
- Tartaglia, L., Fraser, M., Sand, D. J., et al. 2017b, *ApJL*, 836, L12, doi: [10.3847/2041-8213/aa5c7f](https://doi.org/10.3847/2041-8213/aa5c7f)
- Teja, R. S., Singh, A., Sahu, D. K., et al. 2022, *ApJ*, 930, 34, doi: [10.3847/1538-4357/ac610b](https://doi.org/10.3847/1538-4357/ac610b)
- . 2023, *arXiv e-prints*, arXiv:2306.10136, doi: [10.48550/arXiv.2306.10136](https://doi.org/10.48550/arXiv.2306.10136)
- Terreran, G., Margutti, R., Bersier, D., et al. 2019, *ApJ*, 883, 147, doi: [10.3847/1538-4357/ab3e37](https://doi.org/10.3847/1538-4357/ab3e37)
- Tomasella, L., Cappellaro, E., Fraser, M., et al. 2013, *MNRAS*, 434, 1636, doi: [10.1093/mnras/stt1130](https://doi.org/10.1093/mnras/stt1130)
- Tonry, J., Denneau, L., Heinze, A., et al. 2020, *Transient Name Server Discovery Report*, 2020-1094, 1
- Tsvetkov, D. Y., Pavlyuk, N., & Echeistov, V. 2020, *Peremennye Zvezdy*, 40, 1. <https://arxiv.org/abs/2007.05333>
- Tsvetkov, D. Y., Volkov, I. M., Shugarov, S. Y., et al. 2022, *Contributions of the Astronomical Observatory Skalnaté Pleso*, 52, 46, doi: [10.31577/caosp.2022.52.1.46](https://doi.org/10.31577/caosp.2022.52.1.46)
- Tsvetkov, D. Y., Volkov, I. M., Sorokina, E., et al. 2012, *Peremennye Zvezdy*, 32, 6. <https://arxiv.org/abs/1207.2241>
- Tsvetkov, D. Y., Shugarov, S. Y., Volkov, I. M., et al. 2018, *Astronomy Letters*, 44, 315, doi: [10.1134/S1063773718050043](https://doi.org/10.1134/S1063773718050043)

- Tsvetkov, D. Y., Baklanov, P. V., Potashov, M. S., et al. 2019, *Monthly Notices of the Royal Astronomical Society*, 487, 3001–3006, doi: [10.1093/mnras/stz1474](https://doi.org/10.1093/mnras/stz1474)
- Turatto, M., Cappellaro, E., Danziger, I. J., et al. 1993, *MNRAS*, 262, 128, doi: [10.1093/mnras/262.1.128](https://doi.org/10.1093/mnras/262.1.128)
- Utrobin, V. P., & Chugai, N. N. 2015, *A&A*, 575, A100, doi: [10.1051/0004-6361/201424822](https://doi.org/10.1051/0004-6361/201424822)
- Valentini, G., Di Carlo, E., Massi, F., et al. 2003, *ApJ*, 595, 779, doi: [10.1086/377448](https://doi.org/10.1086/377448)
- Van Dyk, S. D. 2013, *AJ*, 146, 24, doi: [10.1088/0004-6256/146/2/24](https://doi.org/10.1088/0004-6256/146/2/24)
- Van Dyk, S. D., Cenko, S. B., Clubb, K. I., et al. 2013a, *The Astronomer’s Telegram*, 4891, 1
- Van Dyk, S. D., Ganeshalingam, M., Silverman, J. M., & Filippenko, A. V. 2012a, *The Astronomer’s Telegram*, 3865, 1
- Van Dyk, S. D., Garnavich, P. M., Filippenko, A. V., et al. 2002, *PASP*, 114, 1322, doi: [10.1086/344382](https://doi.org/10.1086/344382)
- Van Dyk, S. D., Li, W., & Filippenko, A. V. 2003, *PASP*, 115, 1, doi: [10.1086/345748](https://doi.org/10.1086/345748)
- . 2006, *PASP*, 118, 351, doi: [10.1086/500225](https://doi.org/10.1086/500225)
- Van Dyk, S. D., & Matheson, T. 2012, in *Astrophysics and Space Science Library*, Vol. 384, *Eta Carinae and the Supernova Impostors*, ed. K. Davidson & R. M. Humphreys, 249, doi: [10.1007/978-1-4614-2275-4\\_11](https://doi.org/10.1007/978-1-4614-2275-4_11)
- Van Dyk, S. D., Weiler, K. W., Sramek, R. A., & Panagia, N. 1993, *ApJL*, 419, L69, doi: [10.1086/187139](https://doi.org/10.1086/187139)
- Van Dyk, S. D., Li, W., Cenko, S. B., et al. 2011, *ApJL*, 741, L28, doi: [10.1088/2041-8205/741/2/L28](https://doi.org/10.1088/2041-8205/741/2/L28)
- Van Dyk, S. D., Cenko, S. B., Poznanski, D., et al. 2012b, *ApJ*, 756, 131, doi: [10.1088/0004-637X/756/2/131](https://doi.org/10.1088/0004-637X/756/2/131)
- Van Dyk, S. D., Zheng, W., Clubb, K. I., et al. 2013b, *ApJL*, 772, L32, doi: [10.1088/2041-8205/772/2/L32](https://doi.org/10.1088/2041-8205/772/2/L32)
- Van Dyk, S. D., Zheng, W., Fox, O. D., et al. 2014, *AJ*, 147, 37, doi: [10.1088/0004-6256/147/2/37](https://doi.org/10.1088/0004-6256/147/2/37)
- Van Dyk, S. D., Lee, J. C., Anderson, J., et al. 2015, *ApJ*, 806, 195, doi: [10.1088/0004-637X/806/2/195](https://doi.org/10.1088/0004-637X/806/2/195)
- Van Dyk, S. D., Zheng, W., Maund, J. R., et al. 2019, *ApJ*, 875, 136, doi: [10.3847/1538-4357/ab1136](https://doi.org/10.3847/1538-4357/ab1136)
- Van Dyk, S. D., de Graw, A., Baer-Way, R., et al. 2023, *MNRAS*, 519, 471, doi: [10.1093/mnras/stac3549](https://doi.org/10.1093/mnras/stac3549)
- Vinko, J., Sarneczky, K., Hanyecz, O., & Sodor, A. 2017, *The Astronomer’s Telegram*, 10686, 1
- Vinokurov, A., Valeev, A. F., Atapin, K., & Moiseev, A. V. 2021, *The Astronomer’s Telegram*, 15107, 1
- Wagner, R. M., Vrba, F. J., Henden, A. A., et al. 2004, *PASP*, 116, 326, doi: [10.1086/382997](https://doi.org/10.1086/382997)
- Wang, X., Li, W., Filippenko, A. V., et al. 2008, *ApJ*, 677, 1060, doi: [10.1086/529070](https://doi.org/10.1086/529070)
- Weil, K. E., Fesen, R. A., Patnaude, D. J., & Milisavljevic, D. 2020, *ApJ*, 900, 11, doi: [10.3847/1538-4357/aba4b1](https://doi.org/10.3847/1538-4357/aba4b1)
- Wheeler, J. C., & Harkness, R. P. 1990, *Reports on Progress in Physics*, 53, 1467, doi: [10.1088/0034-4885/53/12/001](https://doi.org/10.1088/0034-4885/53/12/001)
- Wiggins, P. 2018, *Transient Name Server Discovery Report*, 2018-53, 1
- . 2020, *Transient Name Server Discovery Report*, 2020-653, 1
- Williams, B. F., Lang, D., Dalcanton, J. J., et al. 2014, *ApJS*, 215, 9, doi: [10.1088/0067-0049/215/1/9](https://doi.org/10.1088/0067-0049/215/1/9)
- Williams, C. L., Panagia, N., Van Dyk, S. D., et al. 2002, *ApJ*, 581, 396, doi: [10.1086/344087](https://doi.org/10.1086/344087)
- Woosley, S. E., & Weaver, T. A. 1986, *ARA&A*, 24, 205, doi: [10.1146/annurev.aa.24.090186.001225](https://doi.org/10.1146/annurev.aa.24.090186.001225)
- Xiang, D., Wang, X., Lin, W., et al. 2021, *ApJ*, 910, 42, doi: [10.3847/1538-4357/abdeba](https://doi.org/10.3847/1538-4357/abdeba)
- Yamanaka, M., Nakaoka, T., Tanaka, M., et al. 2017, *ApJ*, 837, 1, doi: [10.3847/1538-4357/aa5f57](https://doi.org/10.3847/1538-4357/aa5f57)
- Yang, Y., Wang, L., Baade, D., et al. 2017, *ApJ*, 834, 60, doi: [10.3847/1538-4357/834/1/60](https://doi.org/10.3847/1538-4357/834/1/60)
- Yuan, F., Jerkstrand, A., Valenti, S., et al. 2016, *MNRAS*, 461, 2003, doi: [10.1093/mnras/stw1419](https://doi.org/10.1093/mnras/stw1419)
- Zhang, J., & Wang, X. 2016, *Transient Name Server Classification Report*, 2016-12, 1
- Zhang, J., Wang, X., József, V., et al. 2020, *MNRAS*, 498, 84, doi: [10.1093/mnras/staa2273](https://doi.org/10.1093/mnras/staa2273)
- Zhang, T., Wang, X., Wu, C., et al. 2012, *AJ*, 144, 131, doi: [10.1088/0004-6256/144/5/131](https://doi.org/10.1088/0004-6256/144/5/131)
- Zheng, W., Filippenko, A. V., Mauerhan, J., et al. 2017, *ApJ*, 841, 64, doi: [10.3847/1538-4357/aa6dfa](https://doi.org/10.3847/1538-4357/aa6dfa)
- Zheng, W., Stahl, B. E., de Jaeger, T., et al. 2022, *MNRAS*, 512, 3195, doi: [10.1093/mnras/stac723](https://doi.org/10.1093/mnras/stac723)